ROTATIONAL AND VIBRATIONAL SPECTROSCOPY OF SULPHURYL CHLORIDE, SULPHURYL FLUORIDE AND DIMETHYL SULPHONE

JUNYI CHEN

ROTATIONAL AND VIBRATIONAL SPECTROSCOPY OF SULPHURYL CHLORIDE, SULPHURYL FLUORIDE AND DIMETHYL SULPHONE

© JUNYI CHEN
M.Sc. Hunan Normal University,
Changsha, Hunan, People's Republic of China, 1986.

A thesis submitted to the School of Graduate
studies in partial fulfillment of the
requirements for the degree of
Doctor of Philosophy

Department of Chemistry
Memorial University of Newfoundland
St.John's, Newfoundland

February 1991

ISBN 0-315-65339-6

ABSTRACT

The rotational and vibrational spectra of sulphuryl chloride, sulphuryl fluoride and dimethyl sulphone have been extensively studied. The molecular structures of all three molecules and the harmonic force fields of the first two molecules have been derived from the experimental data. Some nuclear quadrupole interactions, Fermi resonance and Coriolis interactions of these molecules have also been investigated.

(1) Cl_2SO_2: The microwave spectra of nine isotopic species of sulphuryl chloride, namely $^{35}Cl_2^{32}S^{16}O_2$, $^{35}Cl^{37}Cl^{32}S^{16}O_2$, $^{35}Cl_2^{32}S^{18}O_2$, $^{35}Cl^{37}Cl^{32}S^{18}O_2$, $^{35}Cl_2^{34}S^{18}O_2$, $^{35}Cl^{37}Cl^{34}S^{18}O_2$, $^{37}Cl_2^{32}S^{16}O_2$, $^{35}Cl_2^{34}S^{16}O_2$ and $^{35}Cl^{37}Cl^{34}S^{16}O_2$, were observed in the ground state over the frequency range from $12000MHz$ to $84000MHz$. The rotational constants and quartic centrifugal distortion constants have been calculated from these spectra. The effective, substitution and scaled structures of this molecule were evaluated from the rotational constants. The nuclear quadrupole hyperfine structures of some transitions were measured. The nuclear quadrupole splittings of $^{35}Cl_2^{32}S^{16}O_2$ transitions have been analyzed to yield the nuclear quadrupole coupling constants of ^{35}Cl as: $\chi_{aa} = -33.25MHz$, $\chi_{bb} = -6.97MHz$, $\chi_{cc} = 40.22MHz$ and $\eta = 1.42$. The Raman spectra of $^{35}Cl_2^{32}S^{16}O_2$, $^{35}Cl_2^{32}S^{18}O_2$ and $^{35}Cl_2^{34}S^{18}O_2$ have also been observed in both the liquid and gas phases. A Fermi resonance between the ν_1 fundamental and the first overtone of the ν_8 mode has been analyzed. A harmonic force field with thirteen force constants has been determined from the quartic centrifugal distortion constants and the vibrational frequencies. The harmonic force field has been used to obtain the average structure for this molecule. The ground state average structural parameters of $^{35}Cl_2^{32}S^{16}O_2$ are: $r_{SO} = 1.41347(11)Å$, $r_{SCl} = 2.01124(10)Å$, $angle_{OSO} = 123.129(15)°$, $angle_{ClSCl} = 100.126(7)°$.

(2) F_2SO_2: The microwave spectra of five isotopic species: $F_2^{32}S^{16}O_2$, $F_2^{32}S^{18}O_2$, $F_2^{32}S^{16}O^{18}O$, $F_2^{34}S^{16}O_2$ and $F_2^{34}S^{18}O_2$ have been measured in the ground state from 6000 to $120000MHz$. A large number of satellite series were also investigated for $F_2^{32}S^{16}O_2$

and $F_2^{32}S^{18}O_2$ and have been assigned to five vibrationally excited state transitions ($v_3 = 1, v_4 = 1, v_5 = 1, v_7 = 1$ and $v_9 = 1$) of $F_2^{32}S^{16}O_2$ and four vibrationally excited state transitions ($v_4 = 1, v_5 = 1, v_7 = 1$ and $v_9 = 1$) of $F_2^{32}S^{18}O_2$. The spectra have been analyzed to yield values for the rotational constants and quartic centrifugal distortion constants for both the ground and excited states. The sextic centrifugal distortion constants of the $F_2^{32}S^{18}O_2$ species have also been determined. An effective geometry has been obtained from the ground state rotational constants. The Coriolis interaction constant ζ_{35}^{c} was derived as 0.264 and 0.24 for $F_2^{32}S^{16}O_2$ and $F_2^{32}S^{18}O_2$ respectively. A complete harmonic force fie.d, with seventeen force constants, has been determined from the quartic distortion constants and vibrational frequencies. The harmonic force constants have been used to calculate the average molecular structure of $F_2^{32}S^{16}O_2$ in the ground state. The average structural parameters are: $r_{SO} = 1.40176(13)Å$, $r_{SF} = 1.53608(16)Å$, $angle_{OSO} = 124.907(20)°$, $angle_{FSF} = 95.?84(13)°$.

(3) $(CH_3)_2SO_2$ The microwave spectra of eight isotopic species,

$(^{12}CH_3)_2^{32}S^{16}O_2$, $(^{12}CD_3)_2^{32}S^{16}O_2$, $(^{12}CH_3)_2^{32}S^{16}O^{18}O$, $(^{12}CH_3)(^{12}CH_2D)^{32}S^{16}O_2(I)$,

$(^{13}CH_3)_2^{32}S^{16}O_2$, $(^{12}CH_3)_2^{34}S^{16}O_2$, $(^{12}CH_3)(^{13}CH_3)^{32}S^{16}O_2$, $(^{12}CH_3)(^{12}CH_2D)^{32}S^{16}O_2(II)$, were observed in the ground state over the frequency range from 40000 to 85000MHz. The rotational constants and quartic centrifugal distortion constants of the eight species have been derived from the experimental data. Effective and substitution structures have been obtained using the ground state rotational constants. The substitution structural parameters of $(^{12}CH_3)_2^{32}S^{16}O_2$ are:

$r_{SO} = 1.4343(23)Å$, $r_{SC} = 1.7728(28)Å$, $r_{CH(I)} = 1.0839(9)Å$, $r_{CH(II)} = 1.0858(2)Å$,

$angle_{OSO} = 120.14(19)°$, $angle_{CSC} = 103.61(16)°$, $angle_{SCH(I)} = 105.59(25)°$,

$angle_{SCH(II)} = 109.51(19)°$, $angle_{H(I)CH(II)} = 110.38(11)°$, $angle_{H(II)CH(II)} = 111.61(5)°$.

ACKNOWLEDGEMENTS

It is a pleasure to acknowledge the friendship and guidance of several people. At first, I wish to express my deep gratitude to my supervisor, Dr. R. W. Davis, for his supervision and help during the course of this work and without whom this thesis would not have been completed. I am indebted to Dr. M. H. Brooker for his guidance in running and interpreting the Raman spectra. My sincere thanks also go to Dr. R. Poirier, who has given me a lot of suggestions for the ab initio calculations and who has also let me use his programs extensively.

Finally, I would like to thank the Memorial University of Newfoundland and the Department of Chemistry of this university for financial support in the form of a Graduate Fellowship.

Table of Contents

LIST OF TABLES

LIST OF FIGURES

CHAPTER 1

INTRODUCTION

The very first microwave spectrum was obtained more than 50 years ago by Cleeton and Williams[64], who investigated the absorption of ammonia vapor at frequencies around $20GHz$ since theoretical calculations had suggested that the absorption due to the inversion motion of the ammonia molecule should be observed in the microwave frequency region. Although the first microwave spectrum was the ground vibrational state inversion spectrum of ammonia, we now usually regard the terms microwave spectroscopy and rotational spectroscopy as being synonymous since microwave studies normally lead to molecular information through the phenomena of changes in molecular rotational energy levels.

The apparatus used by Cleeton and Williams was very simple, the ammonia gas being contained in a rubberised cloth bag at atmospheric pressure. They produced the radiation itself from very small split-anode magnetrons with anode radii of less than $\frac{1}{2}mm$. The microwave powers available, and their detection methods, resulted in low sensitivity for experiment; they were able only to show that there was a broad absorption band centered on a wavelength of about $1.25cm$ [64]. After the second world war, when the enormous advance in microwave techniques occurred because of the interest in radar technology, the development of the klystron and the backward wave oscillator provided microwave sources which could generate microwave radiation at high power levels, the frequency of which could be accurately controlled and measured. The invention of the Stark modulation technique greatly enhanced the sensitivity of microwave spectrometers. Thus it is not surprising that, since then, the theory and the experimental techniques of microwave spectroscopy have both been improved greatly. The introduction of more new experimental techniques is making modern microwave spectrometers increasingly powerful. Modern microwave spectrometers are improving in several respects with higher sensitivity, higher resolution and an expansion of the useful frequency region being most prominent.

Because of the very small population differences of the rotational eigenstates involved in the microwave spectrum, the intensities of microwave pure rotational transitions are particularly low. A useful method of raising sensitivity in microwave spectroscopy experiments involves the double resonance technique and consequent departures from Boltzmann distributions of state populations. An early example, made by Oka[161], of using the microwave-microwave double resonance technique is the detection of $\Delta J = 3$ transitions in the ethyl iodide; the absorption coefficients of these transitions are not greatly in excess of $10^{-11} cm^{-1}$. Now, using the Fourier transformation technique, it is possible to observe very weak rotational transitions in bimolecular species held together by Van der Waals forces, such as $KrHCl$ [67] and, as well, hydrogen bonded complexes such as $H_2O...HF$ [68] and $(CH_3)_3N...HF$ [166]. The observation of microwave transitions in isotopically substituted and nominally nonpolar molecules, such as CH_3CH_2D, CH_2CHD and $CHCD$, the dipole moments of which are usually only 10^{-3} - $10^{-4}D$[162], and very recently, of a complex with nonpolar constituents, $Hg...Ar$ [167], have also been reported.

By far the most striking improvements in resolution have been achieved by the use of molecular beam spectrometers, in which the Doppler widths of lines are largely eliminated. This feature has proved valuable in measuring very dense hyperfine structures, such as multiplets in nuclear quadrupole splittings and especially the Zeeman effect splittings. By using the molecular beam technique, Burie *et.al* [66] obtained very high resolution microwave spectra for CH_3I showing very well resolved iodine nuclear quadrupole hyperfine structures, with a half line width only $3kHz$.

Because the spectra of many fundamental and light molecules fall primarily at shorter wavelengths and also because the strength of the interaction between molecular systems and electromagnetic radiation increases with decreasing wavelength, it has long been an aim to expand the high resolution microwave techniques into the millimeter and submillimeter region of the spectrum[163]-[165]. The Q branch $J_{10,J-9} - J_{11,J-10}$ transitions of SO_2 were the first to be recorded at frequencies above $1000GHz$[165].

Microwave spectroscopy has now become established as a standard tool which is employed to study the molecular structures of molecules in the gas phase. A knowledge of the molecular force field, molecular electric dipole moment and nuclear quadrupole coupling constants can also be obtained from the results of microwave spectroscopic studies.

In this thesis, the microwave spectra of three molecules, namely F_2SO_2, Cl_2SO_2 and $(CH_3)_2SO_2$, have been reported. These have been studied using a conventional Stark modulated spectrometer, and the molecular structures and harmonic force fields of these molecules have been obtained. A very brief outline of the theory needed to interpret microwave spectra is given in subsequent sections of this chapter. A more extensive outline of the existing theory has been given in many excellent publications [1][2][3][4][8][9][63].

1.1 Energy Levels of the Asymmetric Rotor

The three rotational constants A, B and C needed to describe the rotational energies of a rigid three dimensional rotor are related to the corresponding principal moments of inertia by the following equations

$$I_a = \frac{h}{(8\pi^2 A)} \qquad I_b = \frac{h}{(8\pi^2 B)} \qquad I_c = \frac{h}{(8\pi^2 C)} \tag{1.1.1}$$

where

$$\frac{h}{8\pi^2} = 505379.07\ u\dot{A}^2 MHz \tag{1.1.2}$$

where Plank's constant $h = 6.6260755(40)\times 10^{-34} J.sec.$[25].

The principal inertial axes, a, b and c, are usually labeled in such an order that $A \geq B \geq C$ or $I_a \leq I_b \leq I_c$. An asymmetric rotor is one that has no two principal moments of inertia equal, that is

$$I_a < I_b < I_c \tag{1.1.3}$$

In the rigid rotor approximation, the rotational energies of a linear rotor, with $I_a = 0, I_b = I_c$, a spherical rotor, with $I_a = I_b = I_c$, and a symmetric rotor, with $I_a < I_b = I_c$ (prolate symmetric top) or $I_a = I_b < I_c$ (oblate symmetric top), can be expressed in convenient equations because the rigid rotor Hamiltonian can be diagonalized[9]. The non-zero energy matrix elements of symmetric rotors in the field free case are only the diagonal terms, which are

$$\langle JKM|H|JKM\rangle = BJ(J+1) + (A-B)K^2 \tag{1.1.4}$$

and

$$\langle JKM|H|JKM\rangle = BJ(J+1) + (C-B)K^2 \tag{1.1.5}$$

for prolate rotors and oblate rotors, respectively. Here $|JKM\rangle$ is usually used to denote the wavefunction of the symmetric rotor; J is the rotational quantum number related to the total rotational angular momentum, and can assume any non-negative integer value, and K is the rotational quantum number which gives the component of the total rotational angular momentum along the molecule-fixed axis. If an external electric field is present, a third quantum number M, which gives the component of the total rotational angular momentum along the direction of a space fixed axis, is needed to describe the rotational energy. K and M can be any integer in the range from $-J$ to J. In the field-free case, the Hamiltonian of a symmetric top is diagonal in the J and K representation and is double degenerate when $|K|\neq 0$. In addition to the double K degeneracy there is a $(2J+1)$ fold M degeneracy.

For asymmetric rotors the Hamiltonian, however, is not diagonal in the J and K representation and the rotational energies cannot be expressed using convenient equations as is the case with symmetric tops. For nearly prolate asymmetric rotors, the I^r representation[56] is usually chosen and the non-zero matrix elements are

$$\langle JKM|H|JKM\rangle = \frac{1}{2}(B+C)J(J+1) + [A - \frac{1}{2}(B+C)]K^2 \tag{1.1.6}$$

and

$$\langle JK\pm 2M|H|JKM\rangle = \frac{1}{4}(B-C)[J(J+1) - K(K\pm 1)]^{\frac{1}{2}} \\ [J(J+1) - (K\pm 1)(K\pm 2)]^{\frac{1}{2}} \tag{1.1.7}$$

The rigid-rotor Hamiltonian matrix is tridiagonal. The matrix can be factored into four independent submatrices, if it is noticed that there is no matrix element connecting even and odd K values and the Wang transformation[57] is used. Now the total angular momentum J and its projection M on a space-fixed axis are still constants of the motion and are still good quantum numbers. K, however, is no longer a good quantum number and the double K degeneracy of the symmetric rotor is lifted. The energy levels of asymmetric rotors are labeled as $J_{K_a K_c}$. Here K_a and K_c are the $|K|$ values which are obtained from the prolate and oblate symmetric limit, respectively. Another method of designating the levels is using J_τ, with $\tau = K_a - K_c$.

There are various parameters used to indicate the degree of inertial asymmetry. One of them is Ray's asymmetry parameter[58]:

$$\kappa = \frac{2B - A - C}{A - C} \tag{1.1.8}$$

which becomes -1 for a prolate symmetric top and 1 for an oblate symmetric top, varying between -1 and 1 for asymmetric tops. Another parameter, Wang's parameter[59] for a slightly asymmetric prolate top, is:

$$b_p = \frac{C - B}{2A - B - C} = \frac{\kappa + 1}{\kappa - 3} \tag{1.1.9}$$

The value of b_p is zero for a prolate symmetric top, and again increases as the top becomes more and more asymmetric. The Wang parameter for a slightly asymmetric oblate top is:

$$b_o = \frac{A - B}{2C - B - A} = \frac{\kappa - 1}{\kappa + 3} \tag{1.1.10}$$

The value of b_o is zero for an oblate symmetric top and increases as the top becomes more and more asymmetric. For a slightly asymmetric prolate molecule, by using the Wang asymmetry parameter the rigid top Hamiltonian and rotational energy may be conveniently written in the form

$$H_p = \frac{1}{2}(B + C)P^2 + [A - \frac{1}{2}(B + C)]H(b_p) \tag{1.1.11}$$

and

$$E_p = \frac{1}{2}(B + C)J(J + 1) + [A - \frac{1}{2}(B + C)]W_{J_\tau}(b_p) \tag{1.1.12}$$

Similarly for a slightly asymmetric oblate molecule we have

$$H_o = \frac{1}{2}(B + A)P^2 + [C - \frac{1}{2}(B + A)]H(b_o) \tag{1.1.13}$$

and

$$E_o = \frac{1}{2}(B + A)J(J + 1) + [C - \frac{1}{2}(B + A)]W_{J_\tau}(b_o) \tag{1.1.14}$$

with

$$H(b_p) = P_a^2 + b_p(P_c^2 - P_b^2) \tag{1.1.15}$$

and

$$H(b_o) = P_c^2 + b_o(P_a^2 - P_b^2) \tag{1.1.16}$$

The asymmetric top Hamiltonian can also be written in the following form by using Ray's asymmetry parameter

$$H = \frac{1}{2}(A + C)P^2 + \frac{1}{2}(A - C)H(\kappa) \tag{1.1.17}$$

Here

$$H(\kappa) = P_a^2 + \kappa P_b^2 - P_c^2 \tag{1.1.18}$$

The discussion so far has assumed a rigid rotor, with no effects of vibration or centrifugal distortion. This simple rigid rotor approximation can be fairly successfully used to describe low J rotational states. However, as J increases the error becomes larger, because the effects of centrifugal distortion, which shifts the rotational energies from their rigid rotor values, increase. The general theory of centrifugal distortion has been considered in detail by Wilson, Howard and Nielsen[44][60][61][62]. They gave the non-rigid rotor asymmetric top Hamiltonian as:

$$\begin{aligned} H &= H_r + H_d \\ &= AP_a^2 + BP_b^2 + CP_c^2 + \frac{1}{4}\sum_{\alpha,\beta}\tau'_{\alpha\alpha\beta\beta}P_\alpha^2 P_\beta^2 \end{aligned} \tag{1.1.19}$$

Here the τ's are quartic centrifugal distortion constants which are related to the harmonic molecular force field[42], which will be discussed in section 1.6. There are six different τ's, they are τ'_{aaaa}, τ'_{bbbb}, τ'_{cccc}, τ'_{aabb}, τ'_{aacc}, and τ'_{bbcc}; only five combinations of them can be obtained from microwave spectra however[45][46][47]. Convenient combinations of these τ's have been suggested by Watson[45][47] and were used in this work. By using these combinations, the non-rigid rotor Hamiltonian in Watson's S reduction[46][47] is:

$$H = H_r + H_d + H_{d'} + \cdots \tag{1.1.20}$$

Here

$$H_r = A\vec{J}_a^2 + B\vec{J}_b^2 + C\vec{J}_c^2 \tag{1.1.21}$$

$$\begin{aligned} H_d = & -D_J\vec{J}^4 - D_{JK}\vec{J}^2\vec{J}_a^2 - D_K\vec{J}_a^4 \\ & + d_1\vec{J}^2(J_+^2 + J_-^2) + d_2(J_+^4 + J_-^4) \end{aligned} \tag{1.1.22}$$

$$\begin{aligned} H_{d'} = & H_J\vec{J}^6 + H_{JK}\vec{J}^4\vec{J}_a^2 + H_{KJ}\vec{J}^2\vec{J}_a^4 \\ & + H_K\vec{J}_a^6 + h_1\vec{J}^4(J_+^2 + J_-^2) \\ & + h_2\vec{J}^2(J_+^4 + J_-^4) + h_3(J_+^6 + J_-^6) \end{aligned} \tag{1.1.23}$$

Here

$$J_\pm = \vec{J}_b \pm i\vec{J}_c \tag{1.1.24}$$

Because the amount of centrifugal distortion of a molecule does not depend on the sign of the angular rotation, both of H_d and $H_{d'}$ involve only even powers of the angular momentum. Here D_J, D_{JK}, D_K, d_1, and d_2 are quartic distortion constants, which are combinations of the τ 's, as is shown in Table-1.2. H_J, H_{JK}, H_{KJ}, H_K, h_1, h_2 and h_3 are sextic distortion constants, which are related to the cubic force field of the molecule. For the calculations presented in this work, only terms up to $H_{d'}$ were considered. For lighter molecules such as H_2O and H_2S it is necessary to include higher-order terms[63]. If linear combinations of symmetric top wavefunctions are used to construct the asymmetric top wavefunctions, by using the above Hamiltonian the non-zero energy matrix elements satisfy the extended rule $\Delta k = 0, \pm 2, \pm 4, \pm 6$. The non-zero matrix elements are $\langle JKM|H|JKM\rangle$, $\langle JK\pm 2M|H|JKM\rangle$, $\langle JK\pm 4M|H|JKM\rangle$ and $\langle JK\pm 6M|H|JKM\rangle$, which leads to a heptadiagonal non-rigid rotor asymmetric top energy matrix. In the I^r representation it is not difficult to evaluate these energy matrix elements, which are given as the following equations:

$$\langle JKM|H|JKM\rangle = \frac{1}{2}(B+C)J(J+1) + [A - \frac{1}{2}(B+C)]K^2 \tag{1.1.25}$$
$$-D_J J^2(J+1)^2 - D_{JK}J(J+1)K^2 - D_K K^4$$
$$+ H_J J^3(J+1)^3 + H_{JK}J^2(J+1)^2K^2$$
$$+ H_{KJ}J(J+1)K^4 + H_K K^6$$

$$\langle JK\pm2M|H|JKM\rangle = [\frac{1}{4}(B-C) + d_1 J(J+1) + h_1 J^2(J+1)^2] \tag{1.1.26}$$
$$\times\Big\{[J(J+1) - K(K\pm1)][J(J+1)$$
$$-(K\pm1)(K\pm2)]\Big\}$$

$$\langle JK\pm4M|H|JKM\rangle = [d_2 + h_2 J(J+1)][J(J+1) - K(K\pm1)]^{\frac{1}{2}} \tag{1.1.27}$$
$$\times[J(J+1) - (K\pm1)(K\pm2)]^{\frac{1}{2}}[J(J+1)$$
$$-(K\pm2)(K\pm3)]^{\frac{1}{2}}[J(J+1) - (K\pm3)(K\pm4)]^{\frac{1}{2}}$$

$$\langle JK\pm6M|H|JKM\rangle = h_3[J(J+1) - K(K\pm1)]^{\frac{1}{2}}[J(J+1) \tag{1.1.28}$$
$$-(K\pm1)(K\pm2)]^{\frac{1}{2}}[J(J+1) - (K\pm2)(K\pm3)]^{\frac{1}{2}}$$
$$\times[J(J+1) - (K\pm3)(K\pm4)]^{\frac{1}{2}}[J(J+1)$$
$$-(K\pm4)(K\pm5)]^{\frac{1}{2}}[J(J+1) - (K\pm5)(K\pm6)]^{\frac{1}{2}}$$

Here, because of vibrational averaging effects, all of the rotational constants, as well as, the quartic and sextic distortion constants, are effective constants, which vary from one vibrational state to another. Therefore the molecular geometry and force field derived from these constants are also effective and vary with vibrational state. A simpler tridiagonal matrix Hamiltonian, the so-called A reduction Hamiltonian, has also been derived by Watson[46][47]. Because some of the molecules investigated in the present work were nearly symmetric tops Watson's S reduction, which is the necessary choice for molecules which are only slightly asymmetric[47], was used throughout.

The rotational energy states can be obtained from the elements of the required Jacobian matrix, which are usually derived by diagonalizing Watson's reduced Hamiltonian and refining the experimental rotational frequencies. The Jacobians are

$$\begin{aligned}
\frac{\partial E}{\partial A} &= \langle P_a^2 \rangle \\
\cdots &\quad \cdots \\
\frac{\partial E}{\partial D_J} &= \langle P^4 \rangle \\
\cdots &\quad \cdots \\
\frac{\partial E}{\partial H_J} &= \langle P^6 \rangle \\
\cdots &\quad \cdots
\end{aligned} \tag{1.1.29}$$

In this method, an initial trial set of rotational constants are used to calculate the energy eigenvalues, from which the calculated rotational frequences can be derived. The difference between calculated and experimental frequencies can be used to refine the rotational constants or calculate distortion constants. The procedure usually requires two or three iterations to converge.

1.2 Nuclear Spin and Line Intensities of Rotational Spectra

The presence of identical nuclei in a molecule can have important consequences in the determination of the statistical weights of the energy levels and the relative intensities of rotational bands[8][9]. Those wavefunctions which remain unchanged by an exchange of identical nuclei are designated as symmetric functions and those which change sign as antisymmetric. It is found by experience that for Bose particles (with zero or integer spins) the over-all wavefunctions are symmetric, and for Fermi particles (with half-integer spins) the overall wavefunctions are antisymmetric with regard to exchange of the identical particles. The complete wavefunction (Ψ_{total}) is the product of the electronic wavefunction (Ψ_e), the vibrational wavefunction (Ψ_v), the rotational wavefunction (Ψ_r) and the nuclear spin wavefunction (Ψ_n).

$$\Psi_{total} = \Psi_e \Psi_v \Psi_r \Psi_n \tag{1.2.1}$$

The transition dipole moment between states i and j is

$$\mu_{ij} = \int \Psi_i \mu_a \Psi_j d\tau + \int \Psi_i \mu_b \Psi_j d\tau + \int \Psi_i \mu_c \Psi_j d\tau \tag{1.2.2}$$

Here Ψ_i and Ψ_j are complete wavefunctions of state i and state j, respectively. The symmetry operation which merely exchanges the identical nuclei does not change the sign of the dipole moment (μ_a, μ_b, μ_c) and therefore the integral will be zero unless Ψ_i and Ψ_j have the same symmetry along at least one axis. Generally both the ground state electronic wavefunction (Ψ_e) and the ground state vibrational wavefunction (Ψ_v) are symmetric and therefore, the symmetry of the total wavefunction is dependent on the rotational wavefunction (Ψ_r) and the nuclear wavefunction (Ψ_n). Therefore for Bose particles Ψ_r and Ψ_n should have the same symmetry; for Fermi particles Ψ_r and Ψ_n should have different symmetry. For molecules having one pair of identical nuclei with spin I, there are

$$(I+1)(2I+1) \tag{1.2.3}$$

symmetric spin wavefunctions and

$$I(2I+1) \tag{1.2.4}$$

antisymmetric spin wavefunctions. For molecules having three pairs of identical nuclei with spin I, the number of symmetric and antisymmetric wavefunctions are

$$(I+1)^3(2I+1)^3+3(I+1)(2I+1)I^2(2I+1)^2 \tag{1.2.5}$$

and

$$I^3(2I+1)^3+3(I+1)^2(2I+1)^2I(2I+1) \tag{1.2.6}$$

respectively. Table-1.1 gives the spin statistical weights of the molecules considered in this work.

Table-1.1

Spin Statistical Weights of Cl_2SO_2, F_2SO_2 and $(CH_3)_2SO_2$

Molecules		Cl_2SO_2	F_2SO_2	$(CH_3)_2SO_2$	$(CD_3)_2SO_2$
I		3/2	1/2	1/2	1
n		1	1	3	3
a-type	oo-oe	5	3	9	13
	ee-eo	3	1	7	14
b-type	eo-oe	5	3	9	13
	oo-ee	3	1	7	14
c-type	oo-eo	5	3	9	13
	ee-oe	3	1	7	14

Here n is the number of identical atom-pairs and the spins of ^{16}O and ^{12}C both are zero which need not be considered. All the normal species of the three molecules are Fermi particles so that antisymmetric rotational states have more population than symmetric states when they are in the ground electronic and ground vibrational state. The spin statistics of an excited vibrational state are dependent on the symmetry properties of the state. If the excited vibrational state belongs to an A symmetry species (in the C_{2v} point group) antisymmetric rotational states have more intensity than symmetric states, otherwise symmetric rotational states have more intensity than antisymmetric states.

1.3 Molecular Structures from Rotational Spectra

There are two important methods, microwave spectroscopy and electron diffraction, used to determine the molecular structures of gaseous molecules. In comparison with electron diffraction, microwave spectroscopy has several advantages and disadvantages.

Advantages of microwave spectroscopy:

(a) The structures of molecules in the ground state and in various excited vibrational states(if the intensities are high enough for measuring) can be obtained separately and directly.

(b) Sample impurities do not usually affect the microwave measurements. Mixtures are readily studied.

Disadvantages of microwave spectroscopy:

(a) Several isotopic species must usually be studied to obtain the molecular structure.

(b) The coordinates of the atoms which are situated near inertial axes are very difficult to determine accurately.

(c) It can be used only for relatively small molecules.

One of the most important aims of microwave spectroscopy is the accurate measurement of the geometric structures of molecules. The molecular structures are derived from the principal moments of inertia I_a, I_b and I_c

$$\begin{aligned} I_a &= \sum_i m_i (b_i^2 + c_i^2) \\ I_b &= \sum_i m_i (a_i^2 + c_i^2) \\ I_c &= \sum_i m_i (a_i^2 + b_i^2) \end{aligned} \tag{1.3.1}$$

Here a_i, b_i and c_i are the principal axes coordinates of the ith atom and m_i is the mass of the ith atom. The principal moments of inertia are obtained from the rotational constants A , B and C as shown in equation(1.1.1).

The equilibrium structures of diatomic molecules and a few simple polyatomic molecules, since the rotational constants are usually obtained in excited vibrational states as well as in the ground state, in these cases can be derived by extrapolation to allow for removal of the zero point vibrational effects[18][26]. In more complicated cases, however, it is impossible to obtain the required correction of the moments of inertia for vibrational contributions. Because of this several different procedures have been developed, in which various degrees of correction for the effects of molecular vibration have been considered and different conceptions of molecular structures have been defined[9][19][20][21][22]. These structures all deviate from the equilibrium structure to some extent.

Types of molecular structures:

(a) r_e, the equilibrium molecular structure is evaluated by correcting for all the effects of vibration. The r_e structure is the most interesting molecular structure to chemists. r_e is related to the equilibrium rotational constants(A_e , B_e and C_e). The equilibrium rotational constants, however, often cannot be obtained by experiment.

$$
\begin{aligned}
A_e &= A_v + \sum_i^{3N-6} \alpha_i^a (v_i + \frac{d_i}{2}) - \sum_i^{3N-6} \gamma_i^a (v_i + \frac{d_i}{2})^2 + \cdots \\
B_e &= B_v + \sum_i^{3N-6} \alpha_i^b (v_i + \frac{d_i}{2}) - \sum_i^{3N-6} \gamma_i^b (v_i + \frac{d_i}{2})^2 + \cdots \\
C_e &= C_v + \sum_i^{3N-6} \alpha_i^c (v_i + \frac{d_i}{2}) - \sum_i^{3N-6} \gamma_i^c (v_i + \frac{d_i}{2})^2 + \cdots
\end{aligned}
\tag{1.3.2}
$$

Here α and γ, *etc.* are the vibration-rotation interaction constants, d_i is the degeneracy of the ith normal mode and v_i is the vibrational quantum number of the ith normal mode. If γ and higher order vibration-rotation interactions are ignored, the determination of equilibrium rotational constants still requires measurements of the rotational spectra of molecules in excited states of all the fundamental modes of vibration. It is usually impossible using microwave spectroscopy to observe rotational spectra for all of the fundamental modes. For example, the SO symmetric stretch mode(ν_1) of F_2SO_2 has frequency of $1269cm^{-1}$[27] and the population in this state is only 0.23% of the population in the ground vibrational state at room temperature. This population is too low for observation of the pure rotational spectra of this excited state and enough data therefore cannot be obtained to calculate the equilibrium rotation constants. Kuchitsu *et al*[37][38] have suggested estimating the equilibrium bond distances using the following approximate formulas:

$$r_z = r_e + \frac{3au^2}{2} - K \tag{1.3.3}$$

and

$$\delta r_z = \frac{3a\,\delta(u^2)}{2} - \delta K \tag{1.3.4}$$

Here r_e and r_z, which will be discussed later, are the equilibrium and ground state average bond lengths respectively, δ denotes an isotopic difference, u^2 and K are the parallel and perpendicular mean square amplitudes respectively, and a is the Morse anharmonicity parameter. u^2 and K are calculated from the harmonic force field[39].

(b) r_0, the effective molecular structure for the ground vibrational state, is derived from ground vibrational state rotation constants(A_0,B_0,C_0) or moments of inertia(I_a^0,I_b^0,I_c^0), which are obtained directly from experiment. For a diatomic molecule, we have:

$$r_0 = \left(\frac{h}{8\pi^2\mu B_0}\right)^{1/2} = \left(\frac{I^0}{\mu}\right)^{1/2} \tag{1.3.5}$$

Here the rotational constant(B_0) is an effective rotational constant for the ground vibrational state. r_0, however, is not the simple average molecular bond distance in the ground vibrational state, but the reciprocal of the square root of the average inverse square molecular bond distance:

$$r_0 = \left\langle\frac{1}{r^2}\right\rangle^{-1/2} \tag{1.3.6}$$

Because of anharmonic vibrational effects, r_0 is usually longer than r_e.

$$r_0 > r_e \tag{1.3.7}$$

Only three rotational constants can be obtained from one isotopic species(asymmetric top molecule). Therefore, if a molecule has more than three geometrical parameters the rotational spectra of additional isotopic species have to be observed for calculation of the complete r_0 molecular geometry. And for the calculation, we are forced to assume that the effective structure is not affected by isotopic substitution. Actually, however, the r_0 structure is slightly different for different isotopic species, because the zero point vibrational effects change when isotopic substitutions are made[31]. The difference will be largest for a molecule in which the hydrogen atoms contribute a large fraction of the moments of inertia, since usually the deuterated compound is an additional species.

(c) r_s is the substitution molecular structure, which is calculated using the method developed by Kraitchman[28]. In this method the changes of moments of inertia resulting from isotopic substitution of an atom are used to calculate the coordinates of the substituted atom in the molecular principal axis system.

$$\begin{aligned}
|a| &= \left[\frac{P_a' - P_a}{\mu}\left(1 + \frac{P_b' - P_b}{I_a - I_b}\right)\left(1 + \frac{P_c' - P_c}{I_a - I_c}\right)\right]^{1/2} \\
|b| &= \left[\frac{P_b' - P_b}{\mu}\left(1 + \frac{P_a' - P_a}{I_b - I_a}\right)\left(1 + \frac{P_c' - P_c}{I_b - I_c}\right)\right]^{1/2} \\
|c| &= \left[\frac{P_c' - P_c}{\mu}\left(1 + \frac{P_a' - P_a}{I_c - I_a}\right)\left(1 + \frac{P_b' - P_b}{I_c - I_b}\right)\right]^{1/2}
\end{aligned} \tag{1.3.8}$$

Here the I's and P's are the moments of inertia and the principal moments, respectively, of the parent molecule and the P''s are the principal moments of the substituted molecule.

$$\begin{aligned}
P_a &= (I_b + I_c - I_a)/2 \\
P_b &= (I_c + I_a - I_b)/2 \\
P_c &= (I_a + I_b - I_c)/2
\end{aligned} \tag{1.3.9}$$

And

$$\mu = \frac{M(M' - M)}{M'} \tag{1.3.10}$$

Here M and M' are the masses of parent molecule and substituted molecule, respectively.

Costain[31] has suggested that the zero point vibrational effects in substitution constructions are less than in effective constructions and that the variation in the structures obtained from different sets of isotopic species appears to depend only on the uncertainties in the rotational constants. The accuracy is independent of the mass of substituted atom, and therefore light atoms, even hydrogen, are located just as accurately as the heavier atoms. Costain has also suggested that, for simple molecules

$$r_e < r_s < r_0 \tag{1.3.11}$$

Probably the most important quality of the substitution structure r_s is that it often provides a better approximation to the equilibrium structure r_e than does the effective structure r_0; it, however, has no well defined physical meaning.

Once every nonequivalent atom of a molecule is substituted, the substitution structure of the molecule may be readily evaluated. Unfortunately, there are some elements which have only one isotope, such as F and P. If a molecule involves such atoms, Kraitchman's method cannot be used and a substitution structure cannot be obtained. If all nonequivalent atoms but one have been substituted, then the coordinates of the remaining atom may be calculated by the center of mass conditions:

$$\begin{aligned} a_j &= -\frac{\sum_{i \neq j} m_i a_i}{m_j} \\ b_j &= -\frac{\sum_{i \neq j} m_i b_i}{m_j} \\ c_j &= -\frac{\sum_{i \neq j} m_i c_i}{m_j} \end{aligned} \tag{1.3.12}$$

Here a_i, b_i and c_i are the coordinates of the ith atom, which is substituted, in the principal axes system, m_i is the mass of the ith atom, a_j,b_j and c_j are the coordinates of the unsubstituted atom and m_j is the mass of the unsubstituted atom. The center of mass conditions are often used to calculate the coordinates of atoms which are located very close to a principal axis, because in such a case Kraitchman's method is unsatisfactory[29][30]. The molecular geometry obtained using the center of mass conditions is not a true substitution geometry. The difference between this geometry and a true substitution geometry is reflected in the coordinates of the unsubstituted atom. From equations(1.3.12), it is easy to understand why the lighter the unsubstituted atom is, the bigger is the error of its coordinates. The center of mass conditions give poor results for light atoms, particularly for hydrogen atoms[9].

(d) r_ε is the average molecular structure over a specific vibrational state calculated by partially correcting for the effects of vibration. The method suggested by Oka[32], Laurie, *et.al.*[33][34] and Kuchitsu[35][36] makes use of the "average" moment of inertia I_{G_ε} to calculate the r_ε structure. They gave the moment of inertia of the average configuration as

$$I_G^\varepsilon = I_G^e + \sum_l (v_l + \frac{d_l}{2})\varepsilon_{l\,anhar.}^G \tag{1.3.13}$$

$$I_G^\varepsilon = I_G^v - \sum_l (v_l + \frac{d_l}{2})\varepsilon_{l\,har.}^G \tag{1.3.14}$$

If we know the moment of inertia of the ground state I_G^0 we have

$$I_G^\varepsilon = I_G^0 - \sum_l \frac{d_l}{2}\varepsilon_{l\,har.}^G \tag{1.3.15}$$

Use has been made of the fact that the vibration-rotation constants can be separated into harmonic and anharmonic parts.

$$\varepsilon_l^G = \varepsilon_{l\,har.}^G + \varepsilon_{l\,anhar.}^G \tag{1.3.16}$$

The r_ε structure differs from the equilibrium structure only because of the anharmonic effects of molecular vibrations. Therefore it can be derived from the effective rotational constants, if the molecular harmonic force field has been obtained[40]. Kuchitsu has shown that $r_z > r_0$ [37].

(e) The r_m structure calculated by the "mass dependence" method was suggested by Watson[20][41]. In this method, Watson used the inconsistencies in the r_0 determination as a means of estimating the vibrational contributions to the moment of inertia. Approximate equations for the I_0 values can be obtained if the isotopic changes in the vibrational contributions are evaluated to first order in the changes in mass, by a method that is essentially equivalent to first-order perturbation theory. It is then possible to estimate the approximate I_e value of a given isotopomer by isotopically substituting in turn each atom of the molecule. Repetition of this procedure for several parent isotopic molecules can allow a solution for an approximate I_e structure, that is the I_m structure[41]. Watson gave the following simple equation to calculate I_G^m:

$$I_G^m = 2I_G^s - I_G^0 \tag{1.3.17}$$

This method cannot be applied strictly to molecules containing very light atoms, particularly hydrogen atoms, and to molecules containing atoms for which isotopic substitution is impossible.

(f) The r_m^ρ structure is a near-equilibrium molecular structure obtained using a modification and simplification of Watson's mass-dependence method and is called the scaled structure. Harmony *et.al.* [21][22] suggested this structure. The method uses a minimal set of ground state isotopic moment of inertia data to evaluate scaled moments of inertia, I_m^ρ, which in turn lead to structures r_m^ρ. I_m^ρ is computed according to the relation[21][22]:

$$[I_m^\rho]_i = (2\rho - 1)[I^0]_i \tag{1.3.18}$$

and

$$\rho = \frac{[I^s]_P}{[I^0]^P} \tag{1.3.19}$$

Here $[I_m^p]_i$ is the scaled moment of inertia of the ith isotopomer, $[I^0]_i$ is the effective moment of inertia of the ith isotopomer, $[I^s]_p$ and $[I^0]_p$ are the substitution and effective moments of inertia, respectively, of the parent isotopomer. If the ith species is the parent species itself, equation(1.4.20) becomes Watson's equation(1.4.19) and the r_m structure is obtained. For molecules containing no hydrogen atoms, this method leads to structures which are close to the r_e structure and more accurate and reliable than r_0 or r_s structures.

1.4 Fermi Resonance

In polyatomic molecules there are many vibrational modes. These vibrational modes, whether fundamentals, overtones or combinations, are perturbed from their harmonic positions by anharmonicity. It may happen that the transition associated with a given vibrational mode (fundamental, overtone or combination) has an energy level with nearly the same energy as a level involved in another transition associated with a different vibrational mode (fundamental, overtone or combination). If the two modes have the same symmetry, there is a perturbation caused by Fermi resonance. This phenomenon was first recognized by Fermi[1] in the case of CO_2. The effects of Fermi resonance are: (I) to push apart the two near degenerate vibrational levels, and (II) to mix the intensities of the two transitions. The result is that the vibrational bands which are involved in the resonance may be quite far removed in the spectrum from their unperturbed positions and that the overtone or combination band may be more intense than usual. The closer the unperturbed levels lie the greater is the resonance. The major contribution to a Fermi resonance arises out of the anharmonic terms of the intramolecular potential[2]. When the resonating levels have very nearly the same energy, the effect of Fermi resonance can be calculated from the standard quantum mechanical techniques of first-order perturbation theory[3][4]. The result is given by the determinant:

$$\begin{bmatrix} E_i^0 - E & \frac{k}{2} \\ \frac{k}{2} & E_j^0 - E \end{bmatrix} = 0 \tag{1.4.1}$$

Here E_i^0 and E_j^0 are the energies of the unperturbed vibrational levels; k is the cubic force constant relating to the two vibrational levels and E^0-E is the energy shift caused by Fermi resonance.

$$E = \frac{E_i^0 + E_j^0}{2} \pm \frac{[k^2 + (E_i^0 - E_j^0)^2]^{\frac{1}{2}}}{2} \tag{1.4.2}$$

$$= \frac{E_i^0 + E_j^0}{2} \pm \frac{(k^2+\delta_0^2)^{\frac{1}{2}}}{2}$$

$$= \frac{E_i^0 + E_j^0}{2} \pm \frac{\delta}{2}$$

$$\delta = (k^2 + \delta_0^2)^{\frac{1}{2}} \tag{1.4.3}$$

δ_0 and δ represent the separations of the energy levels before and after perturbation, respectively. The eigenfunctions(Ψ') of the resulting states are the linear combinations of the unperturbed eigenfunctions(Ψ^0).

$$\Psi_i' = a\Psi_i^0 + b\Psi_j^0 \tag{1.4.4}$$

$$\Psi_j' = a\Psi_j^0 - b\Psi_i^0 \tag{1.4.5}$$

and

$$a = (\frac{\delta + \delta_0}{2\delta})^{\frac{1}{2}} \tag{1.4.6}$$

$$b = (\frac{\delta - \delta_0}{2\delta})^{\frac{1}{2}} \tag{1.4.7}$$

The unperturbed vibrational transition moments are defined by

$$M_i = \langle \Psi_0 | \mu | \Psi^0{}_i \rangle \tag{1.4.8}$$

$$M_j = \langle \Psi_0 | \mu | \Psi^0{}_j \rangle \tag{1.4.9}$$

The perturbed vibrational transition moments are given by

$$M_i' = \langle \Psi_0 | \mu | \Psi_i' \rangle \tag{1.4.10}$$

$$M_j' = \langle \Psi_0 | \mu | \Psi_j' \rangle \tag{1.4.11}$$

The vibrational line strengths are the squares of the vibrational transition moments. Substituting (1.4.8) and (1.4.9) into (1.4.10) and (1.4.11), using (1.4.4) and (1.4.5), we obtain

(1.4.5), we obtain

$$S_i' = \langle \Psi_0 | \mu | \Psi_i' \rangle^2 \qquad (1.4.12)$$
$$= a^2 M_i^2 + b^2 M_j^2 + 2abM_i M_j$$

$$S_j' = \langle \Psi_0 | \mu | \Psi_j' \rangle^2 \qquad (1.4.13)$$
$$= b^2 M_i^2 + a^2 M_j^2 - 2abM_i M_j$$

Equations (1.4.12) and (1.4.13) show that the Fermi resonance perturbation affects the intensities in the two bands. In the case where one component is a fundamental and the other component is an overtone or a combination with negligible unperturbed intensity relative to the unperturbed fundamental, equations (1.4.12) and (1.4.13) can be simplified. The measurements of the observed intensity ratio $\frac{S_i}{S_j}$ can be used to give values of $\frac{a^2}{b^2}$ by assuming that the unperturbed intensity in the overtone or combination band is zero. The wavenumbers of the observed bands can be corrected for the shift caused by Fermi resonance by

$$\nu = \frac{\nu_i' + \nu_j'}{2} \pm \frac{\nu_i' - \nu_j'}{2}\left(\frac{\rho - 1}{\rho + 1}\right) \qquad (1.4.14)$$

Where ν is the unperturbed wavenumber, ν' is the observed wavenumber and ρ is the observed intensity ratio of the two bands[5][6][7]. Then from the observed frequencies and observed intensities the unperturbed vibrational frequency, which is used to calculate the harmonic force field of the molecule, can be calculated by equation(1.4.14).

This method was used to analyze the Fermi resonance between the ν_6 mode and the $\nu_7 + \nu_8$ mode in methyl cyanide by Duncan, *et.al.*[6], and to investigate the Fermi resonance between the fundamental state of the symmetric CH or CD stretching vibration and the overtone or combination levels involving two quanta of CH_3 or CD_3 deformation motion in CH_3X ($X = F, Cl, Br, I, CCH$) by McKean, *et. al.*[5]. Because it is very difficult to get the cubic force constant, the above approximate method was used in this work to correct for the effects of Fermi resonance.

1.5 Molecular Vibrations and the Molecular Harmonic Force Field

The harmonic force constants of a molecule can be related by several methods to the following experimental data[2][9]:

(a) Vibrational frequencies.

(b) Coriolis coupling constants.

(c) Centrifugal distortion constants.

(d) Inertial defects(planar molecules).

(e) Mean-square amplitudes of vibration.

Coriolis coupling constants, centrifugal distortion constants, inertial defects and mean-square amplitudes of vibration can be determined only for relatively small molecules. Therefore vibrational frequencies are by far the most important experimental source of information for determining the molecular force field. The greatest difficulty encountered in this method is that the number of force constants is in general much larger than the number of observed vibrational frequencies and several simplified approaches, such as the methods called the simplified general valence force field(SGVFF)[10][11] and the Urey-Bradley force field(UBFF)[12], are used for larger molecules to obtain simplified force fields. By larger molecules we mean all those molecules for which it is impossible to obtain enough independent experimental data(vibrational frequencies, Coriolis coupling constants, inertial defects, centrifugal distortion constants and mean-square amplitudes of vibration) to define a general harmonic force field. For small molecules the number of available vibrational frequencies, Coriolis coupling constants and centrifugal distortion constants, *etc.*, often for several isotopic species, is usually greater than the number of the force constants. In such cases it is often possible to calculate the complete harmonic force field[13][14][15][16][17].

For a molecule the vibrational kinetic energy T is a function of the nuclear velocities only and the vibrational potential energy V is a function of the displacements of the nuclei from their equilibrium positions. We have:

$$2T = \tilde{\dot{X}}M\dot{X} = \tilde{\dot{D}}\tilde{B}^{-1}MB^{-1}\dot{D} = \tilde{\dot{D}}G^{-1}\dot{D} \tag{1.5.1}$$

Where G is a matrix which is dependent on the geometry and the masses of the various atoms.

$$G = B^{+}M^{-1}B \tag{1.5.2}$$

and

$$G_{ij} = \sum_{k=1}^{3n} \frac{1}{M_k} B_{ik} B_{kj} \tag{1.5.3}$$

M is the inverse mass matrix. The B matrix is the matrix which transforms the Cartesian coordinates(X) to internal coordinates(D).

$$D = BX \tag{1.5.4}$$

$$\begin{aligned} V &= V_0 + \sum_i f_i D_i + \frac{1}{2}\sum_{i,j} f_{ij} D_i D_j + \frac{1}{6}\sum_{i,j,k} f_{ijk} D_i D_j D_k \\ &+ \frac{1}{24}\sum_{i,j,k,l} f_{ijkl} D_i D_j D_k D_l + \ldots \end{aligned} \tag{1.5.5}$$

Where the constants

$$f_i = \left[\frac{\partial V}{\partial D_i}\right]_0 \tag{1.5.6}$$

$$f_{ij} = \left[\frac{\partial^2 V}{\partial D_i \partial D_j}\right]_0 \tag{1.5.7}$$

$$f_{ijk} = \left[\frac{\partial^3 V}{\partial D_i \partial D_j \partial D_k}\right]_0 \tag{1.5.8}$$

$$f_{ijkl} = \left[\frac{\partial^4 V}{\partial D_i \partial D_j \partial D_k \partial D_l}\right]_0 \tag{1.5.9}$$

are linear, quadratic, cubic and quartic, etc., force constants. The zero point of the energy scale can always be chosen so that V_0 is zero. The molecule in its equilibrium configuration must be at a minimum of energy, so that f_i is zero. The number of cubic and quartic force constants is very large and it is impossible to collect enough spectroscopic data for their calculation, except for a very few small molecules.

Fortunately, the contributions of cubic, quartic and higher order force constants to molecular vibrations are much smaller than quadratic force constants and accordingly the contributions of the higher order constants are ignored in the harmonic force field approximation. Then we have:

$$2V = \sum_{i,j}\left(\frac{\partial^2 V}{\partial D_i \partial D_j}\right)_0 D_i D_j \tag{1.5.10}$$

Once the T and V are obtained, is not difficult to write the molecular vibrational Hamiltonian operator

$$H = T + V \tag{1.5.11}$$

By application of the postulates of quantum mechanics, the Hamiltonian has the form:

$$H_v = -\frac{h^2}{8\pi^2}\sum_{i=1}^{3N-6}\left(\frac{\partial^2}{\partial D_i^2} - \frac{4\pi^2\lambda_i}{h^2}D_i^2\right) \tag{1.5.12}$$

E.B.Wilson Jr. *et al.* [2][23] demonstrated the very important relation between the harmonic force field and vibrational frequencies and obtained the following secular equation:

$$| FG - \lambda E | = 0 \tag{1.5.13}$$

or

$$GFL = L\Lambda \tag{1.5.14}$$

Where E is a unity matrix and

$$\lambda = 4\pi^2\nu^2 \tag{1.5.15}$$

$$L\tilde{L} = G \tag{1.5.16}$$

The F matrix can be obtained from the molecular geometry and vibrational frequencies by using equation(1.5.13). Usually, the symmetry of molecules can be used to simplify the calculation. In Cartesian coordinates F_X is a $3n \times 3n$ matrix, in internal coordinates, F_D is a $(3n-6)\times(3n-6)$ matrix, while in symmetry coordinates and F_S is a $(3n-6)\times(3n-6)$ diagonal blocked matrix. The relations between these F matrices are

$$F_D = BF_X B^+ \tag{1.5.17}$$

and

$$F_S = UF_DU^+ \qquad (1.5.18)$$

It is not difficult to develop the unitary transformation matrix, U, from the group theory, if the molecular structure is known[2][24].

In principle it is no problem to express the force constants as explicit functions of the λ's, which are related to the vibrational frequencies, and of the elements of G, which is related to the molecular geometry and the atomic masses, by expansion of the secular equation(1.5.15). In practice, however, this method is applicable only for very small molecules. A much more powerful and convenient method is that a trial set of force constants is refined to fit the experimental vibrational frequencies and other additional data, such as Coriolis constants, centrifugal distortion constants and so on[53][54][55]. In this method, an initial trial force constant-matrix, F_0, is supposed and is used to compute the eigenvalues λ_0 and eigenvectors L_0. Then the first perturbation theory can be used to refine the elements of F_0 so that the difference between observed and calculated frequencies, $\lambda - \lambda_0$, is minimized. The most elegant way to refine the experimental data is to generate the required Jacobian matrix J [53][54][55]

$$J\Delta F = \Delta\lambda \qquad (1.5.19)$$

and the matrix elements of Jacobian matrix are

$$\frac{\partial\lambda_l}{\partial F_{kk}} = (L_0)_{kl}(L_0)_{kl} \qquad (1.5.20)$$

$$\frac{\partial\lambda_l}{\partial F_{kl}} = (L_0)_{kl}(L_0)_{ll} \qquad (1.5.21)$$

By letting $\Delta F \rightarrow 0$ and $\Delta\lambda \rightarrow 0$ these matrix elements can be obtained. The perturbation procedure must be repeated several times using new trial force constant-matrices and new eigenvectors each time until the difference between observed and calculated frequencies is below a given limit.

1.6 Centrifugal Distortion and Molecular Harmonic Force Field

One fundamental problem in the study of the molecular vibration-rotation spectra of polyatomic molecules is the determination of the normal modes and the potential constants of vibration. Once these normal modes are known, other parameters, such as centrifugal distortion constants and Coriolis coupling constants, which depend on the normal modes, may be calculated. Conversely, if centrifugal distortion constants or Coriolis coupling constants can be obtained from experiment these constants provide additional data for the determinations of the normal coordinates and the harmonic force field[42][43]. A convenient treatment of centrifugal distortion and general relations between centrifugal distortion coefficients and potential constants in asymmetric polyatomic molecules has been given by Wilson and his coworkers[42][44]. The Hamiltonian for the rotational energy of a molecule in the semi-rigid rotor approximation can be written in the form:

$$H = \frac{1}{2}\sum_{\alpha,\beta}\mu^{e}_{\alpha\beta}P_{\alpha}P_{\beta} + \frac{1}{4}\sum_{\alpha,\beta,\gamma,\delta}\tau_{\alpha\beta\gamma\delta}P_{\alpha}P_{\beta}P_{\gamma}P_{\delta} \tag{1.6.1}$$

Here the τ's, the quartic distortion constants, are related to the elements of the inverse harmonic force constants matrix and are given by the expression

$$\begin{aligned} \tau_{\alpha\beta\gamma\delta} &= -\frac{1}{2}\sum_{ij}\mu^{(i)}{}_{\alpha\beta}(f^{-1})_{ij}\mu^{(j)}{}_{\gamma\delta} \\ &= \frac{-1}{2I^{e}_{\alpha\alpha}I^{e}_{\beta\beta}I^{e}_{\gamma\gamma}I^{e}_{\delta\delta}}\sum_{ij}[J^{(i)}_{\alpha\beta}]_e(f^{-1})_{ij}[J^{(j)}_{\gamma\delta}]_e \end{aligned} \tag{1.6.2}$$

Here the I^e's are the equilibrium principal moments of inertia, α,β,γ and δ are the inertial axes, and the $J^{(i)}$'s are the partial derivatives of the components of the inertia tensor with respect to the ith internal coordinate D_i [42]

$$\begin{aligned} \mu^{(i)}{}_{\alpha\beta} &= \left(\frac{\partial\mu_{\alpha\beta}}{\partial D_i}\right)_e \\ &= \frac{-[J^{(i)}{}_{\alpha\beta}]_e}{I^{e}{}_{\alpha\alpha}I^{e}{}_{\beta\beta}} \\ &= \frac{-1}{I^{e}{}_{\alpha\alpha}I^{e}{}_{\beta\beta}}\left(\frac{\partial I_{\alpha\beta}}{\partial D_i}\right) \end{aligned} \tag{1.6.3}$$

and

$$[J_{\alpha\alpha}^{(i)}]_e = \frac{2}{\delta D_i}\sum_j m_j(\beta_j\delta\beta_j + \gamma_j\delta\gamma_j) \tag{1.6.4}$$

$$[J_{\alpha\beta}^{(i)}]_e' = \frac{-2}{\delta D_i I_{\gamma\gamma}}[I_\alpha\sum_j m_j\beta_j\delta\alpha_j + I_\beta\sum_j m_j\alpha_j\delta\beta_j] \tag{1.6.5}$$

Watson derived the relations between the τ's and the experimental distortion constants(Δ_J, Δ_{JK}, Δ_K, δ_J and δ_K [45][46][47]). He expressed the experimental centrifugal distortion constants as linear combinations of the τ's, as given in Table-1.2.

Table-1.2

Relationships Between Centrifugal Distortion Constants

$$\begin{aligned}
T_{xx} &= -D_J + 2d_1 + 2d_2 \\
T_{yy} &= -D_J - 2d_1 + 2d_2 \\
T_{zz} &= -D_J - D_{JK} - D_K \\
T_1 &= -3D_J - D_{JK} - 6d_2 \\
T_2 &= -(B_x + B_y + B_z)D_J - \frac{1}{2}(B_x + B_y)D_{JK} \\
&\quad - (B_x - B_y)d_1 - 6B_z d_2 \\
T_{\alpha\alpha} &= \frac{1}{4}\tau_{\alpha\alpha\alpha\alpha} \\
T_{\alpha\beta} &= \frac{1}{4}\tau_{\alpha\alpha\beta\beta} \\
T_1 &= T_{yz} + T_{xz} + T_{xy} \\
T_2 &= B_x T_{yz} + B_y T_{xz} + B_z T_{xy}
\end{aligned}$$

Here A, B and C are the corrected rotational constants. No more than five linear combinations of τ's can be obtained from the spectra of an asymmetric top molecule.

For simple molecules the centrifugal distortion constants can be used to calculate completely the harmonic force field. One example is the C_{2v} triatomic molecule SCl_2 studied by Davis and Gerry[13]. For larger molecules the distortion constants provide additional data to employ in force field calculations. A combination of vibrational frequencies and distortion constants is now commonly used to derive the harmonic force field of small molecules[48]. As we discussed in (1.5), a set of initially estimated force constants is used to begin the calculation process and to refine the experimental distortion constants. The Jacobians now are

$$\frac{\partial \tau_{\alpha\beta\gamma\delta}}{\partial F_{rt}} = \frac{1}{2I^0_{\alpha\alpha}I^0_{\beta\beta}I^0_{\gamma\gamma}I^0_{\delta\delta}} \sum_{kl} J^k_{\alpha\beta} J^l_{\gamma\delta} \left[(F_0^{-1})_{kr} (F_0^{-1})_{tl} + (F_0^{-1})_{kt} (F_0^{-1})_{rl} \right] \tag{1.6.6}$$

and

$$\frac{\partial \tau_{\alpha\beta\gamma\delta}}{\partial F_{rr}} = \frac{1}{2I^0_{\alpha\alpha}I^0_{\beta\beta}I^0_{\gamma\gamma}I^0_{\delta\delta}} \sum_{kl} J^k_{\alpha\beta} J^l_{\gamma\delta} \left[(F_0^{-1})_{kr} (F_0^{-1})_{rl} \right] \tag{1.6.7}$$

1.7 Coriolis Interactions and the Molecular Harmonic Force Field

The angular momentum of molecular vibrations can interact with the angular momentum of molecular rotation so as to affect the rotational energy levels of the molecule. This kind of interaction is called the Coriolis interaction, which was first reported by Teller[52]. The study of Coriolis interactions furnishes another type of information useful for the refinement of molecular harmonic force fields. Coriolis interactions can be derived from vibrational or rotational spectra. If a nucleus in a molecule is moving linearly in a vibrational motion, and the molecule is also rotating then the nucleus experiences a Coriolis force f_c given by[49]:

$$f_c = 2mV_a\omega\sin\Phi = 2m\vec{V}_a\times\vec{\omega} \tag{1.7.1}$$

Here

m-the mass of nucleus.

$\vec{V}_a$-the apparent velocity with respect to the coordinate system attached to the rotating molecule.

$\vec{\omega}$-the anglar velocity of rotation referred to a molecule fixed coordinate system.

Φ-the angle between the axis of rotation and the direction of motion with velocity $\vec{V}_a$.

The Coriolis interaction perturbs the rotational energy levels and transitions. For linear polyatomic molecules and symmetric top molecules, where there are degenerate vibrational states, there are very strong Coriolis interactions (the first-order Coriolis interaction). For asymmetric top molecules, vibration-rotation coupling through the Coriolis interaction can be large if two vibrational frequencies are very close to each other and the direct product of the symmetry species of the two vibrational states contains a rotational symmetry species[2][3][94].

$$\Gamma(\Psi_v^{'}) \times \Gamma(\Psi_v^{''}) \supset \Gamma(T_x)\ and/or\ \Gamma(T_y)\ and/or\ \Gamma(T_z) \tag{1.7.2}$$

Here $\Gamma(\Psi_v)$ and $\Gamma(T)$ are the group representations of the vibrational and rotational symmetry species, respectively. This kind of interaction is called the second-order Coriolis interaction.

The relationships between the Coriolis coupling constants and their dependence on the potential constants have been developed by Meal and Polo[50][51].

$$\tilde{L}FC^{\sigma}\tilde{L}^{-1} = \Lambda\zeta^{\sigma} \quad (1.7.3)$$

$$\tilde{L}G^{-1}C^{\sigma}\tilde{L}^{-1} = \zeta^{\sigma} \quad (1.7.4)$$

Here F and G are the F matrix and the G matrix, respectively, and L is the matrix which transforms the internal coordinates(D) to symmetry coordinates(S).

$$S = LD \quad (1.7.5)$$

The C^{σ} matrix is defined by

$$C^{\sigma} = BM^{-1/2}\mu^{\sigma}\tilde{B}\tilde{M}^{-1/2} \quad (1.7.6)$$

Here the μ^{σ} are matrices of dimension $3N\times3N$ formed by N identical 3×3 blocks along the diagonal. The blocks, usually denoted by the symbol $(\mu^{\sigma})_{\alpha}$, to specify that each block refers to a given atom α, have the form

$$(\mu^{x})_{\alpha} = \begin{bmatrix} 0 & 0 & 0 \\ 0 & 0 & 1 \\ 0 & -1 & 0 \end{bmatrix} \quad (1.7.7)$$

$$(\mu^{y})_{\alpha} = \begin{bmatrix} 0 & 0 & -1 \\ 0 & 0 & 0 \\ 1 & 0 & 0 \end{bmatrix} \quad (1.7.8)$$

$$(\mu^{z})_{\alpha} = \begin{bmatrix} 0 & 1 & 0 \\ -1 & 0 & 0 \\ 0 & 0 & 0 \end{bmatrix} \quad (1.7.9)$$

From equation(1.7.4), the Coriolis constants ζ^{σ} can be derived from the molecular geometry and atomic masses. Then the calculation of force constants can be accomplished using equation(1.7.3). As discussed before, the Coriolis constants, together with other experimental data(vibrational frequencies and distortion constants, *etc*, are used to refine the force field of the molecule [54][55]. The elements of the Jacobian matrix required for this procedure are

$$\frac{\partial \zeta_{ij}^{\sigma}}{\partial F_{kl}} = \sum_{t \neq i} (\zeta_0^{\sigma})_{jt} \frac{(L_{ki} L_{lt} + L_{li} L_{kt})}{(\lambda_t - \lambda_i)} + \sum_{t \neq j} (\zeta_0^{\sigma})_{it} \frac{(L_{kj} L_{lt} + L_{lj} L_{kt})}{(\lambda_j - \lambda_t)} \tag{1.7.10}$$

$$\frac{\partial \zeta_{ij}^{\sigma}}{\partial F_{kk}} = \sum_{t \neq i} (\zeta_0^{\sigma})_{jt} \frac{L_{ki} L_{kt}}{(\lambda_t - \lambda_i)} + \sum_{t \neq j} (\zeta_0^{\sigma})_{it} \frac{L_{kj} L_{kt}}{(\lambda_j - \lambda_t)} \tag{1.7.11}$$

1.8 The Symmetry Mode Analysis of

Cl_2SO_2, F_2SO_2 and $(CH_3)_2SO_2$

All of the three sulphuryl molecules studied in this work belong to the C_{2v} symmetry point group, and the structure of the representation generated by their vibrational modes is

$$\Gamma_V = 4a_1 + a_2 + 2b_1 + 2b_2 \tag{1.8.1}$$

where the CH_3 group is considered as one atom. The symmetry coordinates of this class of molecules were given by Suthers and Henshall[81] as shown in Table-1.3.

There is a relationship between the three angles in the X_2SO_2 type molecule

$$4cos\frac{\Theta}{2}\cos\frac{\Phi}{2} + \sum_{i=1}^{i=4}\cos\alpha_i = 0 \tag{1.8.2}$$

Partial differentiation of equation(1.8.2) with respect to each angular coordinates derives the redundant symmetry coordinate:

$$(cos\frac{\Phi}{2}\sin\frac{\Theta}{2})\Delta\Theta + (cos\frac{\Theta}{2}\sin\frac{\Phi}{2})\Delta\Phi + \frac{1}{2}\sin\alpha\sum_{i=1}^{i=4}\Delta\alpha_i \tag{1.8.3}$$

$$= \frac{(a\,\Delta\Theta + b\,\Delta\Phi + c\,\Delta\alpha_1 + c\,\Delta\alpha_2 + c\,\Delta\alpha_3 + c\,\Delta\alpha_4)}{(a^2 + b^2 + 4c^2)^{-1/2}} = 0$$

The coefficients, a, b, c, and so on, can be evaluated from the experimental effective angular parameters, Θ, Φ and α, for each molecule , which will be discussed in sections 3.3, 4.3 and 5.3, together with the normalization and orthogonality relations, equation-1.8.4 to 1.8.6.

$$ae - 4c = 0 \tag{1.8.4}$$

$$af + bg - 4c = 0 \tag{1.8.5}$$

$$a^2 + b^2 + 4c^2 = 1 \tag{1.8.6}$$

Then we can obtain the S_3 and S_4 coordinates for each molecule according to its geometry.

Table-1.3 Symmetry Coordinates of the Sulphuryls

Species	Coordinate	Mode
a_1	$S_1 = \frac{(\Delta R_1 + \Delta R_2)}{2^{1/2}}$	$SO_{sym\text{-}stre.}$
	$S_2 = \frac{(\Delta d_1 + \Delta d_2)}{2^{1/2}}$	$SX_{sym\text{-}stre.}$
	$S_3 = \frac{(e\,\Delta\Theta - \Delta\alpha_1 - \Delta\alpha_2 - \Delta\alpha_3 - \Delta\alpha_4)}{(e^2 + 4)^{1/2}}$	OSO_{bend}
	$S_4 = \frac{(f\,\Delta\Theta + g\,\Delta\Phi - \Delta\alpha_1 - \Delta\alpha_2 - \Delta\alpha_3 - \Delta\alpha_4)}{(f^2 + g^2 + 4)^{1/2}}$	XSX_{bend}
a_2	$S_5 = \frac{(\Delta\alpha_1 - \Delta\alpha_2 - \Delta\alpha_3 + \Delta\alpha_4)}{2^{1/2}}$	*Torsion*
b_1	$S_6 = \frac{(\Delta R_1 - \Delta R_2)}{2^{1/2}}$	$SO_{asy\text{-}stre.}$
	$S_7 = \frac{(\Delta\alpha_1 + \Delta\alpha_2 - \Delta\alpha_3 - \Delta\alpha_4)}{2}$	$SO_{2,rock}$
b_2	$S_8 = \frac{(\Delta d_1 - \Delta d_2)}{2^{1/2}}$	$SX_{asy\text{-}stre.}$
	$S_9 = \frac{(\Delta\alpha_1 - \Delta\alpha_2 + \Delta\alpha_3 - \Delta\alpha_4)}{2}$	$SO_{2,wag}$

Table-1.4 Coefficients of Symmetry Coordinates of Sulphuryls

Molecules	e	f	g
Cl_2SO_2	3.3720	-1.1862	7.0631
F_2SO_2	3.1863	-1.2554	7.7516

The Coefficients are derived from the molecular geometries of Cl_2SO_2 and F_2SO_2 obtained in Chapter-3 and Chapter-4, respectively. The coordinate parameters are shown in Figure-1.1 and $X = F, Cl$ or CH_3. All of the modes are both infrared and Raman active, except for the a_2 mode, which is only Raman active.

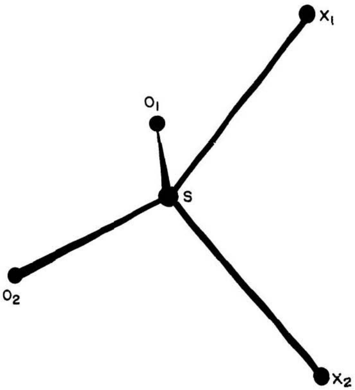

Figure-1.1 The Internal Coordinates of Molecules of Type X_2SO_2.

$R_1 = SO_1$	$\alpha_1 = \langle O_1SX_1$
$R_2 = SO_2$	$\alpha_2 = \langle O_1SX_2$
$d_1 = SX_1$	$\alpha_3 = \langle O_2SX_1$
$d_2 = SX_2$	$\alpha_4 = \langle O_2SX_2$
$\Theta = \langle OSO$	$\Phi = \langle XSX$

1.9 Nuclear Quadrupole Coupling

Nuclear quadrupole effects in molecules were first observed almost fifty years ago by Kellogg *et al.* [142] Since then, quadrupole interactions have been observed as hyperfine structure in the rotational spectra of many molecules. For a quadrupole interaction, it is necessary that the nucleus possesses a nonvanishing nuclear quadrupole moment which results from a nonspherical charge distribution in the nucleus. Such a distribution is found in nuclei with a spin angular momentum greater than $\frac{1}{2}(\frac{h}{2\pi})$.

The most important parameter obtained in a nuclear quadrupole analysis is the electric field gradient, which provides valuable information concerning the electronic environment of the quadrupolar nucleus. The vector model for the quadrupole interaction in the absence of an external field shows that the nuclear spin angular momentum $\vec{I}$ couples with the rotational angular momentum $\vec{J}$ to produce a total angular momentum $\vec{F}$:

$$\vec{F} = \vec{I} + \vec{J} \tag{1.9.1}$$

I and J remain as good quantum numbers whose vector sum is also quantized. However, M_I and M_J, which are the projection quantum numbers of I and J in the uncoupled representation, are no longer constants of the motion. F ranges from $J + I$ to $|J - I|$:

$$F = J + I, J + I - 1, J + I - 2, ..., |J - I|. \tag{1.9.2}$$

The effects of a quadrupole interaction is to split a rotational level into $2I + 1$ levels and a single rotational spectrum into complicated hyperfine structure. The selection rules governing transitions between these energy levels are:

$$\Delta I = 0 \qquad \Delta J = 0, \pm 1 \qquad \Delta F = 0, \pm 1 \tag{1.9.3}$$

The Hamiltonian of Casimir[9] which describes the quadrupole coupling of nuclei in a molecule is of the form:

$$H_Q = \sum_i eQ_i \langle(\frac{\partial^2 V}{\partial Z^2})\rangle_{av.} \left[\frac{3(\vec{J}\cdot\vec{I}_i)^2 + \frac{3}{2}(\vec{J}\cdot\vec{I}_i) - \vec{J}^2\vec{I}_i^2}{2J\,(2J-1)\,I_i\,(2I_i-1)}\right] \tag{1.9.4}$$

Where the quantity Q_i represents the electric quadrupole moment of the ith nucleus, and e the electric charge.

$$\begin{aligned} q_J &= \langle\frac{\partial^2 V}{\partial Z^2})\rangle_{av.} \\ &= \langle M_J = J\,|(\frac{\partial^2 V}{\partial Z^2})|M_J = J\rangle_{av.} \end{aligned} \tag{1.9.5}$$

Here V is the electric field at the quadrupolar nucleus. q_J is the electric field gradient along the space-fixed Z axis averaged over the state $M_J = J$. q_J is the only term in H_Q which changes when an atom combines with other atoms to form a molecule. The characteristic energy values for quadrupole coupling of a single nucleus with spin I and quadrupole moment Q can be written as:

$$E_Q = eQq_J \left[\frac{\frac{3}{4}C\,(C+1) - I\,(I+1)\,J\,(J+1)}{2J\,(2J-1)\,I\,(2I-1)}\right] \tag{1.9.6}$$

where

$$C = F\,(F+1) - I\,(I+1) - J\,(J+1) \tag{1.9.7}$$

For an asymmetric top one can write

$$eQq_J = \frac{2J}{(J+1)(2J+3)} \sum_{g=a,b,c} \chi_{gg} \langle P_g^2\rangle \tag{1.9.8}$$

Where χ_{gg} is called a nuclear coupling constant. Laplace's equation leads to a boundary condition on the nuclear coupling constants

$$\chi_{aa} + \chi_{bb} + \chi_{cc} = 0 \tag{1.9.9}$$

and there are only two independent χ_{gg}'s. Usually the two independent constants are selected as one χ_{gg} and the nuclear quadrupole coupling asymmetry parameter η. For a prolate asymmetric top we have

$$\eta = \frac{(\chi_{bb} - \chi_{cc})}{\chi_{aa}} \tag{1.9.10}$$

Those two constants can be determined from a first order analysis of of nuclear quadrupole hyperfine structure. The first order quadrupole energy has been worked out by Bragg [143]:

$$E_Q = \frac{f(I,J,F)}{J(J+1)}\left[3\langle P_a^2\rangle - J(J+1) + \frac{\eta\langle P_a^2\rangle - \eta W_{J_\tau}(b_p)}{b_p}\right]\chi_{aa} \tag{1.9.11}$$

Where $f(I,J,F)$ is Casimir function

$$f(I,J,F) = \frac{\frac{3}{4}C(C+1) - I(I+1)J(J+1)}{2I(2I-1)(2J-1)(2J+3)} \tag{1.9.12}$$

and W_{J_τ} is Wang's reduced energy[9].

When there is more than one quadrupolar nucleus in a molecule, there exists the possibility of coupling between the individual quadrupole moments by way of molecular rotation. The resulting hyperfine structure can become very complicated. Methods used to treat this problem depend on the relative degrees of coupling of the two nuclei. There are two cases. (1) One of the nuclei couples much more strongly than the other. In this instance, the major contribution to the hyperfine splitting is made by the nuclei which is strongly coupled. The weakly coupled nucleus can be treated as a perturbation on the splittings of the other nucleus. (2) The degrees of coupling of the two nuclei are of the same order of magnitude. This is the case we have to treat in Cl_2SO_2 which has two identical chlorine nuclei with nuclear spin $\frac{3}{2}$. There are two possible coupling schemes if a molecule possesses two quadrupolar nuclei having nuclear spin angular momenta of $\vec{I}_1$ and $\vec{I}_2$, respectively. First, we have

$$\begin{aligned} \vec{J} + \vec{I}_1 &= \vec{F}_1 \\ \vec{F}_1 + \vec{I}_2 &= \vec{F} \end{aligned} \tag{1.9.13}$$

Here $\vec{J}$ is the rotational angular momentum and $\vec{F}$ is the total angular momentum. F_1 and F have the values $J + I_1$ to $|J - I_1|$ and $F_1 + I_2$ to $|F_1 - I_2|$, respectively. Second, we can have

$$\begin{aligned} \vec{I}_1 + \vec{I}_2 &= \vec{I} \\ \vec{I} + \vec{J} &= \vec{F} \end{aligned} \tag{1.9.14}$$

Here $\vec{I}$ is the total nuclear spin angular momentum and I can have the values $I_1 + I_2$ to $|I_1 - I_2|$. F has the values $J + I$ to $|J - I|$. The second scheme was used in our calculation. In an uncoupled representation, the total Hamiltonian is just the sum of two individual quadrupole terms given as

$$\begin{aligned} H_Q(\vec{I}_1\vec{I}_2) &= H_Q(\vec{I}_1,\vec{J}) + H_Q(\vec{I}_2,\vec{J}) \\ &= \frac{(eQq_J)_1}{2J(2J-1)I_1(2I_1-1)}[3(\vec{I}_1\cdot\vec{J})_2 + \frac{3}{2}\vec{I}_1\cdot\vec{J} - I_1^2J^2] \\ &+ \frac{(eQq_J)_2}{2J(2J-1)I_2(2I_2-1)}[3(\vec{I}_2\cdot\vec{J})_2 + \frac{3}{2}\vec{I}_2\cdot\vec{J} - I_2^2J^2] \end{aligned} \tag{1.9.15}$$

The required matrix elements of the Hamiltonian, $\langle H_{Q_T}\rangle$, have been worked out by Robinson and Cornwell[144], and by Flygare and Gwinn[145] in their study of CH_2Cl_2 and $COCl_2$. To first-order, the matrix of H_Q is diagonal in the $|I_1I_2JF\rangle$ basis. When $I_1 = I_2$, the matrix may be written as

$$\langle I|H_Q|I\rangle = \frac{\frac{3X^+}{16}[\Phi^2(I)+\Psi(I)+\Psi(I+1)+2\Phi(I)]-X^+I_1(I_1+1)J(J+1)}{J(2J-1)I_1(2I_1-1)} \tag{1.9.16}$$

$$\langle I|H_Q|I+1\rangle = \frac{3X^+R\Psi^{\frac{1}{2}}(I+1)[\Phi(I)-I]}{8J(2J-1)I_1(2I_1-1)} \tag{1.9.17}$$

$$\langle I|H_Q|I+2\rangle = \frac{3X^+\Psi^{\frac{1}{2}}(I+1)\Psi^{\frac{1}{2}}(I+2)}{16J(2J-1)I_1(2I_1-1)} \tag{1.9.18}$$

Where

$$X_\pm = \frac{1}{2}[(eQq_J)_1 \pm (eQq_J)_2] \tag{1.9.19}$$

$$R = \frac{X^-}{X^+} \tag{1.9.20}$$

$$\Phi(I) = F(F+1) - J(J+1) - I(I+1) \tag{1.9.21}$$

$$\Psi(I) = \frac{[(2I_1+1)^2 - I^2](F+I-J)(F+J-I+1)(F+I+J+1)(I+J-F)}{4I^2 - 1} \tag{1.9.22}$$

The other nonvanishing matrix elements, such as $\langle I+1|H_Q|I\rangle$, $\langle I|H_Q|I-1\rangle$, and so on, may be obtained from the above elements since the matrix is symmetric.

1.10 The Asymmetric Rotor Stark Effect

When an external electric field, $\vec{E}$, is applied to a polar molecule, it interacts with the electric dipole, $\vec{\mu}$, of the molecule, causing a splitting of the rotational energy levels, which results in the appearance of hyperfine structure in the rotational spectrum. This is known as the Stark effect. The Stark Hamiltonian is given by

$$H_{stark} = -\vec{\mu}\bullet\vec{E} \tag{1.10.1}$$

$$= -E \sum_{g=a,b,c} \Phi_{Zg}\mu_g$$

where Φ_{Zg} is the direction cosine between the space-fixed Z-axis and the molecule-fixed g-axis. In symmetric tops, the dipole moment is necessarily directed along the symmetry axis, and hence it has a component along $\vec{J}$, except when $K = 0$. Generally speaking, if the dipole moment $\vec{\mu}$ has a component along the direction of $\vec{J}$, the splitting of the rotational levels by an electric field is directly proportional to the field intensity E, i.e. a first-order Stark effect; if the dipole moment is perpendicular to $\vec{J}$, the splitting depends on the square of E, giving what is known as a second-order Stark effect. Asymmetric top levels do not show K-type degeneracy, and therefore tend to show second-order Stark effects unless a rotational level is accidentally close to another level, or if the asymmetry parameter is very small. Golden and Wilson have calculated the Stark effect of asymmetric rotors by second-order perturbation theory[156]. For cases where the Stark splitting is small compared with the separations of the unpertubed energy level (non-degenerate case) they derived the expression

$$[E_g^{(2)}]_{J,\tau,M_J} = \frac{2\mu_g^2E^2}{(A+C)\,h}[A_J(\kappa,\alpha) + M_J^2B_J(\kappa,\alpha)] \tag{1.10.2}$$

Here μ_g is the component of the dipole moment along the gth principal axis of the molecule, $[E_g^{(2)}]_{J,\tau,M_J}$ is the corresponding second-order energy shift for the M_J component of the J_τ energy level, κ is the asymmetry parameter of the molecule, and $\alpha=(A-C)/(A+C)$. They showed that Eq.-1.10.2 could be put in a form utilizing Cross, Hainer and King's tabulated line strengths[155], $\lambda(J,\tau;J',\tau')$, between levels whose unperturbed energy differences are $E_{J,\tau}^{(0)}$ and $E_{J',\tau'}^{(0)}$, where $J' = J-1, J$, or $J+1$. The resulting relation is

$$[E_q^{(2)}]_{J,\tau,M_J} = \mu_q^2 E^2 \Big[\frac{J^2 - M_J^2}{J(2J-1)(2J+1)} \sum_{\tau'}{}' \frac{\lambda(J,\tau;J-1,\tau')}{E_{J,\tau}^{(0)} - E_{J-1,\tau'}^{(0)}} \tag{1.10.3}$$

$$+ \frac{M_J^2}{J(J+1)(2J+1)} \sum_{\tau'\neq\tau}{}' \frac{\lambda(J,\tau;J,\tau')}{E_{J,\tau}^{(0)} - E_{J+1,\tau'}^{(0)}}$$

$$+ \frac{(J+1)^2 - M_J^2}{(J+1)(2J+1)(2J+3)} \sum_{\tau'}{}' \frac{\lambda(J,\tau;J+1,\tau')}{E_{J,\tau}^{(0)} - E_{J+1,\tau'}^{(0)}} \Big]$$

The line strengths can also be estimated using the eigenvectors of the asymmetric rotor Hamiltonian and the relation

$$\lambda_q(J,\tau;J',\tau') = \sum_{Z,M,M'} |\langle J,\tau,M|\Phi_{Z_q}|J',\tau',M'\rangle|^2 \tag{1.10.4}$$

If there are near degenerate rotational levels or if a transition exhibits nuclear quadrupole hyperfine structure, more complicated treatments are required. These have been discussed in Gordy and Cook's book.[9]

A valuable use of the Stark effect for asymmetric tops lies in the identification of J values of transitions from the number and relative intensities of the Stark components. Two kinds of transition can be defined, those in which $\Delta J = \pm 1$, in which the relative intensities of the components are $(J+1)^2-M^2$ and J^2-M^2 for the upper and lower signs, respectively, and those in which $\Delta J=0$, in which the relative intensities can be shown to be proportional to M^2. If J changes in a transition, there will be $J+1$ Stark components, where J refers to the quantum number of the lower level; these will show a crowding towards the low M values, which are also the most intense. In Q type transitions, where $\Delta J=0$, there are J Stark components, ($M=0$ is missing), and the intensities become greater for larger M, as do the displacements from the zero-field line. Another value of the molecular Stark effect in chemistry is that it allows the measurement of dipole moments. Generally, the dipole moment of an asymmetric rotor does not lie along one of the principal inertial axes of the molecule; therefore the Stark interactions are rather complicated. The analysis of more than one transitions is then necessary, which yields the components of the dipole moment along the principal axes, and from these the total moment can be computed. If the dipole moment of an asymmetric top is directed along a principal axis, such as occurs in Cl_2SO_2, the experiment and calculation are much simpler. In this case, the dipole moment can be determined by measuring Stark shifts for just one Stark component.

CHAPTER 2

EXPERIMENTAL DETAILS

2.1 The Microwave Spectrometer

A conventional microwave spectrometer essentially consists of a tunable source of microwave radiation, an absorption cell containing the gas under investigation, a frequency measurement device and a detector. The system used in this research has been described in a previous report from our laboratory[113].

The spectrometer used for all of the experiments discussed here was a 33kHz Stark modulated instrument. The microwave radiation source was a Hewlett-Packard Model 8341A synthesized sweeper, which generated output frequencies from 10MHz to 20GHz. The working frequencies were produced by using Honeywell Spacekom passive frequency multipliers. Model K2200N, TQ-1 and V2400N frequency multipliers were used to double, triple and quardruple or sextuple the output frequencies generated by the 8341A synthesized sweeper. Therefore, the frequency range from 6000MHz to 120000MHz was available in this work; however, the power available at frequencies higher than 80000MHz was very little and only a few very strong lines were observed in this frequency range. Frequency resolution from 1Hz at 10MHz to 3Hz at 20GHz was available using the microwave synthesizer. The positions of molecular absorption lines could not be measured to better than 20kHz, however, due to the finite linewidth of these lines.

Stark cells of the type used in this research have been described in many previous reports[114][115][116]. Two different Stark cells were used in this study, both of which were 10 feet in length. The first was an X-band cell having cross sectional dimensions of $1.0\times2.2cm$ and the second was a S-band cell with dimensions of $7.2\times3.4cm$. The smaller cell was set in an insulated box of 7 feet in length, which was used to keep dry ice for cooling the cell. Each cell contained a thin copper plate, Stark electrode, parallel to the face of the waveguide and so perpendicular to the microwave electric field. The electrode was held at the center of the cell and isolated from the brass cell by thin teflon. A 33333*Hz* high voltage square wave generator, made in the workshops of Monash University's Chemistry Department, was used to produce the Stark electric field. The output voltage of this generator was 0-3000 volts. The Stark cells were connected to a glass vacuum system and the pressures, measured with a SV-1 Hastings vacuum gauge and a DV-3M vacuum gauge tube, could be pumped to lower than 5microns by a mechanical pump. The samples investigated could be either sealed in the Stark cells or flowed continuously through the cells.

The detector used at frequencies lower than 20000*MHz* was a Hewlett Model X-281A back diode, at frequencies between 20000*MHz* and 40000*MHz* was a Pacific Millimeter Products(PMP) Model 4-42-720-Q2 diode, at frequencies between 40000*MHz* and 60000*MHz* was a PMP MOD-UD diode, while at frequencies higher than 60000*MHz* was a PMP DXP-15 diode.

The microwave synthesizer was controlled by a Hewlett Packard Model 9816S computer, which was also used to process the output data from an EG & G Model 5207 digital lock-in amplifier to obtain accurate line frequencies. In the measurement, bidirectional digitally stepped sweeps were performed. The procedure suggested by Biermann *et al.* [117] was used to smooth the raw output data at first, and then, for symmetric lines, a least squares fit was performed to the smoothed lines, which were assumed to have a Lorentzian line shape, to obtain accurate line frequencies and line widths. The measurement accuracy was 0.02 *MHz* or better for strong lines and 0.05*MHz* or better for weak lines.

2.2 Samples

(i) Cl_2SO_2

Normal Cl_2SO_2 (97%) was obtained from Fisher. The spectra of $^{35}Cl^{37}Cl^{32}S^{16}O_2$, $^{37}Cl_2^{32}S^{16}O_2$, $^{35}Cl_2^{34}S^{16}O_2$ and $^{35}Cl^{37}Cl^{34}S^{16}O_2$ were measured in natural abundance.

$^{35}Cl_2^{32}S^{18}O_2$ and $^{35}Cl_2^{34}S^{18}O_2$ were prepared from sulfur dioxide ($^{32}S^{18}O_2$ and $^{34}S^{18}O_2$, respectively) by using chlorine as the chlorinating agent. $^{34}S^{18}O_2$ was synthesized from ^{34}S enriched sulphur (92.1 atom % of ^{34}S, MSD) and $^{18}O_2$ (99.45 atom % of ^{18}O,BOC).[108] Abc .. 0.05g ^{34}S was introduced into a 150ml bulb; after the air was pumped out an excess of $^{18}O_2$, about 50ml of gas, was introduced; then the bulb was sealed up and heated to about 260°C. The reaction was improved by the help of the discharge of a Tesla coil which produced ozone traces. After the reaction the gas was transferred into another bulb at liquid nitrogen temperature. After the freezing of $^{34}S^{18}O_2$, the remains of oxygen was pumped out and about 50ml of chlorine gas (Canlab) was introduced. The reaction between sulfur dioxide and chlorine proceeded under a UV lamp at room temperature for about two hours. Then the bulb was cooled by dry ice to condense the $^{35}Cl_2^{34}S^{18}O_2$ and the remains of sulfur dioxide and chlorine were pumped out; then $^{35}Cl_2^{34}S^{18}O_2$ was obtained as a colourless liquid.

$$Cl_2 + {}^{34}S^{18}O_2 + h\nu \rightarrow Cl_2^{34}S^{18}O_2 \qquad (2.2.1)$$

$^{35}Cl_2^{32}S^{18}O_2$ was obtained from $^{18}O_2$ and an excess of ^{32}S using the same method as outlined above. ^{32}S was obtained from MCB.

The spectra of $^{35}Cl^{37}Cl^{32}S^{18}O_2$ and $^{35}Cl^{37}Cl^{34}S^{18}O_2$ were both measured in natural abundance.

(ii) F_2SO_2

The method used for the preparation of F_2SO_2 was the fluorination of sulfur dioxide (SO_2) using silver difluoride (AgF_2) as the fluorinating agent [105][106]. A large excess of AgF_2 was put into a small glass tube and dry SO_2 was passed through the tube several times.

$$SO_2 + 2AgF_2 \rightarrow 2AgF + F_2SO_2 \qquad (2.2.2)$$

$F_2^{32}S^{18}O_2$ was prepared from $S^{18}O_2$. $F_2S^{16}O^{18}O$ was prepared using ^{18}O enriched sulfur dioxide(72 atom % of ^{18}O). The spectra of $F_2^{34}S^{16}O_2$ and $F_2^{34}S^{18}O_2$ were measured in natural abundance. AgF_2 and $S^{18}O_2$, in 99 atom % of ^{18}O, were obtained from Alfa. No lines attributable to sulfur dioxide could be detected in the microwave spectra of the product samples.

(iii) $(CH_3)_2SO_2$

$(^{12}CH_3)_2^{32}S^{16}O_2$ (98%), was obtained from Fluka.

$(^{12}CD_3)_2^{32}S^{16}O_2$ was synthesized by oxidizing $(^{12}CD_3)_2^{32}S^{16}O$ (99 atom % of D, MSD), with potassium permanganate.[107] The solution of potassium permanganate in $D_2^{16}O$ was dropped into $(^{12}CD_3)_2^{32}S^{16}O$; after stirring for five minutes $(^{12}CD_3)_2^{32}S^{16}O_2$ was extracted using dichloromethane and dried over anhydrous sodium sulfate. After evaporating the dichloromethane nice white crystals of $(^{12}CD_3)_2^{32}S^{16}O_2$ were obtained.

$$(^{12}CD_3)_2^{32}S^{16}O + KMnO_4 + D_2^{16}O \rightarrow (^{12}CD_3)_2^{32}S^{16}O_2 + KOD + MnO_2 \qquad (2.2.3)$$

$(^{12}CH_3)_2^{32}S^{16}O^{18}O$ was made using an extension of the method suggested by A. Okruszek [109] to prepare labelled $(CH_3)_2SO$. A magnetically stirred solution of $(^{12}CH_3)_2^{32}S$ (0.062g) in CH_2Cl_2 (3ml) was added at room temperature to a solution of $H_2^{18}O$ (1.8g) (97 atom % ^{18}O, MSD) in pyridine (0.5ml) followed by dropwise addition of a solution of bromine (0.88g) in CH_2Cl_2 (3ml). Vigorous stirring was continued for 30 minutes and the excess of bromine was destroyed by the addition of anhydrous $NaHSO_3$ (0.3g). Then the solution was dried with anhydrous Na_2SO_4 and after the solvent was evaporated to yield $(^{12}CH_3)_2^{32}S^{18}O$.

$$({}^{12}CH_3)_2^{32}S + H_2^{18}O + Br_2 + pyridine \rightarrow ({}^{12}CH_3)_2^{32}S^{18}O + HBr \tag{2.2.4}$$

By oxidizing the solution of $({}^{12}CH_3)_2^{32}S^{18}O$ in H_2O, using potassium permanganate, $({}^{12}CH_3)_2^{32}S^{16}O^{18}O$ was obtained as a white crystalline solid.

$({}^{13}CH_3)_2^{32}S^{16}O_2$ was prepared by oxidizing $({}^{13}CH_3)_2^{32}S$. The $({}^{13}CH_3)_2^{32}S$ was synthesized by the reaction of ${}^{13}CH_3I$ (99.3 atom % of ${}^{13}C$, MSD) and $Na_2^{32}S$.[99] 1g of ${}^{13}CH_3I$ in 2.5ml of ethanol (95%) was stirred and refluxed while 0.27g of $Na_2^{32}S$ in 2ml of water was added dropwise as rapidly as possible at room temperature. After the addition was completed the mixture was refluxed for about two hours, then the $({}^{13}CH_3)_2^{32}S$ (boiling point 37-39°C) together with an appreciable quantity of water was distilled out and condensed into another flask. No attempt was made to remove the water since to do so would inevitably have led to an appreciable loss of labelled dimethyl sulfide. Water did not interfere with subsequent workup of the sample. By oxidizing the $({}^{13}CH_3)_2^{32}S$ using potassium permanganate $({}^{13}CH_3)_2^{32}S^{16}O_2$ was obtained as a white solid. A mixture of ${}^{12}CH_3I$(50%) and ${}^{13}CH_3I$(50%) was used to prepare $({}^{12}CH_3)({}^{13}CH_3)^{32}S^{16}O_2$ using the same method.

$${}^{13}CH_3I + Na_2^{32}S \rightarrow ({}^{13}CH_3)_2^{32}S + NaI \tag{2.2.5}$$

$$({}^{13}CH_3)_2^{32}S + KMnO_4 + H_2O \rightarrow ({}^{13}CH_3)_2^{32}S^{16}O_2 + MnO_2 + KOH \tag{2.2.6}$$

$({}^{12}CH_3)_2{}^{34}S^{16}O_2$ was prepared from ${}^{12}CH_3I$ and $Na_2{}^{34}S$ using the method outlined above. $Na_2{}^{34}S$ was obtained from the reaction of Na (99.8%, BDH) and ${}^{34}S$(92.1% atom of ${}^{34}S$,MSD) in liquid ammonia.[110][111] 0.12g of Na and 0.05g of ${}^{34}S$ were put in a tube. After the air had been pumped out, the tube was sealed up and cooled to dry ice temperature and about 15ml of pure liquid ammonia was introduced into it. The tube was kept at about -60°C for about 2 days after which time all of the ${}^{34}S$ had reacted with Na. The remaining Na was destroyed by adding water at ice temperature.

$$2Na + {}^{34}S + (\textit{in liquid ammonia}) \rightarrow Na_2^{34}S \tag{2.2.7}$$

The obtained solution, containing $Na_2^{34}S$, was reacted with $^{12}CH_3I$ to obtain $(CH_3)_2^{34}S$ which was then oxidized to yield the labelled dimethyl sulfone.

$(^{12}CH_3)(^{12}CH_2D)^{32}S^{16}O_2$ was prepared by the oxidation of $(^{12}CH_3)^{32}S(^{12}CH_2D)$, which in turn was prepared by the reduction of monochloromethyl methyl sulfide, $(^{12}CH_3)^{32}S(^{12}CH_2Cl)$, with lithium aluminum deuteride, $LiAlD_4$, in n-butyl ether[112].

$$4(^{12}CH_3)^{32}S(^{12}CH_2Cl) + LiAlD_4 \rightarrow 4(^{12}CH_3)^{32}S(^{12}CH_2D) + LiCl + AlCl_3 \qquad (2.2.8)$$

To a magnetically stirred solution of $(^{12}CH_3)^{32}S(^{12}CH_2Cl)$(3.0g, 95%, Aldrich) in 5ml of n-butyl ether(99%,Aldrich) was added dropwise at room temperature a solution of $LiAlD_4$(0.25g, 98 % atom of D, Aldrich) in n-butyl ether. After the addition was completed the mixture was refluxed for about five minutes. Following this the required $(^{12}CH_3)^{32}S(^{12}CH_2D)$ was distilled out and used in the synthesis of $(^{12}CH_3)(^{12}CH_2D)^{32}S^{16}O_2$.

2.3 Raman Spectra

Raman spectra were measured in digital format with a Coderg PHO spectrometer equipped with a Coherent INNOVA 70-4 Ar ion laser. The 4880Å line was used. The Raman spectra of Cl_2SO_2 were measured in the 100 to 1500 cm^{-1} region. The spectra of $^{35}Cl_2^{32}S^{16}O_2$ and $^{35}Cl_2^{32}S^{18}O_2$ were measured in the both liquid phase and the gas phase. The spectrum of $^{35}Cl_2^{34}S^{18}O_2$ was measured only in the liquid phase, because the sample was too small to permit gas phase measurements. The differences between gas phase and liquid phase frequencies of $^{35}Cl_2^{32}S^{16}O_2$ were used to correct the frequencies of $^{35}Cl_2^{34}S^{18}O_2$ measured in the liquid phase to obtain estimated gas phase frequencies for the latter species.

The Raman spectrum of $(CH_3)_2SO_2$ was measured in the 100 to 1500 cm^{-1} region and the 2900 to 3100 cm^{-1} region. The spectra of $(^{12}CH_3)_2^{32}S^{16}O_2$, $(^{12}CD_3)_2^{32}S^{16}O_2$ and $(^{13}CH_3)_2^{32}S^{16}O_2$ were measured using crystalline samples.

The slit width used to obtain spectra was $1cm^{-1}$ and the scan speed was $50cm^{-1}/min$. Four scans for both solid phase and liquid phase samples and ten scans for gas phase samples were averaged. The resolution was believed to be better than $1.5cm^{-1}$. SO_2, the vibrational frequences of which are known very well[104], was used as the internal standard to correct the vibrational frequencies of the molecules studied in the present work. All of the spectra were obtained at room temperature.

2.4 Infrared Spectra

The infrared spectrum of F_2SO_2 was recorded at low resolution with a Mattson Polaris FTIR spectrometer and at higher resolution with a Perkin-Elmer 283 spectrometer.. Isotope shifts measured with the latter instrument are thought to be accurate to better than $0.5cm^{-1}$. The gaseous sample of F_2SO_2 was enclosed in a $10cm$ cell with $NaBr$ windows and measured at room temperature. $F_2^{34}S^{16}O_2$ was observed in natural abundance. As we mentioned in Section 2.3, $F_2^{32}S^{16}O^{18}O$ was made from a sulfur dioxide mixture containing $^{16}O(28\%)$ and $^{18}O(72\%)$, so that there was about 40% of $F_2^{32}S^{16}O^{18}O$, 52% of $F_2^{32}S^{18}O_2$ and 8% of $F_2^{32}S^{16}O_2$ in the sample used. All of the fundamentals of $F_2^{32}S^{16}O_2$ were measured, except for ν_5, which belongs to the A_2 species and is infrared inactive. Only three or four strong lines were found for the $F_2^{32}S^{18}O_2$,$F_2^{32}S^{16}O^{18}O$ and $F_2^{34}S^{16}O_2$ isotopic species.

CHAPTER 3

THE MICROWAVE SPECTRUM, MOLECULAR STRUCTURE AND HARMONIC FORCE FIELD OF SULPHURYL CHLORIDE

Microwave spectroscopic studies of sulphuryl chloride have earlier been reported by Dubrulle and Boucher[69][70] in 1972 and 1974. In their work, the rotational transitions of $^{35}Cl_2^{32}S^{16}O_2$, for J up to 18 only in R branch, and of $^{35}Cl^{37}Cl^{32}S^{16}O_2$, for J up to 18 in R branch and up to 60 in Q branch, were observed and assigned. From these microwave data the rotational and distortion constants of these two isotopic species were derived. The distortion constants of $^{35}Cl_2^{32}S^{16}O_2$, however, could not be reliable, because only 14 lines of low J R-branch transitions, without Q branch or higher J transitions, were used to derive values for all the 3 rotational constants, 5 quartic distortion constants and 7 sextic distortion constants. The number of the calculated constants was greater than that of the observed lines employed in their calculation. An effective molecular geometry, encompassing only four independent parameters for this molecule, was not derived from the six available rotational constants of the two isotopic species studied in their work. The number of isotopic species was insufficient for them to derive the substitution geometry.

Durbrulle and Boucher[69][70] did not report any chlorine nuclear quadrupole splittings in their work. The nuclear quadrupole coupling constants of sulphuryl chloride were only reported by Suzuki and Yamaguchi[141] in 1981, as $\chi_{xx} = 50.14 MHz$, $\chi_{yy} = 40.37 MHz$ and $\chi_{zz} = -95.51$MHz. However, they only quoted another author's result and did not give any details of the experiment or the calculations.

There is no microwave report on the evaluation of the electric dipole moment of sulphuryl chloride. The dipole moment of this molecule was measured by Coop and

Sutton using a dielectric method in 1939[151][152][153]. They made the measurement using a gas phase sample and obtained the value of 1.795(5)*Debye*.

The r_g geometry of Cl_2SO_2 was obtained by Hargittai from an electron diffraction investigation by using a constant scattering function in 1968[71]. The next year, the geometry was recalculated by using a complex scattering constant, as: $r(SO) = 1.404 \pm 0.004 \mathring{A}$, $r(ClS) = 2.011 \pm 0.005 \mathring{A}$, $\angle(OSO) = 123.5 \pm 0.8°$, $\angle(ClSCl) = 100.0 \pm 0.7°$ and $\angle(ClSO) = 107.7 \pm 0.4$ [72]°. The same author derived the molecular parameters again from a joint least squares refinement of the electron diffraction data and the microwave constants obtained by Boucher[73].

Since 1944 there have been several reports about the vibrational spectra of Cl_2SO_2 [74] using infrared spectroscopy[75], Raman spectroscopy[76][77][78] and theoretical methods[79][80][81]. The first attempt to calculate the force field was made by Siebert[82], who refined a seven parameter valence force field which gave only poor predictions of vibrational frequencies. Stammreich *et al.* [103] performed a normal coordinate analysis, in which only the nine diagonal constants were considered. In this work, they assigned $\nu_7 < \nu_9$ by a very simple calculation. Wilson *et al.* [79] and Suthers *et al.* [81] did this calculation again and obtained nine and thirteen force constants, respectively. In their work, they suggested that $\nu_7 > \nu_9$, contrary to Stammreich's conclusion[103]. Although they obtained reasonable agreement between observed and calculated vibrational frequencies, there were still several difficulties with this work. The first was that only nine vibrational frequencies, observed for one isotopic species were used to calculate nine or more force constants. It is apparent that the data were not sufficient to fit so many force constants. Secondly, the effects of Fermi resonance were not considered in their work. The effects of Fermi resonance in this molecule cannot be ignored as we will discuss later. The third problem was that the molecular geometry available to them was only an early electron diffraction geometry. If more vibrational data for additional isotopic species or data from other sources, such as distortion constants, and a better molecular geometry were available, the force field would obviously be improved a lot.

Therefore, it was worth reinvestigating the spectrum of this molecule in order to define better molecular geometry and harmonic force field. It was the aim of this work.

3.1 Observed Microwave Spectrum and Assignment

The microwave spectra of nine isotopic species of sulphuryl chloride, which were $^{35}Cl_2^{32}S^{16}O_2$, $^{35}Cl^{37}Cl^{32}S^{16}O_2$, $^{35}Cl_2^{32}S^{18}O_2$, $^{35}Cl^{37}Cl^{32}S^{18}O_2$, $^{35}Cl^{34}S^{18}O_2$, $^{35}Cl^{37}Cl^{34}S^{18}O_2$, $^{37}Cl_2^{32}Ssop\,16O_2$, $^{35}Cl_2^{34}S^{16}O_2$ and $^{35}Cl^{37}Cl^{34}S^{16}O_2$ were observed in the frequency range from $12000MHz$ to $84000MHz$. All of these isotopic species have b-type transitions as noted by Dubrulle and Boucher in whose work only the spectra of $^{35}Cl_2^{32}S^{16}O_2$ and $^{35}Cl^{37}Cl^{32}S^{16}O_2$ were measured[69][70]. Therefore the selection rule are $ee-oo$ and $eo-oe$. There should be some very weak a-type transitions for the isotopic species $^{35}Cl^{37}Cl^{32}S^{16}O_2$, $^{35}Cl^{37}Cl^{32}S^{18}O_2$, $^{35}Cl^{37}Cl^{34}S^{18}O_2$ and $^{35}Cl^{37}Cl^{34}S^{16}O_2$; they were, however, not found because the dipole moment component caused by mono-chlorine isotopic substitution to lie along the a principal axes is quite small. Both Q-branch and R-branch transitions were observed for all of the isotopic species except the last three species, for which only R-branch transitions were measured. The number of observed transitions and the highest observed J values for each isotopic species studied are listed in Table-3.1 and the observed transition frequencies are listed from Table-3.2 to Table-3.10.

In addition, many of the transitions studied exhibited nuclear quadrupole hyperfine structure due to the presence of two chlorine nuclei; both the nuclei of ^{35}Cl

and ^{37}Cl have spin 3/2. The hyperfine splitting due to the chlorine nuclear quadrupole interaction was not observed for most of the transitions, which were singlets with nice symmetric line shapes. Some transitions, however, appeared as symmetric triplet hyperfine structures with a strong component at the unsplit line position. The splittings of low J transitions were big but they were always overlapped by stronger higher J lines and, as a result, we were unable to measure very low J lines. Only about twenty hyperfine structures of high J transitions were observed in detail in this work. Two examples obtained by us are given in Figure-3.1.a and Figure-3.1.b, which show the nuclear quadrupole hyperfine structure of $^{35}Cl_2^{32}S^{16}O_2$ for the $43_{15,29} - 43_{14,30}$ transition around 35298.5MHz and of $^{35}Cl^{37}Cl^{32}S^{18}O_2$ for the $37_{25,12}$-$37_{24,13}$ transition around 55232MHz, respectively. The nuclear quadrupole coupling constants of $^{35}Cl_2^{32}S^{16}O_2$ were derived from the hyperfine splittings. The theory for the rotational spectrum of an asymmetric top containing two nuclei of nuclear sp $\frac{3}{2}$ presented by Robinson and Cornwell[157] shows that four degenerate hyperfine components always exist at the unsplit position when the two quadrupolar nuclei are equivalent. Actually the spectra generally showed symmetric patterns, Figure-3.1.a and Figure-3.1.b; therefore, average frequencies of all the peaks or the frequency of the center peak were assigned to the rotational transition and used to calculate the rotational constants and distortion constants for this molecule.

The rotational constants and distortion constants of $^{35}Cl_2^{32}S^{16}O_2$ and $^{35}Cl^{37}Cl^{32}S^{16}O_2$ from the previous work of Dubrulle and Boucher[69][70] were used as the initial values to predict the spectra of these two species. The transitions of other isotopic species were located with little difficulty by using the rotational constants calculated from a preliminary effective structure, which could be obtained after good rotational constants of $^{35}Cl_2^{32}S^{16}O_2$ and $^{35}Cl^{37}Cl^{32}S^{16}O_2$ had been derived from their spectra. Some of the lines measured in Bubrulle and Boucher's work were remeasured in this work; the frequencies differ in the two works by about $0.2MHz$. Because of the spin statistics, as discussed in Section-1.2, the eo-oe transitions are stronger than the ee-oo transitions for all of the $^{35}Cl_2$- and $^{37}Cl_2$- species, which helped greatly in the assignment of the transitions.

All of the measurements were done in a $1.0\times2.2cm$ Stark cell cooled to dry ice temperature. The samples were pumped continuously through the cell, in which the presure was controlled in the range 1-5 microns. Very high Stark fields, typically 2000-$4000V/cm$, were employed for the measurements.

Table-3.1

Number of Observed Transitions(N) and the Highest J Values(J) Observed

for Cl_2SO_2 Isotopomers

Isotopic Species	Q-Branch (J)	Q-Branch (N)	R-Branch (J)	R-Branch (N)	Total (N)
$^{35}Cl_2^{32}S^{16}O_2$	84	95	20	50	145
$^{35}Cl^{37}Cl^{32}S^{16}O_2$	87	116	25	47	163
$^{35}Cl^{32}S^{18}O_2$	75	68	22	43	111
$^{35}Cl^{37}Cl^{32}S^{18}O_2$	78	73	21	33	109
$^{35}Cl_2^{34}S^{18}O_2$	59	18	19	26	44
$^{37}Cl_2^{32}S^{16}O_2$			21	24	24
$^{35}Cl^{37}Cl^{34}s^{18}O_2$	66	17	21	27	44
$^{35}Cl_2^{34}S^{16}O_2$			20	45	45
$^{35}Cl^{37}Cl^{34}S^{16}O_2$			21	14	14

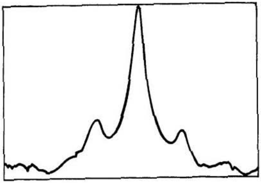

Figure-3.1.a The $43_{15,29}-43_{14,30}$ Transition of $^{35}Cl_2^{32}S^{16}O_2$ Showed a Symmetric Triplet Nuclear Quadrupole Hyperfine Structure with Frequencies of 35297.575, 35298.425 and 35299.262 MHz.

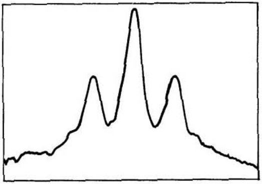

Figure-3.1.b The $37_{25,12}-37_{24,13}$ Transition of $^{35}Cl^{37}Cl^{32}S^{18}O_2$ Showed a Symmetric Triplet Nuclear Quadrupole Hyperfine Structure with Frequencies of 55231.995, 55232.635 and 55233.268 MHz.

Table-3.2

Observed Rotational Transition Frequencies(in MHz) of $^{35}Cl_2^{32}S^{16}O_2$.

J'	K_a'	K_c'	-	J''	K_a''	K_c''	Frequency	Deviation
7	4	4	-	6	3	3	38776.749	-0.020
8	4	4	-	7	3	5	44932.233	0.007
9	9	0	-	8	8	1	61409.128	0.031
9	2	8	-	8	1	7	37356.287	0.030
9	1	9	-	8	0	8	35554.928	0.005
10	10	0	-	9	9	1	68379.513	0.062
10	9	1	-	9	8	2	65714.248	-0.017
10	9	2	-	9	8	1	65714.248	-0.014
10	7	3	-	9	6	4	60364.177	-0.042
10	5	5	-	9	4	6	55723.059	0.006
10	0	10	-	9	1	9	39407.105	-0.013
10	3	7	-	9	4	6	39422.109	0.024
11	2	10	-	10	1	9	44922.587	0.000
11	10	2	-	10	9	1	72684.864	0.018
11	9	2	-	10	8	3	70016.638	0.004
11	9	3	-	10	8	2	70016.638	0.032
11	7	5	-	10	6	4	64615.489	-0.051
13	3	10	-	12	4	9	54735.358	0.040
14	1	13	-	13	2	12	56458.582	-0.026
14	3	11	-	13	4	10	59140.624	0.009
14	5	10	-	13	4	9	65266.166	0.042
14	4	11	-	13	3	10	60515.144	0.011
14	0	14	-	13	1	13	54849.139	-0.044
15	2	13	-	14	3	12	61926.921	-0.065
15	4	12	-	14	3	11	64004.996	-0.043
15	2	14	-	14	1	13	60320.395	-0.052
15	3	13	-	14	2	12	61976.153	-0.056
15	0	15	-	14	1	14	58709.163	0.015
16	9	7	-	16	8	8	21613.493	0.029
16	1	16	-	15	0	15	62569.021	-0.027
16	5	12	-	15	4	11	70777.595	-0.031
16	0	16	-	15	1	15	62569.021	-0.018
17	4	14	-	16	3	13	71404.002	0.025
17	4	13	-	16	5	12	72272.946	0.069
17	7	10	-	16	8	9	57387.771	0.008
17	6	12	-	16	7	9	56504.279	-0.029
17	6	12	-	16	5	11	79134.054	-0.005
17	0	17	-	16	1	16	66428.866	0.011
17	1	17	-	16	0	16	66428.866	0.008
18	0	18	-	17	1	17	70288.560	-0.031
18	9	9	-	18	8	10	20684.201	-0.054
18	2	16	-	17	3	15	73514.667	0.000
18	5	14	-	17	4	13	77342.629	0.007
18	1	18	-	17	0	17	70288.560	-0.032
19	4	16	-	19	3	17	24932.883	0.033

Table-3.2 Continued(1)

J'	K_a'	K_c'	-	J''	K_a''	K_c''	Frequency	Deviation
20	0	20	-	19	1	19	78007.838	0.041
20	5	15	-	20	4	16	21065.160	0.000
21	5	16	-	21	4	17	22992.806	0.017
24	6	19	-	24	5	20	28333.321	0.011
24	7	17	-	24	6	18	20970.385	0.010
25	12	13	-	25	11	14	28064.652	-0.025
26	12	14	-	26	11	15	27407.934	0.020
26	8	18	-	26	7	19	20369.007	-0.020
26	6	20	-	26	5	21	28993.283	0.03[illegible]
27	9	19	-	27	8	20	25416.999	0.033
28	8	20	-	28	7	21	25549.885	-0.005
28	12	16	-	28	11	17	25325.233	-0.006
28	9	20	-	28	8	21	26966.051	-0.040
30	12	18	-	30	11	19	21957.165	-0.018
31	10	21	-	31	9	22	21372.147	0.012
32	13	19	-	32	12	20	25321.856	-0.055
32	11	21	-	32	10	22	18207.473	0.003
32	8	25	-	32	7	26	36618.360	0.012
33	13	21	-	33	12	22	28849.709	0.016
33	11	22	-	33	10	23	20404.321	-0.036
33	12	21	-	33	11	22	18012.888	0.036
34	14	21	-	34	13	22	31152.769	-0.020
35	16	19	-	35	15	20	37426.424	0.036
35	12	23	-	35	11	24	19768.847	0.045
36	17	19	-	36	16	20	40539.216	-0.007
36	14	22	-	36	13	23	24740.482	0.016
36	13	23	-	36	12	24	19343.159	0.031
36	11	25	-	36	10	26	29214.157	-0.081
37	24	14	-	37	23	15	61547.357	0.002
37	17	20	-	37	16	21	40038.426	-0.007
37	16	22	-	37	15	23	36505.143	0.039
37	12	25	-	37	11	26	25059.555	0.020
38	15	23	-	38	14	24	28282.972	-0.041
39	15	24	-	39	14	25	26079.623	-0.034
39	10	29	-	39	9	30	40177.670	0.036
40	13	27	-	40	12	28	26902.463	0.052
40	17	23	-	40	16	24	37850.359	-0.053
41	11	30	-	41	10	31	40585.013	-0.032
41	15	26	-	41	14	27	22514.024	0.084
43	18	25	-	43	17	26	39694.864	0.003
43	15	29	-	43	14	30	35298.395	-0.019
44	16	28	-	44	15	29	23764.438	-0.005
44	17	28	-	44	16	29	36623.914	-0.031
44	15	29	-	44	14	30	24477.617	0.008
44	5	39	-	44	4	40	61036.490	0.044
47	17	31	-	47	16	32	37289.570	-0.028

Table-3.2 Continued(2)

J'	K_a'	K_c'	-	J''	K_a''	K_c''	Frequency	Deviation
47	17	30	-	47	16	31	25006.765	0.038
47	19	28	-	47	18	29	40171.697	0.030
47	7	40	-	47	6	41	61429.695	-0.057
48	17	31	-	48	16	32	24623.002	0.020
48	17	32	-	48	16	33	38139.648	0.016
48	8	40	-	48	7	41	60736.290	-0.007
50	17	33	-	50	16	34	27640.261	-0.057
50	19	32	-	50	18	33	40353.959	-0.025
51	19	33	-	51	18	34	40299.243	-0.016
51	18	33	-	51	17	34	25940.702	-0.046
52	18	34	-	52	17	35	26961.793	0.035
52	20	32	-	52	19	33	37733.532	-0.006
53	19	34	-	53	18	35	27474.346	-0.018
53	18	36	-	53	17	37	42725.872	-0.079
57	20	37	-	57	19	38	28580.780	0.007
59	22	38	-	59	21	39	45838.358	-0.005
59	22	37	-	59	21	38	37643.431	0.022
60	25	36	-	60	24	37	56696.702	-0.008
60	25	35	-	60	24	36	56559.781	-0.035
60	22	39	-	60	21	40	45813.745	0.052
60	21	40	-	60	20	41	45849.972	-0.051
61	25	36	-	61	24	37	55675.067	-0.021
61	20	41	-	61	19	42	39758.754	-0.005
63	22	41	-	63	21	42	31229.912	0.074
64	27	38	-	64	26	39	62013.763	0.008
65	27	38	-	65	26	39	61209.717	-0.056
65	26	40	-	65	25	41	57006.305	-0.011
65	23	42	-	65	22	43	32381.485	-0.056
66	24	42	-	66	23	43	37142.063	0.001
66	22	44	-	66	21	45	39322.291	-0.022
68	25	43	-	68	24	44	41346.012	-0.036
69	28	41	-	69	27	42	62228.159	0.052
73	29	45	-	73	28	46	63430.394	0.039
73	23	50	-	73	22	51	56201.667	-0.026
74	29	46	-	74	28	47	62509.833	0.087
74	25	49	-	74	24	50	40394.914	-0.014
76	27	49	-	76	26	50	38300.840	0.051
78	25	53	-	78	24	54	56742.819	0.027
78	27	51	-	78	26	52	37890.197	-0.016
79	32	48	-	79	31	49	71676.493	-0.024
79	28	52	-	79	27	53	56975.815	0.026
80	32	49	-	80	31	50	70812.545	0.007
80	25	55	-	80	24	56	63033.117	0.000
80	30	51	-	80	29	52	61538.322	-0.078
81	24	57	-	81	23	58	70605.347	0.056
82	29	53	-	82	28	54	40636.246	0.004
84	33	51	-	84	32	52	71400.974	-0.010

Table-3.3
Observed Rotational Transition Frequencies(in MHz) of $^{35}Cl^{37}Cl^{32}S^{16}O_2$.

J'	K_a'	K_c'	-	J''	K_a''	K_c''	Frequency	Deviation
6	5	2	-	5	4	1	37438.686	0.018
6	5	1	-	5	4	2	37453.050	-0.092
9	9	0	-	8	8	1	60911.700	0.037
9	9	1	-	8	8	0	60911.700	0.037
9	0	9	-	8	1	8	34778.813	0.059
9	1	9	-	8	0	8	34791.760	-0.080
10	10	0	-	9	9	1	67829.065	0.006
10	10	1	-	9	9	0	67829.065	0.006
10	9	1	-	9	8	2	65122.501	-0.005
10	9	2	-	9	8	1	65122.403	-0.100
10	1	10	-	9	0	9	38563.194	-0.033
10	1	9	-	9	2	8	40086.161	0.027
10	0	10	-	9	1	9	38558.110	-0.020
10	2	9	-	9	1	8	40270.564	0.050
11	11	0	-	10	10	1	74746.141	0.014
11	11	1	-	10	10	0	74746.141	0.014
11	10	1	-	10	9	2	72040.110	-0.007
11	10	2	-	10	9	1	72040.110	-0.006
12	11	2	-	11	10	1	78957.253	-0.071
12	8	4	-	11	7	5	70804.759	-0.036
13	7	6	-	12	6	7	72284.604	0.013
14	8	7	-	13	7	6	79105.869	-0.009
14	8	6	-	13	7	7	79160.245	-0.079
14	2	13	-	13	1	12	55269.957	0.078
15	2	14	-	14	1	13	59042.187	-0.058
15	3	13	-	14	2	12	60697.935	0.031
16	3	14	-	15	2	13	64449.126	-0.027
16	0	16	-	15	1	15	61213.800	0.033
16	1	16	-	15	0	15	61213.800	0.020
17	1	17	-	16	0	16	64989.132	-0.028
17	0	17	-	16	1	16	64989.132	-0.023
18	1	18	-	17	0	17	68764.496	0.026
18	0	18	-	17	1	17	68764.496	0.028
18	2	16	-	17	3	15	71975.120	-0.018
18	3	16	-	17	2	15	71979.879	-0.024
19	1	18	-	18	2	17	74139.191	-0.038
19	1	19	-	18	0	18	72539.753	0.051
19	0	19	-	18	1	18	72539.753	0.052
19	2	18	-	18	1	17	74139.191	-0.090
20	1	19	-	19	2	18	77913.923	0.030
20	2	19	-	19	1	18	77913.923	0.010
20	0	20	-	19	1	19	76314.934	0.087
20	1	20	-	19	0	19	76314.934	0.087
22	8	14	-	22	7	15	12700.211	0.067
23	11	12	-	23	10	13	26045.193	-0.015
24	24	1	-	24	23	2	63507.214	-0.003

Table-3.3 Continued(1)

J'	K_a'	K_c'	-	J''	K_a''	K_c''	Frequency	Deviation
24	24	0	-	24	23	1	63507.214	-0.003
24	9	15	-	24	8	16	14392.813	0.026
25	15	10	-	24	16	9	64658.445	-0.064
25	9	16	-	25	8	17	14129.150	0.026
25	15	11	-	24	16	8	64658.445	-0.061
25	14	11	-	24	15	10	67709.483	-0.021
25	14	12	-	24	15	9	67709.483	0.048
25	12	13	-	25	11	14	28730.576	0.030
26	19	7	-	26	18	8	49593.912	-0.068
26	15	11	-	25	16	10	69121.577	-0.010
26	15	12	-	25	16	9	69121.577	0.001
27	23	4	-	27	22	5	60637.717	-0.022
27	23	5	-	27	22	6	60637.717	-0.022
28	14	14	-	28	13	15	34401.970	0.063
29	23	6	-	29	22	7	60517.458	-0.019
29	23	7	-	29	22	8	60517.458	-0.019
29	21	8	-	28	22	7	64714.006	0.010
29	21	9	-	28	22	6	64714.006	0.010
29	15	15	-	29	14	16	37329.980	-0.039
29	14	15	-	29	13	16	34012.064	0.063
30	15	15	-	30	14	16	37002.181	-0.068
30	14	16	-	30	13	17	33544.250	-0.034
31	14	18	-	31	13	19	33222.544	-0.008
31	14	17	-	31	13	18	32968.402	0.076
31	15	16	-	31	14	17	36628.960	0.024
31	7	25	-	31	6	26	37153.654	0.001
32	15	17	-	32	14	18	36192.230	0.060
32	12	20	-	32	11	21	19704.711	0.072
33	15	19	-	33	14	20	35814.775	0.005
34	12	22	-	34	11	23	18319.751	0.011
34	15	19	-	34	14	20	35032.608	-0.065
35	10	26	-	35	9	27	35624.418	0.051
35	15	21	-	35	14	22	34830.878	-0.041
36	17	20	-	36	16	21	41461.800	-0.017
36	16	21	-	36	15	22	37937.349	0.011
36	16	20	-	36	15	21	37765.631	-0.027
37	26	12	-	37	25	13	68246.861	-0.018
37	26	11	-	37	25	12	68246.861	-0.018
37	16	22	-	37	15	23	37418.161	0.002
37	16	21	-	37	15	22	37065.260	0.056
38	14	24	-	38	13	25	22477.700	0.089
38	17	22	-	38	16	23	40553.227	-0.067
38	17	21	-	38	16	22	40457.261	0.009
38	16	23	-	38	15	24	36877.191	0.035
39	30	9	-	39	29	10	79248.727	0.058
39	16	24	-	39	15	25	36341.382	-0.017

Table-3.3 Continued(2)

J'	K_a'	K_c'	-	J''	K_a''	K_c''	Frequency	Deviation
39	17	23	-	39	16	24	40032.583	-0.024
40	30	10	-	40	29	11	79176.301	0.059
40	24	17	-	40	23	18	62150.376	-0.058
40	24	16	-	40	23	17	62150.376	-0.058
40	14	26	-	40	13	27	21053.768	0.100
40	17	23	-	40	16	24	39068.825	0.022
41	30	11	-	41	29	12	79097.955	0.089
41	16	26	-	41	15	27	35462.846	0.005
41	17	24	-	41	16	25	38113.631	-0.012
41	18	23	-	41	17	24	42547.629	0.032
41	18	24	-	41	17	25	42661.105	0.038
42	15	27	-	42	14	28	22606.611	0.046
42	18	24	-	42	17	25	41869.118	-0.078
43	18	26	-	43	17	27	41509.395	-0.022
43	18	25	-	43	17	26	41046.062	0.029
44	16	29	-	44	15	30	35509.659	0.033
44	18	27	-	44	17	28	40898.144	0.088
44	17	28	-	44	16	29	37404.842	0.015
44	25	19	-	44	24	20	64393.401	-0.007
45	17	29	-	45	16	30	37165.505	0.017
46	24	23	-	46	23	24	60904.615	-0.037
46	5	42	-	46	4	43	65988.588	0.080
46	24	22	-	46	23	23	60904.615	-0.033
46	18	29	-	46	17	30	39756.885	-0.047
46	4	42	-	46	3	43	65988.588	0.080
47	18	30	-	47	17	31	39328.104	0.021
47	24	24	-	47	23	25	60632.425	-0.058
47	24	23	-	47	23	24	60632.425	-0.046
48	22	26	-	48	21	27	53655.913	-0.008
48	17	32	-	48	16	33	38023.685	0.071
48	18	31	-	48	17	32	39076.618	0.068
49	22	28	-	49	21	29	53195.644	-0.028
51	28	24	-	51	27	25	71965.676	-0.049
51	28	23	-	51	27	24	71965.676	-0.049
55	24	31	-	55	23	32	57432.225	0.020
56	31	26	-	56	30	27	79945.254	0.087
56	31	25	-	56	30	26	79945.254	0.087
56	25	32	-	56	24	33	60603.782	-0.022
56	24	32	-	56	23	33	56847.996	-0.006
57	24	33	-	57	23	34	56198.679	0.003
58	24	34	-	58	23	35	55467.966	0.021
59	31	28	-	59	30	29	79278.566	0.069
59	24	35	-	59	23	36	54631.206	-0.033
60	26	35	-	60	25	36	62207.991	-0.030
60	26	34	-	60	25	35	62199.244	-0.028
62	26	36	-	62	25	37	60965.081	-0.029

Table-3.3 Continued(3)

J'	K_a'	K_c'	-	J''	K_a''	K_c''	Frequency	Deviation
62	25	38	-	62	24	39	56851.506	-0.067
63	26	37	-	63	25	38	60248.780	-0.007
67	27	40	-	67	26	41	61412.429	-0.097
68	27	42	-	68	26	43	60770.295	-0.007
70	28	42	-	70	27	43	63369.121	-0.052
70	28	43	-	70	27	44	63552.022	-0.013
72	28	45	-	72	27	46	61832.045	-0.008
73	28	46	-	73	27	47	60[illegible]75.652	-0.033
74	28	47	-	74	27	48	60022.905	0.082
74	29	46	-	74	28	47	64646.607	0.020
75	29	47	-	75	28	48	63737.348	-0.018
75	30	46	-	75	29	47	68309.983	0.008
76	29	48	-	76	28	49	62804.026	0.035
79	27	52	-	79	26	53	38126.957	0.086
80	30	50	-	80	29	51	61569.437	0.016
81	31	51	-	81	30	52	67525.099	-0.051
82	32	51	-	82	31	52	71347.247	-0.016
82	25	57	-	82	24	58	65721.515	-0.051
85	32	54	-	85	31	55	68398.598	-0.018
87	33	55	-	87	32	56	71288.411	-0.023

Table-3.4

Observed **R**otational Transition Frequencies(in MHz) of $^{35}Cl_2^{32}S^{18}O_2$.

J'	K_a'	K_c'	-	J''	K_a''	K_c''	Frequency	Deviation
11	11	0	-	10	10	1	69852.433	-0.042
11	10	2	-	10	9	1	67602.504	-0.008
11	10	1	-	10	9	2	67602.504	-0.009
11	11	1	-	10	10	1	69852.433	-0.042
12	12	0	-	11	11	1	76303.799	-0.028
12	10	3	-	11	9	2	71801.875	-0.025
12	10	2	-	11	9	3	71801.875	-0.032
12	11	2	-	11	10	1	74054.335	0.025
12	11	1	-	11	10	2	74054.335	0.025
12	12	1	-	11	11	0	76303.799	-0.028
14	1	13	-	13	2	12	55106.290	0.036
15	2	13	-	14	3	12	60336.244	0.015
15	0	15	-	14	1	14	57443.809	0.045
15	1	15	-	14	0	14	57443.809	0.035
16	0	16	-	15	1	15	61224.890	0.021
16	1	16	-	15	0	15	61224.890	0.018
16	1	15	-	15	2	14	62667.674	0.062
17	5	13	-	16	4	12	71346.574	-0.002
17	0	17	-	16	1	16	65005.814	-0.092
17	1	17	-	16	0	16	65005.814	-0.093
17	3	14	-	16	4	13	69349.926	0.024

Table-3.4 Continued(1)

J'	K_a'	K_c'	-	J''	K_a''	K_c''	Frequency	Deviation
17	3	15	-	16	2	14	67902.733	0.001
17	4	14	-	16	3	13	69416.863	-0.014
18	5	14	-	17	4	13	74881.629	0.067
18	0	18	-	17	1	17	68786.897	0.028
18	1	18	-	17	0	17	68786.897	0.028
18	1	17	-	17	2	16	70228.576	-0.014
18	2	17	-	17	1	16	70228.576	-0.046
18	2	16	-	17	3	15	71678.634	-0.068
18	3	15	-	17	4	14	73139.538	0.021
19	3	16	-	18	4	15	76920.534	-0.042
19	0	19	-	18	1	18	72567.787	0.035
19	1	19	-	18	0	18	72567.787	0.035
19	1	18	-	18	2	17	74009.050	0.001
19	2	18	-	18	1	17	74009.050	-0.010
20	2	19	-	19	1	18	77789.418	-0.059
20	0	20	-	19	1	19	76348.530	-0.019
20	1	20	-	19	0	19	76348.530	-0.019
20	1	19	-	19	2	18	77789.418	-0.055
21	1	21	-	20	0	20	80129.208	-0.046
21	0	21	-	20	1	20	80129.208	-0.046
22	1	22	-	21	0	21	83909.919	0.057
22	0	22	-	21	1	21	83909.919	0.057
38	26	13	-	38	25	14	56438.779	0.091
38	26	12	-	38	25	13	56438.779	0.091
39	27	13	-	39	26	14	58707.196	0.013
39	27	12	-	39	26	13	58707.196	0.013
42	27	16	-	42	26	17	58331.619	0.017
42	27	15	-	42	26	16	58331.619	0.017
45	28	18	-	45	27	19	60324.326	-0.032
45	28	17	-	45	27	18	60324.326	-0.032
48	9	39	-	48	8	40	52951.509	0.012
48	10	39	-	48	9	40	52951.509	0.012
48	5	43	-	48	4	44	60804.233	-0.011
48	6	43	-	48	5	44	60804.233	-0.011
49	28	22	-	49	27	23	59598.354	-0.061
49	28	21	-	49	27	22	59598.354	-0.061
49	6	43	-	49	5	44	60367.141	0.000
49	7	43	-	49	6	44	60367.141	0.000
51	11	40	-	51	10	41	53107.746	0.012
51	12	40	-	51	11	41	53107.746	0.004
51	28	24	-	51	27	25	59147.986	0.041
51	28	23	-	51	27	24	59147.986	0.041
52	32	21	-	52	31	22	69032.872	-0.031
52	32	20	-	52	31	21	69032.872	-0.031
53	32	22	-	53	31	23	68869.517	0.018
53	32	21	-	53	31	22	68869.517	0.018
54	32	23	-	54	31	24	68695.137	-0.046

Table-3.4 Continued(2)

J'	K_a'	K_c'	-	J''	K_a''	K_c''	Frequency	Deviation
54	32	22	-	54	31	23	68695.137	-0.046
56	32	25	-	56	31	26	68311.146	-0.058
56	32	24	-	56	31	25	68311.146	-0.058
56	12	45	-	56	11	46	60564.972	0.000
56	11	45	-	56	10	46	60564.972	0.000
59	32	28	-	59	31	29	67635.629	-0.070
59	32	27	-	59	31	28	67635.629	-0.070
59	14	46	-	59	13	47	60668.491	0.002
59	13	46	-	59	12	47	60668.491	0.003
61	33	29	-	61	32	30	69757.802	0.046
61	33	28	-	61	32	29	69757.802	0.046
61	32	30	-	61	31	31	67108.772	0.000
61	32	29	-	61	31	30	67108.772	0.000
61	14	47	-	61	13	48	61413.410	0.006
61	15	47	-	61	14	48	61413.410	0.002
62	33	30	-	62	32	31	69501.838	0.000
62	33	29	-	62	32	30	69501.838	0.000
63	12	52	-	63	11	53	70871.197	0.039
63	11	52	-	63	10	53	70871.197	0.039
67	35	33	-	67	34	34	73472.568	-0.013
67	35	32	-	67	34	33	73472.568	-0.013
67	14	54	-	67	13	55	72588.162	-0.043
67	13	54	-	67	12	55	72588.162	-0.043
69	35	35	-	69	34	36	72877.872	-0.048
69	35	34	-	69	34	35	72877.872	-0.048
70	35	36	-	70	34	37	72553.526	-0.002
70	35	35	-	70	34	36	72553.526	-0.001
70	34	36	-	70	33	37	69714.643	0.000
70	16	55	-	70	15	56	72708.958	0.003
70	15	55	-	70	14	56	72708.958	0.003
70	34	37	-	70	33	38	69714.643	-0.014
71	35	37	-	71	34	38	72209.486	0.034
71	34	38	-	71	33	39	69322.806	-0.040
71	34	37	-	71	33	38	69322.806	-0.005
71	35	36	-	71	34	37	72209.486	0.038
72	36	37	-	72	35	38	74678.210	0.008
72	35	37	-	72	34	38	71844.261	-0.021
72	35	38	-	72	34	39	71844.261	-0.029
72	36	36	-	72	35	37	74678.210	0.009
74	36	39	-	74	35	40	73974.073	-0.013
74	36	38	-	74	35	39	73974.073	-0.008
75	36	40	-	75	35	41	73590.124	0.021
75	36	39	-	75	35	40	73590.124	0.032

Table-3.5
Observed Rotational Transition Frequencies(in MHz) of $^{35}Cl^{37}Cl^{32}S^{18}O_2$.

J'	K_a'	K_c'	-	J''	K_a''	K_c''	Frequency	Deviation
9	9	0	-	8	8	1	56484.849	-0.049
9	9	1	-	8	8	0	56484.849	-0.049
11	11	1	-	10	10	0	69289.964	-0.005
11	10	2	-	10	9	1	66998.526	0.037
11	10	1	-	10	9	2	66998.526	0.036
11	11	0	-	10	10	1	69289.964	-0.005
12	11	1	-	11	10	2	73401.009	-0.025
12	10	3	-	11	9	2	71107.230	-0.007
12	10	2	-	11	9	3	71107.230	-0.013
12	11	2	-	11	10	1	73401.009	-0.025
13	12	1	-	12	11	2	79803.277	0.043
13	12	2	-	12	11	1	79803.277	0.043
16	1	16	-	15	0	15	59902.244	0.002
16	0	16	-	15	1	15	59902.244	0.007
17	4	14	-	16	3	13	68015.821	-0.013
17	0	17	-	16	1	16	63600.718	-0.002
17	1	17	-	16	0	16	63600.718	-0.004
18	3	16	-	17	2	15	70186.658	-0.005
18	0	18	-	17	1	17	67299.151	0.020
18	1	18	-	17	0	17	67299.151	0.020
18	1	17	-	17	2	16	68737.692	0.028
18	2	17	-	17	1	16	68737.692	-0.017
18	2	16	-	17	3	15	70184.905	-0.021
18	3	15	-	17	4	14	71640.454	-0.027
19	2	18	-	18	1	17	72435.562	-0.012
19	0	19	-	18	1	18	70997.477	0.013
19	1	19	-	18	0	18	70997.477	0.013
19	1	18	-	18	2	17	72435.562	0.005
20	1	20	-	19	0	19	74695.736	0.024
20	0	20	-	19	1	19	74695.736	0.024
21	2	20	-	20	1	19	79831.211	-0.029
21	1	20	-	20	2	19	79831.211	-0.027
34	26	9	-	34	25	10	57914.254	0.007
34	26	8	-	34	25	9	57914.254	0.007
37	26	12	-	37	25	13	57649.282	0.001
37	26	11	-	37	25	12	57649.282	0.001
37	25	13	-	37	24	14	55232.635	-0.011
37	25	12	-	37	24	13	55232.635	-0.011
38	24	15	-	38	23	16	52653.261	0.010
38	24	14	-	38	23	15	52653.261	0.010
39	26	14	-	39	25	15	57430.176	0.001
39	26	13	-	39	25	14	57430.176	0.001
44	24	21	-	44	23	22	51525.025	0.001
44	24	20	-	44	23	21	51525.025	0.005

Table-3.5 Continued(1)

J'	K_a'	K_c'	-	J''	K_a''	K_c''	Frequency	Deviation
47	7	40	-	47	6	41	55266.660	-0.005
47	8	40	-	47	7	41	55266.660	-0.005
50	9	41	-	50	8	42	55570.606	0.020
50	10	41	-	50	9	42	55570.606	0.019
51	31	21	-	51	30	22	68097.670	-0.028
51	31	20	-	51	30	21	68097.679	-0.019
51	10	41	-	51	9	42	54918.443	0.002
51	11	41	-	51	10	42	54918.443	0.001
51	27	25	-	51	26	26	57779.638	-0.009
51	27	24	-	51	26	25	57779.638	-0.007
52	32	21	-	52	31	22	70434.079	0.020
52	12	41	-	52	11	42	54205.877	-0.006
52	32	20	-	52	31	21	70434.079	0.020
52	31	22	-	52	30	23	67935.792	0.000
52	31	21	-	52	30	22	67935.792	0.000
52	27	25	-	52	26	26	57507.889	0.010
52	27	26	-	52	26	27	57507.889	0.003
52	11	41	-	52	10	42	54205.877	0.001
53	32	22	-	53	31	23	70279.761	0.009
53	10	43	-	53	9	44	57877.463	-0.010
53	32	21	-	53	31	22	70279.761	0.009
53	31	22	-	53	30	23	67762.905	0.019
53	31	23	-	53	30	24	67762.905	0.019
53	11	43	-	53	10	44	57877.463	-0.010
54	32	23	-	54	31	24	70115.201	-0.035
54	13	42	-	54	12	43	54940.506	-0.010
54	31	24	-	54	30	25	67578.333	0.008
54	31	23	-	54	30	24	67578.333	0.008
54	12	42	-	54	11	43	54940.506	0.008
54	32	22	-	54	31	23	70115.201	-0.035
55	32	24	-	55	31	25	69939.915	-0.011
55	32	23	-	55	31	24	69939.915	-0.011
58	33	26	-	58	32	27	71927.730	0.009
58	33	25	-	58	32	26	71927.730	0.009
59	34	26	-	59	33	27	74292.545	0.012
59	33	26	-	59	32	27	71727.106	-0.060
59	33	27	-	59	32	28	71727.106	-0.060
59	34	25	-	59	33	26	74292.545	0.012
60	33	27	-	60	32	28	71514.100	-0.005
60	33	28	-	60	32	29	71514.100	-0.005
61	34	28	-	61	33	29	73899.818	0.047
61	33	29	-	61	32	30	71287.789	-0.012
61	33	28	-	61	32	29	71287.789	-0.012
61	34	27	-	61	33	28	73899.818	0.047
68	35	34	-	68	34	35	74860.882	-0.019
68	35	33	-	68	34	34	74860.882	-0.019

Table-3.5 Continued(2)

J'	K_a'	K_c'	-	J''	K_a''	K_c''	Frequency	Deviation
69	35	35	-	69	34	36	74574.596	0.049
69	35	34	-	69	34	35	74574.596	0.049
69	34	35	-	69	33	36	71775.932	0.036
69	34	36	-	69	33	37	71775.932	0.034
70	35	36	-	70	34	37	74271.326	-0.028
70	35	35	-	70	34	36	74271.326	-0.028
71	34	38	-	71	33	39	71068.500	-0.017
71	34	37	-	71	33	38	71068.500	-0.004
73	36	38	-	73	35	39	76124.788	-0.012
73	36	37	-	73	35	38	76124.788	-0.011
74	36	38	-	74	35	39	75787.411	0.186
76	37	40	-	76	36	41	77964.627	-0.008
76	37	39	-	76	36	40	77964.627	-0.007
78	37	42	-	78	36	43	77236.534	0.002
78	37	41	-	78	36	42	77236.534	0.007

Table-3.6
Observed Rotational Transition Frequencies(in MHz) of $^{35}Cl_2^{34}S^{18}O_2$.

J'	K_a'	K_c'	-	J''	K_a''	K_c''	Frequency	Deviation
11	11	0	-	10	10	1	69661.121	-0.046
11	10	2	-	10	9	1	67427.094	0.017
11	10	1	-	10	9	2	67427.094	0.016
11	11	1	-	10	10	0	69661.121	-0.046
12	12	0	-	11	11	1	76094.376	-0.026
12	10	3	-	11	9	2	71624.172	0.005
12	10	2	-	11	9	3	71624.172	-0.002
12	11	2	-	11	10	1	73860.816	0.054
12	11	1	-	11	10	2	73860.816	0.054
12	12	1	-	11	11	0	76094.376	-0.026
15	1	15	-	14	0	14	57352.459	-0.002
15	0	15	-	14	1	14	57352.459	0.006
16	1	16	-	15	0	15	61127.382	-0.001
16	0	16	-	15	1	15	61127.382	0.002
17	4	14	-	16	3	13	69315.961	0.047
17	3	15	-	16	2	14	67803.724	-0.042
18	4	15	-	17	3	14	73062.881	-0.005
18	0	18	-	17	1	17	68677.015	-0.008
18	1	18	-	17	0	17	68677.015	-0.009
18	1	17	-	17	2	16	70121.360	0.011
18	2	17	-	17	1	16	70121.360	-0.016
18	3	15	-	17	4	14	73037.964	0.007
19	3	16	-	18	4	15	76812.155	-0.013
19	0	19	-	18	1	18	72451.740	0.013
19	1	19	-	18	0	18	72451.740	0.013
19	1	18	-	18	2	17	73895.638	0.002

Table-3.6 Continued

J'	K_a'	K_c'	-	J''	K_a''	K_c''	Frequency	Deviation
19	2	18	-	18	1	17	73895.638	-0.008
49	32	18	-	49	31	19	68930.117	0.041
49	32	17	-	49	31	18	68930.117	0.041
50	32	19	-	50	31	20	68792.448	-0.055
50	32	18	-	50	31	19	68792.448	-0.055
50	28	22	-	50	27	23	58881.592	-0.014
50	28	23	-	50	27	24	58881.592	-0.014
51	28	23	-	51	27	24	58641.666	0.012
51	28	24	-	51	27	25	58641.666	0.011
52	28	24	-	52	27	25	58383.564	-0.019
52	28	25	-	52	27	26	58383.564	-0.021
53	32	22	-	53	31	23	68320.602	0.018
53	28	25	-	53	27	26	58106.011	0.028
53	28	26	-	53	27	27	58106.011	0.024
53	32	21	-	53	31	22	68320.602	0.018
56	32	25	-	56	31	26	67747.195	0.010
56	32	24	-	56	31	25	67747.195	0.010
59	32	28	-	59	31	29	67052.696	-0.015
59	32	27	-	59	31	28	67052.696	-0.015

Table-3.7

Observed Rotational Transition Frequencies(in MHz) of $^{37}Cl_2^{32}S^{16}O_2$.

J'	K_a'	K_c'	-	J''	K_a''	K_c''	Frequency	Deviation
9	9	1	-	8	8	0	60377.384	0.023
10	10	1	-	9	9	0	67237.236	0.000
10	9	2	-	9	8	1	64497.477	-0.040
12	9	3	-	11	8	4	72728.255	-0.067
12	9	4	-	11	8	3	72728.255	0.040
13	10	4	-	12	9	3	79590.906	0.041
14	1	13	-	13	2	12	54100.673	0.066
15	1	14	-	14	2	13	57794.530	-0.012
15	1	15	-	14	0	14	56200.719	-0.060
15	0	15	-	14	1	14	56200.719	-0.013
15	2	14	-	14	1	13	57797.398	-0.040
16	1	16	-	15	0	15	59893.983	0.010
16	0	16	-	15	1	15	59893.983	0.028
17	1	17	-	16	0	16	63587.131	0.016
18	0	18	-	17	1	17	67280.193	0.003
18	1	18	-	17	0	17	67280.193	0.001
18	4	14	-	17	5	13	73227.723	-0.004
20	0	20	-	19	1	19	74666.104	-0.007
20	1	19	-	19	2	18	76257.537	0.045
20	1	20	-	19	0	19	74666.104	-0.007
20	2	19	-	19	1	18	76257.537	0.019
21	1	20	-	20	2	19	79949.849	-0.034
21	0	21	-	20	1	20	78358.972	0.033
21	2	20	-	20	1	19	79949.849	-0.044

Table-3.8
Observed Rotational Transition Frequencies(in MHz) of $^{35}Cl^{37}Cl^{34}S^{18}O_2$.

J'	K_a'	K_c	-	J''	K_a''	K_c'	Frequency	Deviation
11	11	0	-	10	10	1	69093.139	0.003
11	10	2	-	10	9	1	66817.999	0.019
11	10	1	-	10	9	2	66817.999	0.019
11	11	1	-	10	10	0	69093.139	0.003
12	11	1	-	11	10	2	73201.863	-0.021
12	10	3	-	11	9	2	70924.376	0.023
12	10	2	-	11	9	3	70924.376	0.017
12	11	2	-	11	10	1	73201.863	-0.020
13	7	7	-	12	6	6	67774.025	-0.064
16	5	12	-	15	4	11	66670.798	-0.018
16	0	16	-	15	1	15	59804.065	0.010
16	1	16	-	15	0	15	59804.065	0.006
17	4	14	-	16	3	13	67912.764	-0.077
17	0	17	-	16	1	16	63496.329	0.002
17	1	17	-	16	0	16	63496.329	0.001
18	3	15	-	17	4	14	71538.443	0.048
18	0	18	-	17	1	17	67188.533	0.006
18	1	18	-	17	0	17	67188.533	0.005
18	1	17	-	17	2	16	68629.610	0.024
18	2	17	-	17	1	16	68629.610	-0.015
18	2	16	-	17	3	15	70079.313	0.062
19	1	19	-	18	0	18	70880.653	0.002
19	0	19	-	18	1	18	70880.653	0.002
20	1	20	-	19	0	19	74572.692	0.000
20	0	20	-	19	1	19	74572.692	0.000
21	1	21	-	20	0	20	78264.627	-0.018
21	0	21	-	20	1	20	78264.627	-0.018
49	31	18	-	49	30	19	67856.659	0.001
50	31	19	-	50	30	20	67711.203	-0.037
51	31	20	-	51	30	21	67555.700	-0.013
52	31	21	-	52	30	22	67389.499	0.015
53	31	22	-	53	30	23	67211.960	0.045
57	32	26	-	57	31	27	68973.612	-0.001
57	32	25	-	57	31	26	68973.612	-0.001
59	32	28	-	59	31	29	68524.458	0.007
59	32	27	-	59	31	28	68524.458	0.007
61	32	30	-	61	31	31	68015.441	0.022
61	32	29	-	61	31	30	68015.441	0.022
64	33	32	-	64	32	33	69885.932	-0.027
64	33	31	-	64	32	32	69885.932	-0.026
65	33	33	-	65	32	34	69589.144	-0.037
65	33	32	-	65	32	33	69589.144	-0.036
66	33	34	-	66	32	35	69273.673	0.032
66	33	33	-	66	32	34	69273.673	0.034

Table-3.9
Observed Rotational Transition Frequencies(in MHz) of $^{35}Cl_2{}^{34}S^{16}O_2$.

J'	K_a'	K_c'	-	J''	K_a''	K_c''	Frequency	Deviation
15	1	15	-	14	0	14	58599.250	-0.010
15	0	15	-	14	1	14	58599.250	0.014
16	1	16	-	15	0	15	62451.685	-0.037
16	0	16	-	15	1	15	62451.685	-0.029
17	5	13	-	16	4	12	73732.397	0.020
17	0	17	-	16	1	16	66304.119	0.000
17	1	17	-	16	0	16	66304.119	-0.003
17	2	15	-	16	3	14	69537.120	-0.003
17	3	14	-	16	4	13	71135.596	0.016
17	3	15	-	16	2	14	69544.693	-0.018
17	4	14	-	16	3	13	71276.566	0.009
17	4	13	-	16	5	12	72228.179	0.022
18	4	15	-	17	3	14	75075.234	-0.025
18	0	18	-	17	1	17	70156.480	0.033
18	1	18	-	17	0	17	70156.480	0.032
18	2	16	-	17	3	15	73388.182	0.004
18	3	15	-	17	4	14	75012.338	0.001
18	3	16	-	17	2	15	73391.236	-0.005
19	2	18	-	18	1	17	75618.888	-0.047
19	0	19	-	18	1	18	74008.727	0.038
19	1	19	-	18	0	18	74008.727	0.037
19	1	18	-	18	2	17	75618.888	-0.017
20	2	19	-	19	1	18	79470.571	-0.039
20	0	20	-	19	1	19	77860.858	0.017
20	1	20	-	19	0	19	77860.858	0.017
20	1	19	-	19	2	18	79470.571	-0.028

Table-3.10
Observed Rotational Transition Frequency(in MHz) of $^{35}Cl^{37}Cl^{34}S^{16}O_2$.

J'	K_a'	K_c'	-	J''	K_a''	K_c''	Frequency	Deviation
15	1	15	-	14	0	14	57328.239	-0.018
15	0	15	-	14	1	14	57328.239	0.014
16	1	16	-	15	0	15	61096.250	-0.008
16	0	16	-	15	1	15	61096.250	0.004
18	1	18	-	[illegible]	[illegible]	17	68632.077	0.002
18	0	18	-	[illegible]	1	17	68632.077	0.004
19	2	18	-	[illegible]	1	17	74002.257	-0.022
19	0	19	-	18	1	18	72399.866	-0.002
19	1	19	-	18	0	18	72399.866	-0.002
19	1	18	-	18	2	17	74002.257	0.022
20	1	20	-	19	0	19	76167.586	0.011
20	0	20	-	19	1	19	76167.586	0.011
21	1	21	-	20	0	20	79935.179	-0.008
21	0	21	-	20	1	20	79935.179	-0.008

3.2 The Calculation of the Rotational Constants and Distortion Constants of Sulphuryl Chloride.

Watson's S reduction Hamiltonian in the I^r representation[45][47], equations (1.1.20) to (1.1.28), was used to fit the observed rotational frequencies and calculate the required constants. The constants of $^{35}Cl_2^{32}S^{16}O_2$ and $^{35}Cl^{37}Cl^{32}S^{16}O_2$ obtained by Dubrulle and Boucher[69][70] were used as trial values in these refinements. For these two species, more and higher J transitions, including some very high J lines with low K_a, which are very weak and not observed in previous work[69][70], were measured and much improved constants were eventually derived, as shown in Table-3.14. Both R-branch(J up to about 25) and Q-branch(J up to 80) transitions were measured and so it was not difficult to calculate values for the rotational constants and all of the quartic distortion constants, for six species, which were $^{35}Cl_2^{32}S^{16}O_2$, $^{35}Cl^{37}Cl^{32}S^{16}O_2$, $^{35}Cl_2^{32}S^{18}O_2$, $^{35}Cl^{37}Cl^{32}S^{18}O_2$, $^{35}Cl_2^{34}S^{18}O_2$ and $^{35}Cl^{37}Cl^{34}S^{18}O_2$. Because the experiments on the species $^{37}Cl_2^{32}S^{16}O_2$, $^{35}Cl_2^{34}S^{16}O_2$ and $^{35}Cl^{37}Cl^{34}S^{16}O_2$ were done in natural abundance, only a limited set of R-branch lines could be observed. It was impossible to derive all the quartic distortion constants from only the R-branch transitions. In order to fit the rotational frequencies for these three species, the following procedure was used. At first, a harmonic force field was derived from the distortion constants of the previous six species, together with the vibrational frequencies. Then the distortion constants of the latter three species were calculated from the harmonic force field. The calculated values for distortion constants were then used to fit the experimental microwave frequencies. Good fits, yielding values for three rotational constants and several distortion constants were obtained for $^{37}Cl_2^{32}S^{16}O_2$ and $^{35}Cl_2^{34}S^{16}O_2$. Only $J_{0J} \leftarrow (J-1)_{1,J-1}$ and $J_{1J} \leftarrow (J-1)_{0,J-1}$ transitions were measured for $^{35}Cl^{37}Cl^{34}S^{16}O_2$ and so a good estimate for the A rotational constant could not be derived. A value for the rotational constant A calculated from the effective structure, which was obtained from the first six species, was used to fit the experimental lines and to allow refinement of the other two rotational constants of this species. All of the resulting rotational constants and distortion constants, including the calculated constants of the last three species, are given in Tables 3.11 to 3.13.

No sextic distortion constants were required to fit the experimental frequencies, even though transitions with J up to 80 and beyond were assigned for some species. The standard deviations of the fit were smaller than $0.05 MHz$ for all isotopomers investigated, as shown in Table-3.13.

Table-3.11 Effective Rotational Constants of Cl_2SO_2 Isotopomers

Isotopomer	A (MHz)	B (MHz)	C (MHz)	κ
$^{35}Cl_2^{32}S^{16}O_2$	3485.85392(54)	2344.24647(55)	1930.31011(57)	-0.468
$^{35}Cl^{37}Cl^{32}S^{16}O_2$	3459.36647(46)	2293.79236(49)	1888.07484(44)	-0.484
$^{35}Cl_2^{32}S^{18}O_2$	3226.49981(59)	2278.77573(75)	1890.88090(70)	-0.419
$^{35}Cl^{37}Cl^{32}S^{18}O_2$	3201.87425(43)	2230.92443(67)	1849.59852(78)	-0.436
$^{35}Cl_2^{34}S^{18}O_2$	3217.44368(71)	2278.8688(16)	1887.7939(15)	-0.412
$^{35}Cl^{37}Cl^{34}S^{18}O_2$	3192.55831(78)	2230.9922(27)	1846.4880(13)	-0.429
$^{37}Cl_2^{32}S^{16}O_2$	3430.6048(18)	2245.567(13)	1846.9493(16)	-0.497
$^{35}Cl_2^{34}S^{16}O_2$	3473.6588(15)	2344.3374(14)	1926.5949(10)	-0.460
$^{35}Cl^{37}Cl^{34}S^{16}O_2$	3446.7949(*)	2293.8655(51)	1884.3577(57)	-0.476

Table-3.12 Effective Moments of Inertia of Cl_2SO_2 Isotopomers

Isotopomer	I^0_A $(amuA^2)$	I^0_B $(amuA^2)$	I^0_C $(aumA^2)$
$^{35}Cl_2^{32}S^{16}O_2$	144.97997(2)	215.58271(5)	261.81234(8)
$^{35}Cl^{37}Cl^{32}S^{16}O_2$	146.09005(2)	220.32465(5)	267.66894(8)
$^{35}Cl_2^{32}S^{18}O_2$	156.63382(3)	221.77654(7)	267.27173(10)
$^{35}Cl^{37}Cl^{32}S^{18}O_2$	157.83848(2)	226.53345(7)	273.23713(12)
$^{35}Cl_2^{34}S^{18}O_2$	157.07470(3)	221.76748(15)	267.70878(22)
$^{35}Cl^{37}Cl^{34}S^{18}O_2$	158.29907(4)	226.52657(27)	273.69742(19)
$^{37}Cl_2^{32}S^{16}O_2$	147.31484(8)	225.05632(131)	273.62906(23)
$^{35}Cl_2^{34}S^{16}O_2$	145.48896(6)	215.57435(14)	262.31721(14)
$^{35}Cl^{37}Cl^{34}S^{16}O_2$	146.62288(*)	220.31762(49)	268.19695(8)

*--Calculated from the effective molecular structure.

Table-3.13 Quartic Distortion Constants of Cl_2SO_2 Isotopomers

Isotopomer	$D_J(kHz)$	$D_{JK}(kHz)$	$D_K(kHz)$
$^{35}Cl_2^{32}S^{16}O_2$	0.4704(11)	-0.7362(2)	1.6750(5)
$^{35}Cl^{37}Cl^{32}S^{16}O_2$	0.4468(5)	-0.7102(2)	1.6557(3)
$^{35}Cl_2^{32}S^{18}O_2$	0.4268(10)	-0.6218(5)	1.3281(7)
$^{35}Cl^{37}Cl^{32}S^{18}O_2$	0.4143(10)	-0.5999(3)	1.3121(3)
$^{35}Cl_2^{34}S^{18}O_2$	0.4296(21)	-0.6189(21)	1.3266(21)
$^{35}Cl^{37}Cl^{34}S^{18}O_2$	0.4197(21)	-0.6013(14)	1.3180(20)
$^{37}Cl_2^{32}S^{16}O_2$	0.4335(88)	-0.6957(39)	1.6597(*)
$^{35}Cl_2^{34}S^{16}O_2$	0.4647(15)	-0.7362(*)	1.6638(*)
$^{35}Cl^{37}Cl^{34}S^{16}O$	0.4480(73)	-0.7104(*)	1.6634(*)

Isotopomer	$d_1(kHz)$	$d_2(kHz)$	$\varepsilon\ (MHz)$
$^{35}Cl_2^{32}S^{16}O_2$	-0.12751(1)	-0.000033(7)	0.0360
$^{35}Cl^{37}Cl^{32}S^{16}O_2$	-0.12322(3)	-0.00094(2)	0.0491
$^{35}Cl_2^{32}S^{18}O_2$	-0.11338(2)	0.00190(1)	0.0385
$^{35}Cl^{37}Cl^{32}S^{18}O_2$	-0.1096(1)	0.00118(3)	0.0228
$^{35}Cl_2^{34}S^{18}O_2$	-0.1146(7)	0.0012(4)	0.0287
$^{35}Cl^{37}Cl^{34}S^{18}O_2$	-0.1120(4)	0.0013(*)	0.0294
$^{37}Cl_2^{32}S^{16}O_2$	-0.1196(53)	-0.0010(*)	0.0448
$^{35}Cl_2^{34}S^{16}O_2$	-0.1278(*)	0.0001(*)	0.0262
$^{35}Cl^{37}Cl^{34}S^{16}O_2$	-0.1233(*)	-0.0005(*)	0.0134

*--Calculated from the harmonic force field of Table-3.25.

ε--Standard deviation of the fit.

3.3 The Calculation of the Molecular Structure of Sulphuryl Chloride

The effective principal moments of inertia of all isotopic species studied are given in Table-3.12; these were derived from the effective rotational constants of Table-3.11. The ground state effective structural parameters, r_0, were calculated principally using the effective rotational constants of ${}^{35}Cl_2^{32}S^{16}O_2$, ${}^{35}Cl^{37}Cl^{32}S^{16}O_2$, ${}^{35}Cl_2^{32}S^{18}O_2$, ${}^{35}Cl^{37}Cl^{32}S^{18}O_2$, ${}^{35}Cl_2^{34}S^{18}O_2$ and ${}^{35}Cl^{37}Cl^{34}S^{18}O_2$. An uncertainty 0.1% Of the observed value was assigned to these rotational constants in a weighted least squares fit. The principal moments of inertia of ${}^{37}Cl_2^{32}S^{16}O_2$ and ${}^{35}Cl_2^{34}S^{16}O_2$ were also used in this calculation but a bigger uncertainty, 0.2%, was set for them, because they were obtained from only R-branch transitions. The principal moments of inertia of ${}^{35}Cl^{37}Cl^{34}S^{16}O_2$, which were not well determined in this work, were not considered in this calculation. Since there is no light atom in this molecule, the differences in the effects of zero point vibrations for different isotopic species are expected to be very small[31]. The resulting effective structure is listed in the first row of Table-3.14. The effective structure was used in the calculation of force constants, which will be discussed later.

We have obtained sufficient isotopic data to calculate all of the structural parameters of this molecule. Two partial substitution structures have been obtained for the ground state. One used ${}^{35}Cl_2^{32}S^{18}O_2$ as the parent species and ${}^{35}Cl_2^{32}S^{16}O_2$ and ${}^{35}Cl^{37}Cl^{32}S^{18}O_2$ as the substituted species. The other used ${}^{35}Cl_2^{32}S^{16}O_2$ as the parent species and ${}^{35}Cl_2^{32}S^{18}O_2$ and ${}^{35}Cl^{37}Cl^{32}S^{16}O_2$ as the substituted species. The coordinates of Cl and O were derived using Kraitchman's method, equation(1.3.8). Due to the symmetry of this molecule, the sulphur atom is on the symmetry axis and both the sulfur a coordinate and the sulphur c coordinate are zero. Because the sulphur atom is located too close to the mass center, a good estimate of its b coordinate could not be obtained by Kraitchman's method[29][30] and the b coordinate of sulphur was therefore calculated using the center mass condition, equation(1.3.12). The principal axes coordinates of $^{35}Cl_2^{32}S^{16}O_2$ and $^{35}Cl_2^{32}S^{18}O_2$ are given in Table-3.15 and Table-3.16, respectively. The substitution parameters are listed in Table-3.14, which shows that the two substitution structures are almost the same.

Two different scaled geometries have also been calculated with $^{35}Cl_2^{32}S^{18}O_2$ and $^{35}Cl_2^{32}S^{16}O_2$ as the parent species, respectively. The scaled constants derived from equation(1.3.19) were $\rho_A = 0.99256$, $\rho_B = 0.99812$ and $\rho_C = 0.997146$ for $^{35}Cl_2^{32}S^{18}O_2$ and $\rho_A = 0.999610$, $\rho_B = 0.998324$ and $\rho_C = 0.997528$ for $^{35}Cl^{32}S^{16}O_2$. The scaled moments of inertia were obtained using the above scaled constants and the effective moments of inertia, in Table-3.12, according to equation(1.3.18). The same procedure, which was used to calculate the effective structure from the effective rotational constants, was applied here to derive the scaled structure from the scaled rotational constants. The results are also shown in Table-3.14.

The calculation of the harmonic force field will be discussed later, however, the resulting force constants, Table-3.25, are used in this section to derive the harmonic vibration-rotation interaction constants, the zero point mean square amplitude, u^2, and the zero point perpendicular amplitude, K, from which the average structure and equilibrium structure of sulphuryl chloride could be evaluated. The average rotational constants, A_z, B_z and C_z, were obtained by equation-1.3.15 and are listed in Table-3.17. At least two isotopic species are required to derive all of the four geometrical parameters, therefore the isotopic variations of the bond lengths should be considered in the calculation of the average structure. The isotopic variations of bond lengths were calculated from u^2 and K, both of which were derived from the harmonic force field[39], using Equation-1.3.4. The values of the Morse anharmonic parameter were $a(SO) = 2.072\text{Å}^{-1}$ and $a(SCl) = 1.706\text{Å}^{-1}$, both taken from Kuchitsu and Morino's publication[92], where the value of $a(SCl)$ was the average of $a(S_2)$ and $a(Cl_2)$. The mean square amplitude of vibration of the bonds and the mean perpendicular amplitude, as well as their corresponding isotopic changes, are given in Table-3.19 and Table-3.20. The isotopic variations of the average bond lengths δr_z were evaluated using equation-1.3.4 and are listed in Table-4.18, which shows that the values are about 10^{-5} to 10^{-4}Å. The obtained average rotational constants and the isotopic variations of the average bond lengths were applied to derive the average structure for this molecule by a least squares procedure, which we had used as well to calculate the effective structure. A crude equilibrium structure was evaluated from the average structure, with the help of equation-1.3.3. In the calculations of both of these structures, the normal species $^{35}Cl_2^{32}S^{16}O_2$ was the parent species. The results are collected in Table-3.14. A theoretical structure of this molecule was also derived, for comparison with the experimental structures, using the 6-31G* basis set and the Gaussian-86 program[83].

The different structures show only slight variations from one to another. The SCl bond lengths follow the trend $r_z > r_0 > r_s > r_m^\rho > r_e > r_{ab\text{-}initio}$. The SO bond lengths also follow this order, except r_0, which is a little shorter than r_s. Table-3.21 gives a comparison of the structure of Cl_2SO_2 with that of SO_2 [95][96], Cl_2SO [95][136] and SCl_2 [13]. The SO bond of Cl_2SO_2 is about 0.015Å and 0.02Å shorter than that of Cl_2SO and SO_2, respectively. The SCl bond of Cl_2SO_2 is only 0.004Å shorter than that of SCl_2, but more than 0.06Å shorter than that of Cl_2SO. The OSO angle is about 4.7° bigger than that of SO_2. The $ClSCl$ angle is about 3.2° bigger but 2.6° smaller than that of Cl_2SO and of Cl_2S, respectively. Figure-3.2 and Figure-3.3 give the principal axes orientations of $^{35}Cl_2^{32}S^{16}O_2$ and $^{35}Cl^{37}Cl^{32}S^{16}O_2$, respectively. Because of the unsymmetric isotopic substitution of ^{37}Cl, the $^{35}Cl^{37}Cl^{32}S^{16}O_2$ species has C_s symmetry and the principal axis b no longer divides the $ClSCl$ angle equally. The angle between $S^{35}Cl$ bond and the principal axes b is 40.552° and the principal axis b has been shifted from the OSO plane by about 1.82°.

Table-3.14

The Molecular Geometries of Cl_2SO_2

Parameter	$Bond_{SO}$/Å	$Bond_{SCl}$/Å	$Angle_{OSO}$/°	$Angle_{ClSCl}$/°
r_0	1.41217(10)	2.01065(10)	123.230(15)	100.117(7)
r_s(I)	1.41249(74)	2.00934(167)	123.300(72)	100.099(92)
r_s(II)	1.41232(95)	2.00978(178)	123.326(90)	100.081(95)
r_m^ρ(III)	1.41211(10)	2.00866(10)	123.476(15)	100.035(6)
r_m^ρ(IV)	1.41227(10)	2.00897(9)	123.447(15)	100.033(6)
r_z	1.41347(11)	2.01124(10)	123.129(15)	100.126(7)
r_e	1.41186(21)	2.00705(18)	**	**
$r^*_{ab-initio}$	1.4096(2)	1.9985(0)	123.571(0)	101.257(0)

(I) Obtained using $^{35}Cl_2^{32}S^{18}O_2$ as the parent isotopomer.

(II) Obtained using $^{35}Cl_2^{32}S^{16}O_2$ as the parent isotopomer.

(III) Scaled geometry, using $^{35}Cl_2^{32}S^{18}O_2$ as the parent species.

(IV) Scaled geometry, using $^{35}Cl_2^{32}S^{16}O_2$ as the parent species.

(*) The ab-initio calculation was done by using the GAUSSIAN-86 program with a 6-31G* basis set[83].

(**) The angles were assumed to equal the value obtained in the r_z structure.

Table-3.15

The Substitution Principal Axes Coordinates (Å) of $^{35}Cl_2^{32}S^{16}O_2$.

Atoms	a	b	c
S	0.0	0.51404(29)	0.0
$O1$	0.0	1.18440(8)	1.24308(7)
$O2$	0.0	1.18440(8)	-1.24308(7)
$Cl1$	1.54049(10)	-0.77674(21)	0.0
$Cl2$	-1.54049(10)	-0.77674(21)	0.0

Table-3.16

The Substitution Principal Axes Coordinates (Å) of $^{35}Cl_2^{32}S^{18}O_2$

Atoms	a	b	c
S	0.0	0.47925(19)	0.0
$O1$	0.0	1.14998(7)	1.24308(7)
$O2$	0.0	1.14998(7)	-1.24308(7)
$Cl1$	1.54036(13)	-0.81100(28)	0.0
$Cl2$	-1.54036(13)	-0.81100(28)	0.0

Table-3.17 Average Rotational Constants of Cl_2SO_2

Species	A_z (MHz)	B_z (MHz)	C_z (MHz)
$^{35}Cl_2^{32}S^{16}O_2$	3481.984	2341.976	1929.010
$^{35}Cl^{37}Cl^{32}S^{16}O_2$	3455.537	2291.592	1886.825
$^{35}Cl_2^{32}S^{18}O_2$	3223.070	2276.646	1889.601
$^{35}Cl^{37}Cl^{32}S^{18}O_2$	3198.484	2228.854	1848.359
$^{35}Cl_2^{34}S^{18}O_2$	3214.024	2276.739	1886.514
$^{35}Cl^{37}Cl^{34}S^{18}O_2$	3189.178	2228.922	1845.258
$^{37}Cl_2^{32}S^{16}O_2$	3426.825	2243.417	1845.739
$^{35}Cl_2^{34}S^{16}O_2$	3469.799	2342.077	1925.305
$^{35}Cl^{37}Cl^{34}S^{16}O_2$	3442.985	2291.656	1883.108

Table-3.18 The Isotopic Variation (Å) of Average Bond Lengths of Cl_2SO_2

Species	δr_{SO}	$\delta r_{S^{35}Cl}$	$\delta r_{S^{37}Cl}$
$^{35}Cl_2^{32}S^{16}O_2$			
$^{35}Cl^{37}Cl^{32}S^{16}O_2$			-0.0000474
$^{35}Cl_2^{32}S^{18}O_2$	-0.0000196		
$^{35}Cl^{37}Cl^{32}S^{18}O_2$	-0.0000276	-0.0000290	-0.0000718
$^{35}Cl_2^{34}S^{18}O_2$	-0.0000401	-0.0000748	
$^{35}Cl^{37}Cl^{34}S^{18}O_2$	-0.0000481	-0.0000848	-0.0001221
$^{37}Cl_2^{32}S^{16}O_2$	-0.000016		-0.0000567
$^{35}Cl_2^{34}S^{16}O_2$	-0.0000192	-0.0000505	
$^{35}Cl^{37}Cl^{34}S^{16}O_2$	-0.0000272	-0.0000605	-0.0000984

Table-3.19

The Parallel Mean Square Amplitudes (Å) of Cl_2SO_2

Species		SO	$S^{35}Cl$	$S^{37}Cl$
$^{35}Cl_2^{32}S^{16}O_2$	u^2	0.0011982	0.0019712	
$^{35}Cl^{37}Cl^{32}S^{16}O_2$	u^2	0.0011982	0.0019712	0.0019421
	$\delta\langle u^2\rangle$	0.0	0.0	-0.0000291
$^{35}Cl_2^{32}S^{18}O_2$	u^2	0.0011507	0.0019690	
	$\delta\langle u^2\rangle$	-0.0000475	0.0	
$^{35}Cl^{37}Cl^{32}S^{18}O_2$	u^2	0.0011507	0.0019690	0.001940
	$\delta\langle u^2\rangle$	-0.0000475	0.0	-0.0000316
$^{35}Cl_2^{34}S^{18}O_2$	u^2	0.0011396	0.0019435	
	$\delta\langle u^2\rangle$	-0.0000586	-0.0000277	
$^{35}Cl^{37}Cl^{34}S^{18}O_2$	u^2	0.0011396	0.00194435	0.0019140
	$\delta\langle u^2\rangle$	-0.0000586	-0.0000277	-0.0000571
$^{37}Cl_2^{32}S^{16}O_2$	u^2	0.0011981		0.0019420
	$\delta\langle u^2\rangle$	0.0		-0.0000292
$^{35}Cl_2^{34}S^{16}O_2$	u^2	0.0011875	0.0019456	
	$\delta\langle u^2\rangle$	-0.0000107	-0.0000256	
$^{35}Cl^{37}Cl^{34}S^{16}O_2$	u^2	0.0011875	0.0019456	0.0019163
	$\delta\langle u^2\rangle$	-0.0000107	-0.0000256	-0.0000549

Table-3.20

The Perpendicular Mean Amplititudes (K) of Cl_2SO_2

Species		SO	$S^{35}Cl$	$S^{37}Cl$
$^{35}Cl_2^{32}S^{16}O_2$	K	0.002109	0.000851	
$^{35}Cl^{37}Cl^{32}S^{16}O_2$	K	0.002117	0.000861	0.000824
	δK	0.000008	0.000010	-0.000027
$^{35}Cl_2^{32}S^{18}O_2$	K	0.001981	0.000870	
	δK	-0.000128	0.000019	
$^{35}Cl^{37}Cl^{32}S^{18}O_2$	K	0.001989	0.000880	0.000842
	δK	-0.000120	0.000029	-0.000009
$^{35}Cl_2^{34}S^{18}O_2$	K	0.001967	0.000855	
	δK	-0.000142	0.000004	
$^{35}Cl^{37}Cl^{34}S^{18}O_2$	K	0.001975	0.000865	0.000827
	δK	-0.000134	0.000014	-0.000024
$^{37}Cl_2^{32}S^{16}O_2$	K	0.002125		0.000833
	δK	0.000016		-0.000018
$^{35}Cl_2^{34}S^{16}O_2$	K	0.002095	0.000836	
	δK	-0.000014	-0.000015	
$^{35}Cl^{37}Cl^{34}S^{16}O_2$	K	0.002103	0.000846	0.000809
	δK	-0.000006	-0.000005	-0.000042

Table-3.21

Comparison between the Structure of Cl_2SO_2

and these of SO_2 [95][96], Cl_2SO [95][136] and SCl_2 [13]

Parameter		$Bond_{SO}/\AA$	$Bond_{SCl}/\AA$	$Angle_{OSO}/°$	$Angle_{ClSCl}/°$
r_0	Cl_2SO_2	1.41217(10)	2.01065(10)	123.230(15)	100.117(7)
	Cl_2SO	1.4278(5)	2.0744(3)		96.955(1)
	SCl_2		2.0140(30)		102.74(30)
	SO_2	1.43217		119.535	
r_e	Cl_2SO_2	1.41186(21)	2.00705(18)		
	SO_2	1.4308		119.33	
r_s	Cl_2SO_2	1.41249(74)	2.00934(167)	123.300(72)	100.099(92)
	Cl_2SO	1.4347(7)	2.0744(3)		96.820(14)
	SCl_2		2.0141(20)		102.64(20)

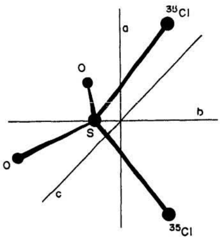

Figure-3.2 Principal Axes

Orientation of $^{35}Cl_2^{32}S^{16}O_2$

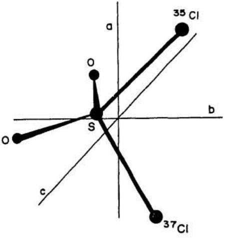

Figure-3.3 Principal Axes

Orientation of $^{35}Cl^{37}Cl^{32}S^{16}O_2$

3.4 The Harmonic Force Field of Sulphuryl Chloride

As discussed at the beginning of this chapter, there have been several papers concerned with the molecular vibrations of sulphuryl chloride[74][75][76][77][78][79][80][81]. In these works, however, there still are some problems which have not been satisfactorily resolved. The first is the assignment of the ν_7 and ν_9 modes. There are two lines around the frequency $370cm^{-1}$; it is very difficult to determine which of them is ν_7 or ν_9 using only the vibrational spectrum. That is because both of the modes belong to b symmetry species and are related to the vibrational motions of the OSO group, so that both the depolarization properties of the Raman spectra and the isotopic substitution shifts of the vibrational spectra do not distinguish between the two modes. The second is that Fermi resonance has never been considered in previous reports. The third is that the force field of this molecule has not been well refined using a sufficiently large data set. Therefore in this work we remeasured the Raman spectra for this molecule in both the liquid and gas phases and reinvestigated the force field using both our vibrational spectra and rotational spectroscopic data.

The Raman spectra of $^{35}Cl_2^{32}S^{16}O_2$, $^{35}Cl_2^{32}S^{18}O_2$ and $^{35}Cl_2^{34}S^{18}O_2$were measured in both the liquid and gas phases. The spectra of these three species in the liquid phase are given in Figure-3.4. The gas phase spectra were weak and the ν_7 and ν_9 lines were not observed. Figures 3.5, 3.6 and 3.7 show the gas phase Raman spectra of the three species over the frequency range of $1100cm^{-1}$ to $1250cm^{-1}$. There are three transitions; in each case the strongest line was assigned to ν_1 and the lowest frequency line was assigned to the symmetric stretch of a sulfur dioxide impurity[104]. The third lines could be overtone $2\nu_2$ or $2\nu_8$ bands or a combination band $\nu_2 + \nu_8$. Martz *et al* [75] assigned this line to $2\nu_2$ or $\nu_2 + \nu_8$ in their infrared work. After analysis of our Raman data, we did not assign this line to $2\nu_2$ nor to $\nu_2 + \nu_8$. Because the $\nu_2 + \nu_8$ mode belongs to the b_2 symmetry species and the ν_1 mode to the a_1 species, there is no Fermi resonance between these two modes and therefore the third line could not belong to $\nu_2 + \nu_8$ mode. By making a comparison between Figure-3.5 and Figure-3.6, we found that the frequencies of the ν_1 mode and SO_2 are about 60-70cm^{-1} decreased, however, the frequency of the third line is only about 7cm^{-1} decreased, because of the double ^{18}O substitution. In $^{35}Cl_2^{32}S^{16}O_2$, the third line has a lower frequency than ν_1; conversely, in $^{35}Cl_2^{32}S^{18}O_2$ and $^{35}Cl^{34}S^{18}O_2$, the third lines have higher frequencies than the correspondenting ν_1 modes. As we know that the ν_2 mode is the OSO scissors mode and the ν_8 mode is SCl asymmetric stretch, the ^{18}O substitution should change the frequency of ν_2 and therefore $2\nu_2$ a lot, but not that of ν_8 and $2\nu_8$. Actually, the ν_2 fundamentals are observed at frequencies 567.5cm^{-1}, 552.5cm^{-1} and 545.7cm^{-1}, Table-3.22 to 3.24, so that the frequencies of overtones $2\nu_2$ should be about 1135.0cm^{-1}, 1105.0cm^{-1} and 1091.4cm^{-1}, for $^{35}Cl_2^{32}S^{16}O_2$, $^{35}Cl_2^{32}S^{18}O_2$ and $^{35}Cl_2^{34}S^{18}O_2$, respectively. Therefore we assigned the third band in each case to $2\nu_8$. The ν_8 line were too weak to observe in the gas phase; however, the $2\nu_8$ lines were very strong due to the Fermi resonance between the ν_1 and $2\nu_8$ modes. Group theory also tells us that both the ν_1 and $2\nu_8$ modes belong to the same symmetry species, a_1. The method discussed in section-1.4 was used to correct for the effects of Fermi resonance. The intensities of the involved lines were calculated by assuming their line-shape functions were Lorentzian functions. The observed intensity ratios, ρ, were 0.194, 0.349 and 0.803 for $^{35}Cl_2^{32}S^{16}O_2$, $^{35}Cl_2^{32}S^{18}O_2$ and $^{35}Cl_2^{34}S^{18}O_2$, respectively. Here

$$\rho = \frac{I_{2\nu_8}}{I_{\nu_1}} \tag{3.4.1}$$

where $I_{2\nu_8}$ and I_{ν_1} are the observed line intensities of $2\nu_8$ and ν_1, respectively. The bigger the value of ρ, the stronger is the effect of the Fermi resonance. Then the corrected frequencies of ν_1 and $2\nu_8$ were derived from equation(1.4.14). The observed and Fermi resonance corrected frequencies of these modes are listed in Tables 3.22 to

3.24. The calculation showed that in $^{35}Cl_2^{32}S^{18}O_2$ and $^{35}Cl_2^{34}S^{18}O_2$ the Fermi resonance is much stronger than in $^{35}Cl_2^{32}S^{16}O_2$. The effect in $^{35}Cl_2^{34}S^{18}O_2$ is the strongest; the intensity of $2\nu_8$ is in this case almost as great as that of ν_1. The reason is that the substitution of ^{18}O and ^{34}S makes the frequencies of ν_1 and $2\nu_8$ shift towards each other. The Fermi resonance increases the frequency of ν_1 for the $^{35}Cl_2^{32}S^{16}O_2$ species by about $5.4 cm^{-1}$, but decreases that of $^{35}Cl_2^{32}S^{18}O_2$ and $^{35}Cl_2^{34}S^{18}O_2$ by 11.0 and $13.9 cm^{-1}$, respectively.

This molecule belongs to the C_{2v} symmetry point group and the structure of the representation generated by its vibrational modes has been given in equation(1.8.1). Because of the asymmetric substitution of ^{37}Cl, the C_{2v} symmetry is decreased to C_s symmetry. The a_1 and b_2 species of C_{2v} group construct the a' species in the C_s group, and the b_1 and a_2 species of the C_{2v} construct the a'' species of the C_s. C_s symmetry was used in the force field calculation. The symmetry coordinates were derived using the method discussed in section-1.8. The effective structure was employed in the force field refinement process.

The vibrational frequencies, Table-3.22 to Table-3.24, and the quartic distortion constants, Table-3.13, were used to derive the force field for this molecule. All of the gas phase Raman frequencies were used and 1% uncertainty was assumed. For the ν_7 and ν_9 modes, because no gas phase frequency was obtained, the liquid spectra data were used and a 3% uncertainty was assumed. Half the Fermi resonance corrected frequency of $2\nu_8$ was assigned to ν_8 and used in the calculation. The distortion constants of $^{35}Cl^{32}S^{16}O_2$, $^{35}Cl^{37}Cl^{32}S^{16}O_2$, $^{35}Cl^{32}S^{18}O_2$, $^{35}Cl^{37}Cl^{32}S^{18}O_2$ and $^{35}Cl_2^{34}S^{18}O_2$ were considered in the force field calculation, the distortion constants of other species were not used in the calculation; however, they were used to check the calculations. Duncan[48] suggested that in force constant calculations, uncertainties of some 2-5% of the individual values of the distortion constants should be used, even if the precision of their experimental determination was much greater. In this work a 3% uncertainty was assumed for these distortion constants.

Because the frequency of ν_1 is much higher than that of ν_2, ν_3 and ν_4, the data obtained is insensitive to the off-diagonal force constants $f_{1,2}$, $f_{1,3}$ and $f_{1,4}$, these were constrained to be zero in the calculation. For the same reason, the force constant $f_{6,7}$ was also assumed to be zero.

Two different calculations were done to facilitate the assignment of the ν_7 and ν_9 modes. The first calculation(I) assumed that the frequency of ν_7 was lower than that of ν_9 as suggested by Stammreich[103]. In the second one(II) the frequency of ν_7 was assumed to be higher than that of ν_9, as was suggested by references [79] and [81]. All the other conditions were the same for the two methods.

The calculated vibrational frequencies are listed in Table-3.22 to Table-3.24, the force constants are given in Table-3.25 and the quartic distortion constants are shown in Table-3.26.

The force constants derived from method(I) and method(II) are almost the same for the a_1 and a_2 symmetry species; for the b_1 and b_2 symmetry species $f_{7,7}$, $f_{9,9}$ and $f_{8,9}$ show big differences. The vibrational frequencies calculated by the two methods both agree well with the observed data. Therefore, it is very difficult to determine which assignment, (I) or (II), is correct, using only the vibrational frequencies. The quartic distortion constants, however, show some important differences between method(I) and method(II). In method(I), all of the calculated distortion constants agree very well with the constants obtained from the microwave spectra. In method(II), only the distortion constants D_J, D_{JK}, D_K, and d_1 are in accord with the observed data; d_2 cannot be fit at all as Table-4.26 shows. Therefore we assigned the ν_7 mode to have a higher frequency than the ν_9 mode. The harmonic force field calculated from method(I) was used to derive the average and equilibrium structures for this molecule, section-3.3. The calculated quartic distortion constants of $^{37}Cl_2^{32}S^{16}O_2$, $^{35}Cl_2^{34}S^{16}O_2$, $^{35}Cl^{37}Cl^{34}S^{16}O_2$ and $^{35}Cl^{37}Cl^{34}S^{18}O_2$ were used to fit the rotational frequencies.

In another calculation we tried to use the same procedure as above, but did not correct for the Fermi resonance. The observed ν_1 vibrational frequencies could not be fit well in this case. The differences between the calculated and observed vibrational frequencies were 1 to $15cm^{-1}$, for the three isotopomers, which were much bigger than those obtained in method(I) and method(II).

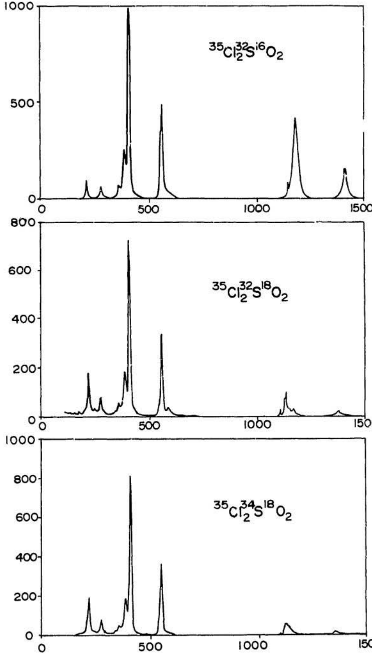

Figure-3.4

The Raman Spectra (cm^{-1}) of $^{35}Cl_2^{32}S^{16}O_2$, $^{35}Cl_2^{32}S^{18}O_2$ and $^{35}Cl_2^{34}S^{18}O_2$, in the Liquid Phase.

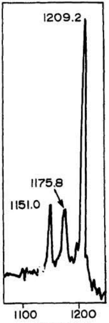

Figure-3.5

Gas Phase Raman Spectrum of $^{35}Cl_2^{32}S^{16}O_2$, which Shows Fermi Resonance between ν_1 and $2\nu_8$. The Lowest Frequency Line is $^{32}S^{16}O_2$.

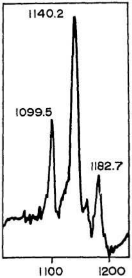

Figure-3.6

Gas Phase Raman Spectrum of $^{35}Cl_2^{32}S^{18}O_2$, which Shows Fermi Resonance between ν_1 and $2\nu_8$. The Lowest Frequency Line is $^{32}S^{18}O_2$.

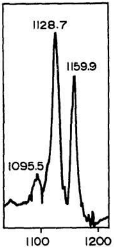

Figure-3.7

Gas Phase Raman Spectrum of $^{35}Cl_2^{34}S^{18}O_2$, which Shows Fermi Resonance between ν_1 and $2\nu_8$. The Lowest Frequency Line is $^{34}S^{18}O_2$.

Table-3.22

Vibrational Frequencies (in cm^{-1}) of $^{35}Cl_2^{32}S^{16}O_2$.

Mode		Raman		Inf.	Calculated	
ν	Liquid[a]	Liquid[b]	Gas[b]	Gas[a]	(I)	(II)
ν_1	1182.	1186.6	1209.2	1205.	1203.99	1204.19
			1203.8[c]			
ν_2	560.	564.1	567.5	577.	567.62	567.53
ν_3	408.	410.0	406.2		406.57	407.55
ν_4	218.	214.7	210.8		212.64	211.82
ν_5	282.	280.7	285.0		284.50	284.30
ν_6	1414.	1414.9	1436.7	1434.	1436.59	1436.46
ν_7	388.	364.0			362.96	386.67
ν_8	580.	590.0		586.	590.57	590.71
			590.6[d]			
ν_9	362.	390.0			388.02	364.98
$2\nu_8$			1175.8			
			1181.2[c]			

a--Reference[73]

b--This work.

c--Fermi resonance corrected.

d--Half the frequency of the Fermi resonance corrected $2\nu_8$ overtone.

(I)--Assumes that $\nu_7 < \nu_9$.

(II)-Assumes that $\nu_7 > \nu_9$.

Table-3.23

Vibrational Frequencies (in cm^{-1}) of $^{35}Cl_2^{32}S^{18}O_2$.

Mode	Raman		Calculated	
ν	Liquid	Gas	(I)	(II)
ν_1	1123.4	1140.2	1151.86	1153.58
		1151.2[a]		
ν_2	547.2	552.5	553.19	551.92
ν_3	398.5	396.5	396.88	397.58
ν_4	211.0	208.5	210.70	210.19
ν_5	266.3	272.2	272.01	271.83
ν_6	1370.5	1392.6	1394.14	1393.50
ν_7	352.0		350.60	373.64
ν_8		585.9[b]	585.48	588.57
ν_9	377.2		378.33	354.08
$2\nu_8$		1182.7		
		1171.7[a]		

a--Fermi resonance corrected.

b--Half the frequency of the $2\nu_8$ Fermi resonance corrected overtone.

(I)--Assumes that $\nu_7 < \nu_9$.

(II)-Assumes that $\nu_7 > \nu_9$.

Table-3.24

Vibrational Frequencies (in cm^{-1}) of $^{35}Cl_2^{34}S^{18}O_2$.

Mode	Raman		Calculated	
ν	Liquid	Gas	(I)	(II)
ν_1	1114.9	1128.7	1143.02	1143.90
		1142.6[a]		
ν_2	540.7	545.7	545.84	545.19
ν_3	398.6	396.2	396.86	397.53
ν_4	210.6	207.2	210.29	209.71
ν_5	266.2	272.1	272.01	271.83
ν_6	1351.8	1374.0	1373.25	1372.86
ν_7	348.2		348.31	371.13
ν_8		573.0[b]	572.60	576.10
ν_9	377.3		378.33	353.79
$2\nu_8$		1159.9		
		1146.0[a]		

a--Fermi resonance corrected.

b--Half the frequency of the Fermi resonance corrected $2\nu_8$ overtone.

(I)--Assumes that $\nu_7 < \nu_9$.

(II)-Assumes that $\nu_7 > \nu_9$.

Table-3.25 The Force Constants of Cl_2SO_2

a_1	1(I)	10.6842(1322)			
	1(II)	10.6842(751)			
	2(I)	0.0000	2.7874(650)		
	2(II)	0.0000	2.8092(450)		
	3(I)	0.0000	-0.2026(261)	1.1998(333)	
	3(II)	0.0000	-0.1828(168)	1.2040(222)	
	4(I)	0.0000	0.2652(192)	-0.2390(373)	1.2678(321)
	4(II)	0.0000	0.2439(118)	-0.1867(285)	1.2237(230)
a_2	5(I)	0.9018(95)			
	5(II)	0.9034(55)			
b_1	6(I)	10.6801(1276)			
	6(II)	10.6351(736)			
	7(I)	0.0000	1.2134(261)		
	7(II)	0.0000	1.4016(186)		
b_2	8(I)	2.3399(1517)			
	8(II)	2.7543(1162)			
	9(I)	-0.5020(613)	1.8327(1505)		
	9(II)	-0.3669(255)	1.3487(587)		

(I)--It was assumed for this refinement that $\nu_7 < \nu_9$

(II)-It was assumed for this refinement that $\nu_7 > \nu_9$

The units are $aJ\AA^{-2}$ for stretch-stretch, $aJ\AA^{-1}$ for stretch-bend and aJ for bend-bend constants.

Table-3.26 Quartic Distortion Constants of Cl_2SO_2

	Parameters	$^{35}Cl_2^{32}S^{16}O_2$	$^{35}Cl^{37}Cl^{32}S^{16}O_2$	$^{37}Cl_2^{32}S^{16}O_2$
D_J	Observed	0.4704	0.4468	0.4335
	Calculated(I)	0.4693	0.4517	0.4369
	Calculated(II)	0.4700	0.4527	0.4380
D_{JK}	Observed	-0.7362	-0.7102	-0.6957
	Calculated(I)	-0.7318	-0.7068	-0.7023
	Calculated(II)	-0.7368	-0.7128	-0.7092
D_K	Observed	1.6750	1.6557	
	Calculated(I)	1.6760	1.6564	1.6597
	Calculated(II)	1.6774	1.6586	1.6625
d_1	Observed	-0.1275	-0.1232	-0.1196
	Calculated(I)	-0.1273	-0.1229	-0.1195
	Calculated(II)	-0.1272	-0.1228	-0.1194
d_2	Observed	0.0000	-0.0009	
	Calculated(I)	-0.0001	-0.0006	-0.0010
	Calculated(II)	-0.0011	-0.0016	-0.0019

Table-3.26 Continued(1)

	Parameters	$^{35}Cl_2^{34}S^{16}O_2$	$^{35}Cl^{37}Cl^{34}S^{16}O_2$	$^{35}Cl_2^{32}S^{18}O_2$
D_J	Observed	0.4647	0.4480	0.4268
	Calculated(I)	0.4686	0.4510	0.4316
	Calculated(II)	0.4693	0.4519	0.4311
D_{JK}	Observed			-0.6218
	Calculated(I)	-0.7362	-0.7104	-0.6231
	Calculated(II)	-0.7435	-0.7187	-0.6189
D_K	Observed			1.3281
	Calculated(I)	1.6838	1.6634	1.3345
	Calculated(II)	1.6881	1.6883	1.3284
d_1	Observed			-0.1134
	Calculated(I)	-0.1278	-0.1233	-0.1132
	Calculated(II)	-0.1277	-0.1233	-0.1128
d_2	Observed		-0.0007	0.0019
	Calculated(I)		-0.0005	0.0018
	Calculated(II)	-0.0009	-0.0014	0.0006

Table-3.26 Continued(2)

	Parameters	$^{35}Cl^{37}Cl^{32}S^{18}O_2$	$^{35}Cl_2^{34}S^{18}O_2$	$^{35}Cl^{37}Cl^{34}S^{18}O_2$
D_J	Observed	0.4243	0.4296	0.4197
	Calculated(I)	0.4155	0.4312	0.4150
	Calculated(II)	0.4153	0.4307	0.4148
D_{JK}	Observed	-0.5999	-0.6188	-0.6013
	Calculated(I)	-0.5992	-0.6275	-0.6029
	Calculated(II)	-0.5963	-0.6251	-0.6018
D_K	Observed	1.3132	1.3259	1.3180
	Calculated(I)	1.3167	1.3419	1.3233
	Calculated(II)	1.3116	1.3380	1.3204
d_1	Observed	-0.1096	-0.1146	-0.1120
	Calculated(II)	-0.1095	-0.1135	-0.1098
	Calculated(II)	-0.1091	-0.1132	-0.1095
d_2	Observed	0.0012	0.0012	
	Calculated(I)	0.0012	0.0020	0.0013
	Calculated(II)	0.0000	0.0008	0.0002

(I)--Assumes that $\nu_7 < \nu_9$.

(II)-Assumes that $\nu_7 > \nu_9$.

3.5 The Nuclear Quadrupole Coupling in Sulphuryl Chloride

An initial prediction of the hyperfine splitting of $^{35}Cl_2^{32}S^{16}O_2$ was derived from the rotational constants and distortion constants calculated from the observed unsplit line transition frequencies and the quadrupole coupling constants given by Suzuki and Yamaguchi[141]. Analysis of our observed splittings by a least squares fit yielded the quadrupole coupling constant values reported here. All of the hyperfine structure observed in the present study was treated with a first order Hamiltonian. The method discussed in Section-1.9 was used in the calculations.

For $^{35}Cl^{32}S^{16}O_2$, the rotation C_2^b interchanges identical chlorine nuclei and the total wave function must be antisymmetric with respect to this operation. There are a total of $(2I_1+1)(2I_2+1)=16$ spin functions. The total nuclear spin, I, can have the values of 0, 1, 2, and 3. In this molecule, both I_1 and I_2 are $\frac{3}{2}$, so the nuclear state with the lowest I value should be antisymmetric. Therefore for symmetric rotational levels, ee-oo, only antisymmetric nuclear states, those with $I=0,2$ exist and there are $(2\times0+1)+(2\times2+1)=6$ nuclear states. For antisymmetric rotational levels, eo-oe, only symmetric nuclear states, $I=1,3$ exist and there are $(1\times2+1)+(3\times2+1)=10$ nuclear states. The splittings of the antisymmetric rotational levels are more complicated than those of symmetric rotational levels as shown by the prediction, Table-3.27.

Figure-3.8 and Figure-3.9 show the calculated quadrupole splittings and intensities of one symmetric rotational transition, $43_{15,29}$-$43_{14,30}$, and one antisymmetric rotational transition, $48_{17,32}$-$48_{16,33}$, and the comparison with the observed patterns. For each of these transitions there were some peaks predicted to have bigger splittings, however they were too weak to be observed; therefore only the three strongest peaks were measured in this work. Table-3.27 gives some samples of the calculated and observed quadrupole splitting frequencies.

The values of the coupling constants obtained are $\chi_{aa} = -33.25 MHz$ and $\eta = 1.42$. Because of the C_{2v} symmetry of this molecule, we have[9], assuming the SCl bond to be a principal axis of the quadrupole coupling tensor

$$\chi_{xx} = \frac{\chi_{aa}\sin^2\theta_{za} - \chi_{bb}\cos^2\theta_{za}}{\sin^2\theta_{za} - \cos^2\theta_{za}} \tag{3.5.1}$$

$$\chi_{yy} = \chi_{cc} \tag{3.5 2}$$

$$\chi_{zz} = \frac{\chi_{aa}\cos^2\theta_{za} - \chi_{bb}\sin^2\theta_{za}}{\cos^2\theta_{za} - \sin^2\theta_{za}} \tag{3.5.3}$$

The principal values of the quadrupole coupling constants are given in Table-3.28 together with some data for related molecules. In the calculation of χ_{xx} and χ_{zz}, the effective geometry obtained in Section-3.3, $\theta_{za} = \frac{1}{2}\theta_{ClSCl} = 50.0585°$, was used.

Table-3.27 Examples of Hyperfine Structure in Transitions of $^{35}Cl_2^{32}S^{16}O_2$

F'	F''	I'	I''	$Frequency_{obs.}/MHz$	$Frequency_{cal.}/MHz$
$6_{5,1}$	←	$5_{4,2}$			
6	5	0	0	37835.117	37835.131
4	3	2	2	37833.719	37833.742
5	4	2	2	37833.719	37833.742
7	6	2	2	37833.719	37833.742
6	5	2	2	37833.719	37832.353
$9_{2,8}$	←	$8_{1,7}$			
9	8	0	0	37354.939	37354.974
7	6	2	2	37356.229	37356.257
8	7	2	2	37356.229	37356.257
10	9	2	2	37356.229	37356.257
9	8	2	2	37357.489	37357.540
$9_{6,4}$	←	$8_{5,3}$			
9	8	2	2	53345.477	53345.438
7	6	2	2	53346.438	53346.462
8	7	2	2	53346.438	53346.462
10	9	2	2	53346.438	53346.462
9	8	0	0	53347.447	53347.486
$10_{5,5}$	←	$9_{4,6}$			
10	9	2	2	55720.877	55720.826
8	7	2	2	55723.019	55723.053
9	8	2	2	55723.019	55723.053
11	10	2	2	55723.019	55723.053
10	9	0	0	55725.220	55725.279
$34_{8,26}$	←	$34_{7,27}$			
34	34	2	2	37283.272	37283.294
32	32	2	2	37284.810	37284.825
33	33	2	2	37284.810	37284.825
35	35	2	2	37284.810	37284.825
36	36	2	2	37284.810	37284.825
34	34	0	0	37286.386	37286.356

Table-3.27 Continued

F'	F''	I'	I''	$Frequency_{obs.}/MHz$	$Frequency_{cal.}/MHz$
$36_{9,27}$	←	$36_{8,28}$			
36	36	2	2	37860.015	37860.078
34	34	2	2	37861.488	37861.524
35	35	2	2	37861.488	37861.524
37	37	2	2	37861.488	37861.524
38	38	2	2	37861.488	37861.524
36	36	0	0	37862.952	37862.971
$43_{15,29}$	←	$43_{14,30}$			
43	43	2	2	35297.575	35297.604
41	41	2	2	35298.425	35298.455
42	42	2	2	35298.425	35298.455
44	44	2	2	35298.425	35298.455
45	45	2	2	35298.425	35298.455
43	43	0	0	35299.262	35299.306
$39_{10,29}$	←	$39_{9,30}$			
38	38	1	1	40177.624	40177.657
37	37	3	3	40177.624	40177.449
40	40	3	3	40177.624	40177.660
41	41	3	3	40177.624	40177.710
39	39	1	1	40176.267	40176.324
36	36	3	3	40176.267	40176.273
42	42	3	3	40176.267	40176.374
38	38	3	3	40178.954	40178.944
39	39	3	3	40178.954	40178.991
40	40	1	1	40178.954	40179.043

Table-3.28

Chlorine Nuclear Quadrupole Coupling Constants(MHz)

of $^{35}Cl\,^{32}S\,^{16}O_2$ and Related Molecules

χ	$^{35}Cl_2^{32}S^{16}O_2$		$^{35}Cl_2^{32}S^{b}$	$^{35}Cl_2^{12}CH_2^{c}$	$^{35}Cl_2^{28}SiH_2^{d}$
χ_{aa}	-33.25(0.18)		-37.85		
χ_{bb}	-6.97(0.07)		-10.01		
χ_{cc}	40.22(0.39)		47.86		
η	1.42(0.01)		1.53		
χ_{xx}	54.70	55.14[a]	39.17	37.09	21.00
χ_{yy}	40.22	40.37[a]	47.86	39.83	21.00
χ_{zz}	-94.92	-95.51[a]	-87.03	-76.92	-42.0

a-Reference[141]

b-Reference[13]

c-Reference[145]

d-Reference[146]

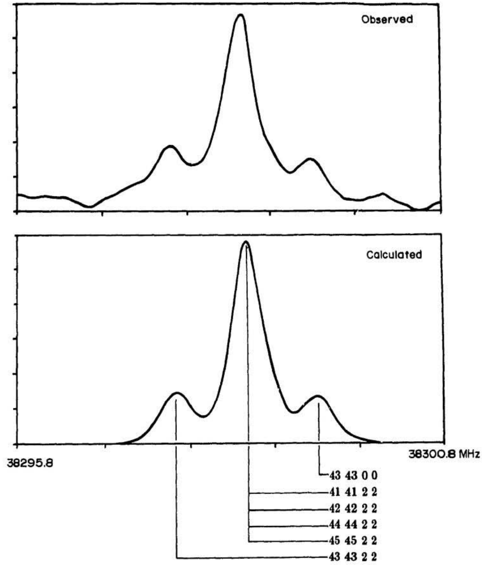

Figure-3.8 Nuclear Quadrupole Hyperfine Structure of $^{35}Cl_2^{32}S^{16}O_2$ in the $43_{15,29}$ - $43_{14,30}$ Transition.

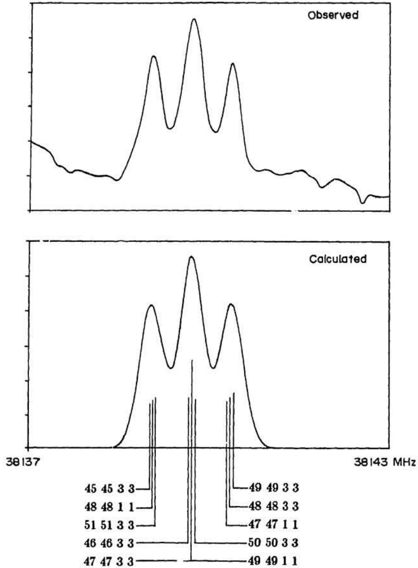

Figure-3.9 Nuclear Quadrupole Hyperfine Structure of $^{35}Cl_2^{32}S^{16}O_2$ in the $48_{17,32}$ - $48_{16,33}$ Transition.

3.6 The Dipole Moment of Sulphuryl Chloride

The Stark effect of the $6_{4,2} \leftarrow 5_{3,3}$ transition of ${}^{35}Cl_2^{32}S^{16}O_2$ was used to measure the dipole moment. The calculated zero-field nuclear quadrupole hyperfine splitting of this transition is small and actually both the zero-field and Stark-shifted lines showed no evidence of hyperfine structure. Because of the C_{2v} symmetry, the electric dipole moment of ${}^{35}Cl_2^{32}S^{16}O_2$ coincides with the b-principal inertial axis. Therefore the dipole moment can be determined by measuring Stark shifts for just one Stark component. The frequencies of the Stark component were measured in the field range from $3000 Vcm^{-1}$ up to $5000 Vcm^{-1}$. Because the Stark effect was second-order and very slow, in the lower field range the Stark component was overlapped by the zero field lines. The electrode spacing was measured precisely by observing the Stark effect in the $1_{1,1\,M=0} \leftarrow 0_{0,0\,M=0}$ transition of ${}^{32}S^{16}O_2$ whose dipole moment is accurately known. A very accurate measurement of the electric dipole moment of ${}^{32}S^{16}O_2$ has been made by Patel *et al*; their value of $1.63305(4)$ *Debye* [154] was used here. The electrode spacing was obtained as $0.4601(14) cm$. The observed frequencies(ν) and shift ($\delta\nu$) of the Stark component of ${}^{35}Cl_2^{32}S^{16}O_2$ are given together with the applied Stark voltages in Table-3.29. The results show that the Stark effect is second order. The expression for the Stark shift has been derived using equation-1.10.3 to be

$$\delta\nu(6_{4,2\,M=0} \leftarrow 5_{3,3\,M=0}) = 2.38886\times10^{-8}\mu_b^2E^2 \tag{3.6.1}$$

where $\delta\nu$ is the frequency shift in MHz and E is the electric field in Vcm^{-1}. A linear least squares analysis of the Stark data gave the slope $\frac{\delta\nu}{V^2} = 3.372(9)\times10^{-7}\ MHz\ V^{-2}$, which was converted to the required value $\frac{\delta\nu}{E^2}$ of $7.138(19)\times10^{-8} MHz V^{-2} cm^{-2}$ by using the electrode spacing of $0.4601 cm$. The electric dipole moment $\mu_b = 1.729(13)$ *Debye* was calculated using Equation-3.6.1. The previous value obtained by using dielectric measurement was $1.795(5)$ *Debye* [151][152][153].

Table-3.29

Stark Shifts in the $6_{4,2\ M=0} \leftarrow 5_{3,3\ M=0}$ Transition of $^{35}Cl_2^{32}S^{16}O_2$

V	$\nu(MHz)$	$\delta\nu(MHz)$	$\nu_{obs.} - \nu^{*}_{cal.}\ (MHz)$
0000	35327.596	0.000	-0.015
13[illegible]0	35328.159	0.563	-0.009
1442	35328.273	0.677	-0.009
1615	35328.475	0.864	0.015
1782	35328.625	1.029	-0.027
1864	35328.723	1.127	-0.029
1996	35328.918	1.322	-0.006
2140	35329.170	1.574	0.045
2245	35329.312	1.716	0.032
2388	35329.495	1.899	-0.009
2417	35329.531	1.935	-0.020

*--$\nu_{cal.}$ was calculated by using $\nu_0 = 35327.596 MHz$ and

$\frac{\delta\nu}{V^2} = 0.033721\ MHz\ V^{-2}$.

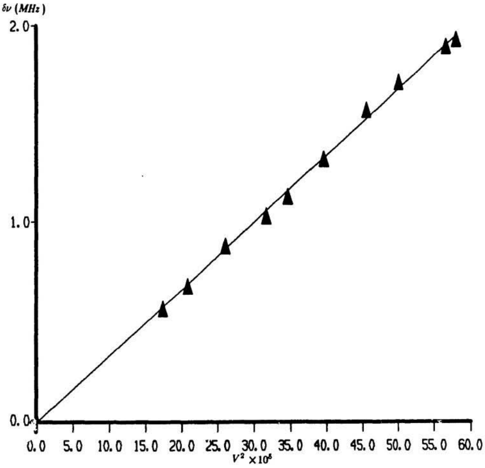

Figure-3.10 The Stark Shift in the $6_{4,2\ M=0} \leftarrow 5_{3,3\ M=0}$ Transition of ${}^{35}Cl_2^{\ 32}S^{16}O_2$

CHAPTER 4

THE MICROWAVE SPECTRUM, MOLECULAR STRUCTURE AND HARMONIC FORCE FIELD OF SULPHURYL FLUORIDE

The first investigation of the microwave spectrum of sulphuryl fluoride was reported in 1951 by Fristrom[84]. Seven ground state lines were measured, six of which were assigned to the $J = 1 \rightarrow 2$ and $J = 2 \rightarrow 3$ transitions of $F_2^{32}S^{16}O_2$ and the other to the $1_{1,1} \rightarrow 2_{1,2}$ transition of $F_2^{34}S^{16}O_2$. The spectrum showed that the molecule is an almost-spherical rotor and that the molecular symmetry axis is coincident with the principal inertial axis a for both of these two isotopic species. Lide and Mann reinvestigated the microwave spectrum[85][86] and found only a few new ground state lines for the two species in the same series, $J = 1 \rightarrow J = 2$ and $J = 2 \rightarrow J = 3$. Because no high J transitions were observed, centrifugal distortion constants cannot be obtained from this data alone. The rotational constants were calculated using the rigid rotor approximation and were used to derive an effective molecular geometry for F_2SO_2, Table-4.25. A number of satellite transitions were also measured in this work and assigned to three different vibrationally excited states($v_4 = 1$ or $v_5 = 1$, and $v_7 = 1$ or $v_9 = 1$) according to their symmetry. The average value of the dipole moment obtained from Stark effect measurements on three $J = 1 \rightarrow 2$ transitions was 1.110(15) *Debye*. A Coriolis interaction between the fundamentals $v_4(a_1)$ and $v_5(a_2)$ was suggested to explain the anomalies in the rotational constants reported for the excited states.

The gas-phase electron diffraction geometry of F_2SO_2 was determined in an early study by Stevenson and Russel[87] and later refined by Hedberg *et al.* [88]. Hedberg *et al.* pointed out that an accurate geometry for this type of near spherical top is not readily obtained by electron diffraction and that a spectroscopic structure determination should also include a careful treatment of vibrational effects.

Many studies of the vibrational spectrum of F_2SO_2 have been carried out[73][86][89][90][91][93], which, however, have yielded neither a definitive nor a complete vibrational assignment. Nevertheless some force field calculations have been performed[79][80][81] using the vibrational frequencies of the normal isotopic species only. A nine force constant Urey-Bradley force field was obtained by Toyuki[80] and several valence force fields with seven to nine force constants were derived by Wilson[79]. In all of the force field calculations, Lide's microwave geometry[86] was used. As we discussed above, because of the limited isotopic data and the neglect of vibrational effects the reliability of Lide's structural parameters was unclear.

We wished to determine a very accurate molecular geometry for F_2SO_2, to establish unambiguously the assignment of vibrational fundamentals, and also to determine an accurate harmonic force field for this molecule. This required the precise determination of rotational constants and, for the first time, centrifugal distortion constants for isotopic sulfuryl fluorides and, as well, additional vibrational data. In the present work the microwave and infrared spectra of F_2SO_2 were reinvestigated. The microwave spectra of five isotopic species, $F_2^{32}S^{16}O_2$, $F_2^{32}S^{18}O_2$, $F_2^{32}S^{16}O^{18}O$, $F_2^{34}S^{16}O_2$ and $F_2^{34}S^{18}O_2$, were measured, of which the last two were done in natural abundance. All together more than 550 transitions were observed. Several vibrational lines of $F_2^{32}S^{18}O_2$, $F_2^{32}S^{16}O^{18}O$ and $F_2^{34}S^{16}O_2$ were obtained. The Coriolis coupling constants between the ν_4 and ν_5, and between the ν_3 and ν_7 states have also been calculated. From these data, good effective, average and approximate equilibrium geometries and, as well, the molecular harmonic force field were derived.

4.1 The Observed Microwave Transitions and Assignments for Sulphuryl Fluoride

The rotational transition frequencies and rotational constants of $F_2^{32}S^{16}O_2$ and $F_2^{34}S^{16}O_2$ obtained by Lide[8c] were used to obtain the initial high frequency predictions for these two species. Both of these species have a-type transitions with $oo-oe$ lines stronger than $ee-eo$ lines, Table-1.1. Because the Q-branch transitions of these two species were out of the microwave frequency range used in this work, only R-branch lines were found. At high Stark fields, several hundred to one thousand $volt.cm^{-1}$, the low K_a lines were strong and symmetric. For high K_a transitions, however, low modulation fields, typically 5-20 $volt.cm^{-1}$, were suitable. As the Stark field increased the high K_a lines were broadened somewhat as a consequence of their very fast Stark effect and a slight non-zero basing of the square wave modulation voltage. Several very weak lines of $F_2^{32}S^{16}O_2$ with $\Delta K_a = 2$, such as $4_{2,2} \leftarrow 3_{0,3}$, were measured, and greatly improved the accuracy of the values determined for both the A rotational constant and the quartic centrifugal distortion constants.

An effective structure derived from the rotational constants of the above two species was used to obtain the initial predictions of the rotational frequencies for $F_2^{32}S^{18}O_2$. Because, as we know, $F_2^{32}S^{16}O_2$ and $F_2^{34}S^{16}O_2$ both are nearly spherical tops, it was very difficult to decide what type of transitions $F_2^{32}S^{18}O_2$ had when we made the initial prediction. Therefore three predictions, with a-type, b-type and c-type selection rules, were made. The experimental spectrum was characterized by b-type transitions, which means that the $^{18}O_2$ substitution rotates the principal axes of the molecule. Due to the nuclear spin of fluorine, $eo-oe$ transitions were three times stronger than $ee-oo$ transitions. Figure-4.1 gives two b-type transitions $4_{0,4} \leftarrow 3_{1,3}$ and $4_{1,4} \leftarrow 3_{0,3}$, with frequency 37400.431MHz and 37410.035MHz respectively, which show the nuclear spin statistics of fluorine. Both R-branch and Q-branch transitions were eventually found.

Some very weak lines with $\Delta K_a = 3$ or $\Delta K_c = 3$, such as $4_{3,2} \leftarrow 3_{0,3}$, $4_{2,3} \leftarrow 3_{3,0}$ and $27_{17,10} \leftarrow 27_{14,13}$, have also been assigned.

Both a-type and b-type R-branch transitions but only b-type Q-branch transitions were found for $F_2^{32}S^{16}O^{18}O$. In fact, examination of the relative intensities of a-type and b-type lines for this isotopomer showed that the μ_a and μ_b dipole moment components were of very nearly equal magnitude, Figure-4.2. For this species many Q-branch transitions were measured. Figure-4.3 illustrates the $J_{30,J-30} \leftarrow J_{29,J-29}$ and $J_{38,J-38} \leftarrow J_{37,J-37}$ series Q-branch lines, which show almost identical spacings between two neighbouring transitions; small Q-branch splittings are observed since this isotopomer is a near symmetric rotor. These Q-branch bands formed a band head at the higher frequency side with the transitions $J_{J,0} \leftarrow J_{J-1,1}$, which helped a lot in the assignment of the Q-branch lines. The intensity of the Q-branch lines increased with J up to a maximum, then decreased. This isotopic species was the only species studied for this molecule not to have C_{2v} symmetry, and Figures 4.2, 4.3 and 4.4 show no effects due to nuclear spin statistics.

The spectrum of $F_2^{34}S^{18}O_2$ was obtained in natural abundance and only 17 R-branch frequencies were measured. This species also has b-type transitions.

A large number of satellite series were found for $F_2^{32}S^{16}O_2$ and $F_2^{32}S^{18}O_2$ and these have been assigned to five vibrationally excited states of $F_2^{32}S^{16}O_2$ and four vibrationally excited states of $F_2^{32}S^{18}O_2$, respectively. The five satellite series of $F_2^{32}S^{16}O_2$, that were labeled as the X-, Y-, U-, W- and Z- states following Lide[85][86], all had a-type transitions except for the Y-series, which had c-type transitions. All of the four satellite series, that were labeled as the K-, L-, M- and N- states, of $F_2^{32}S^{18}O_2$ exhibited b-type selection rules. The five lowest vibrational fundamentals of $F_2^{32}S^{16}O_2$, ν_3, ν_4, ν_5, ν_7 and ν_9, have vibrational frequencies $552.2cm^{-1}$, $385.0cm^{-1}$, $384.0cm^{-1}$, $544.0cm^{-1}$ and $539.3cm^{-1}$, respectively. At room temperature, ν_4 and ν_5 state satellite series lines have about 16% of the ground state intensity, and v_3, v_7 and v_9 state lines are only half as strong as the v_4 and v_5 state lines. The transitions of the ^{34}S species have only 5% of the ground state intensity of the normal species and the ratio does not change with temperature, therefore it was no problem to differentiate ^{34}S species and excited state satellite series. Another very important source of information, which helped a lot in the assignment of the satellite frequencies, comes from the molecular symmetry and the nuclear spin statistics. From the normal mode analysis[73][81], v_3, v_4 and v_5 states belong to either a_1 or a_2 species, v_7 and v_9 to either b_1 or b_2 species. As we know, see Section 1.3, that, for A species, the $oo-oe$ lines are stronger than the $ee-eo$ lines(a-type), the $eo-oe$ lines are stronger than the $oo-ee$ lines(b-type) and the $oo-eo$ lines are stronger than the $ee-oe$ lines(c-type); for B species the case is the opposite. After comparing the intensities of the satellite series, Figure-4.4, and considering the spin statistics, Figure-4.5, we assigned the U-state to v_3, the X- and Y- states to v_4 or v_5, the W- and Z- states to v_7 or v_9 for $F_2^{32}S^{16}O_2$, and the K- and L- states to v_4 or v_5, and the M- and N- states to v_7 or v_9 for $F_2^{32}S^{18}O_2$. Because there is no difference between the intensities and spin statistics of v_4 and v_5 and of v_7 and v_9, it is very difficult to distinguish between them. After we discuss the Coriolis interaction between these excited states, we can assign them; this will be discussed in Section-4.5.

The ground state lines were measured at dry ice temperature and the excited states at room temperature. All of the experiments were carried out using a $1.0\times2.2cm$ Stark cell, in which the sample presure was controlled in the range of 5-10microns. The frequencies between 6000-120000MHz were investigated. The observed frequencies are collected in Tables 4.2 to 4.15.

Table-4.1

The Number of Observed Transitions(N) and the Highest J Observed

for F_2SO_2 Isotopomers

Isotopic Species	R-branch J	R-branch N	Q-branch J	Q-branch N	Total N
$F_2^{32}S^{16}O_2$	10	56			56
$F_2^{32}S^{18}O_2$	11	88	60	52	140
$F_2^{32}S^{16}O^{18}O$	8	70	70	244	314
$F_2^{34}S^{16}O_2$	7	26			26
$F_2^{34}S^{18}O_2$	8	17			17

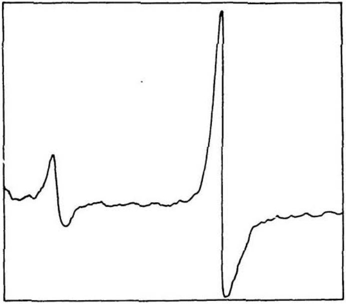

Figure-4.1 The $4_{0,4} \leftarrow 3_{1,3}$ and $4_{1,4} \leftarrow 3_{0,3}$ Transitions, with Frequency 37400.431MHz and 37410.035MHz Respectively, of $F_2^{32}S^{18}O_2$, Which Show the F Nuclear Spin Statistics.

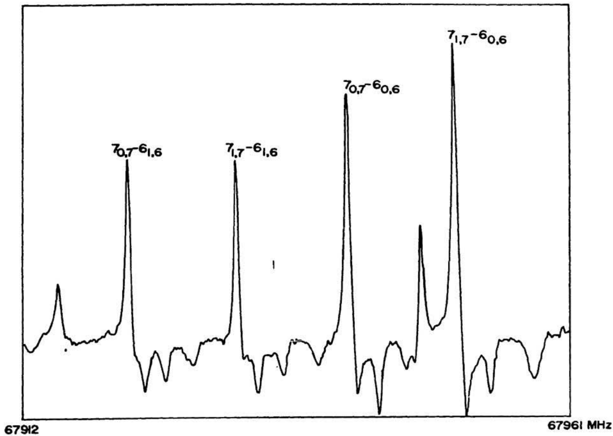

Figure-4.2 The $J = 7 \leftarrow 6$ Transitions of $F_2^{32}S^{16}O^{18}O$.

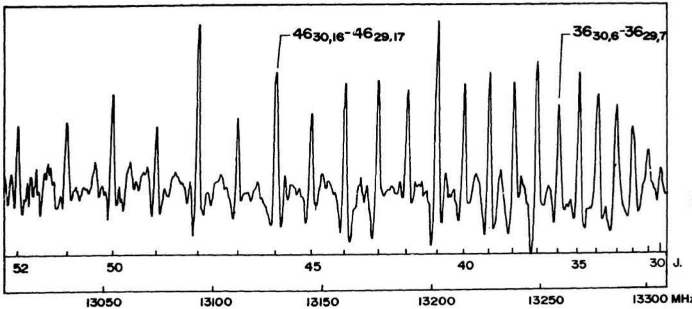

Figure-4.3a The Lower J Lines of the K_a=30←29 b-Type Q-Branch Series of $F_2^{32}S^{16}O^{18}O$

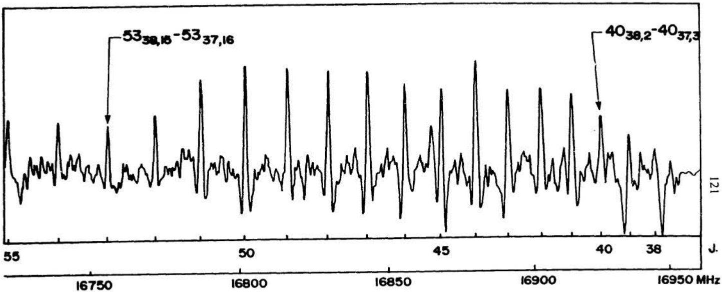

Figure-4.3b The Lower J Lines of the $K_a=38\leftarrow37$ b-Type Q-Branch Series of $F_2^{32}S^{16}O^{18}O$

Figure-4.4 The Intensities of $7_{0,7} - 6_{1,6}$ Transitions for the Ground State(65281.984MHz) and the K-Excited State(65281.165MHz) of $F_2^{32}S^{18}O_2$.

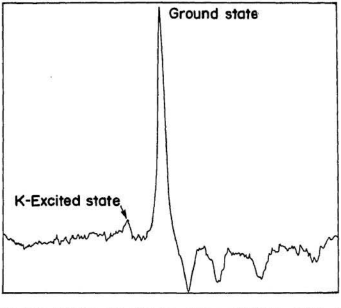

Figure-4.5 The Spin Statistics of L-State Transitions of $F_2^{32}S^{18}O_2$, Which Shows that $7_{1,6} - 6_{2,5}$(65581.129MHz) is Stronger than $7_{2,6} - 6_{1,5}$(65602.965MHz).

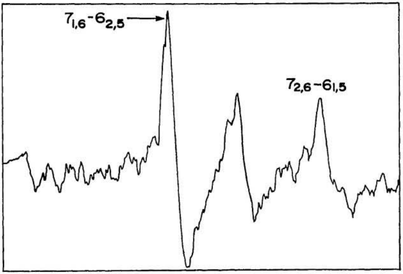

Table-4.2

Observed Rotational Transition Frequencies(in MHz) of $F_2^{32}S^{16}O_2$.

J'	K_a'	K_c'	-	J''	K_a''	K_c''	Frequency	Deviation
2	1	2	-	1	1	1	20244.21*	0.001
2	0	2	-	1	0	1	20257.48*	-0.011
2	1	1	-	1	1	0	20276.25*	0.006
3	1	2	-	2	1	1	30412.41*	0.014
3	1	3	-	2	1	2	30364.64*	-0.006
3	0	3	-	2	0	2	30379.791	-0.023
3	2	2	-	2	2	1	30390.31*	0.045
3	2	1	-	2	2	0	30400.748	0.029
4	2	2	-	3	0	3	40847.354	0.093
4	0	4	-	3	0	3	40496.618	0.002
4	1	4	-	3	1	3	40483.513	0.050
4	3	1	-	3	3	0	40526.667	-0.031
4	1	3	-	3	1	2	40545.743	-0.023
4	2	2	-	3	2	1	40541.540	-0.072
4	2	3	-	3	2	2	40518.114	0.081
5	2	3	-	4	2	2	50683.926	0.014
5	0	5	-	4	0	4	50609.771	-0.036
5	1	5	-	4	1	4	50600.675	0.028
5	1	4	-	4	1	3	50674.855	0.025
5	3	3	-	4	3	2	50656.822	0.088
5	3	2	-	4	3	1	50662.563	-0.051
6	3	3	-	5	1	4	61285.232	0.007
6	1	6	-	5	1	5	60716.397	-0.024
6	0	6	-	5	0	5	60721.841	-0.015
6	2	5	-	5	2	4	60767.488	0.036
6	5	2	-	5	5	1	60786.894	0.002
6	5	1	-	5	5	0	60786.894	-0.020
6	3	4	-	5	3	3	60787.895	0.033
6	1	5	-	5	1	4	60798.056	0.005
6	3	3	-	5	3	2	60802.271	-0.004
6	2	4	-	5	2	3	60824.389	-0.018
6	2	4	-	5	0	5	61249.193	0.036
7	3	5	-	6	1	6	71696.313	-0.038
7	1	6	-	6	3	3	70427.710	-0.023
7	1	7	-	6	1	6	70831.080	-0.026
7	0	7	-	6	0	6	70834.001	-0.006
7	2	6	-	6	2	5	70888.631	0.031
7	1	6	-	6	1	5	70914.930	0.023
7	6	2	-	6	6	1	70917.404	-0.023
7	6	1	-	6	6	0	70917.404	-0.025
7	5	3	-	6	5	2	70919.271	0.061
7	5	2	-	6	5	1	70919.271	-0.059
7	3	4	-	6	3	3	70945.722	-0.020
7	2	5	-	6	2	4	70960.864	0.016

*-Reference [86]

Table-4.2 Continued(2)

J'	K_a'	K_c'	-	J''	K_a''	K_c''	Frequency	Deviation
7	3	4	-	6	1	5	71432.901	-0.015
7	4	3	-	6	2	4	71667.810	0.008
7	5	2	-	6	3	3	72002.300	-0.001
8	4	4	-	7	4	3	81062.259	-0.006
8	1	8	-	7	1	7	80945.010	0.005
8	1	7	-	7	1	6	81026.884	0.006
8	3	6	-	7	3	5	81045.310	0.003
8	7	2	-	7	7	1	81047.861	0.007
8	6	3	-	7	6	2	81049.379	0.032
10	3	7	-	9	3	6	101373.805	-0.015
10	2	8	-	9	2	7	101332.622	-0.015
10	5	5	-	9	5	4	101322.518	0.032

Table-4.3
Observed Rotational Transition Frequencies(in MHz) of $F_2^{32}S^{18}O_2$.

J'	K_a'	K_c'	-	J'	K_a''	K_c''	Frequency	Deviation
2	2	1	-	1	1	0	19471.597	-0.036
2	0	2	-	1	1	1	18734.015	-0.001
2	1	2	-	1	0	1	18880.952	0.074
3	2	1	-	2	1	2	29737.609	0.009
3	0	3	-	2	1	2	28090.255	-0.003
3	[illegible]	3	-	2	0	2	28134.916	-0.023
3	1	2	-	2	2	1	28271.043	-0.004
3	2	2	-	2	1	1	28764.355	0.039
4	4	1	-	3	1	2	40602.327	-0.019
4	0	4	-	3	1	3	37400.431	0.024
4	1	4	-	3	0	3	37410.035	0.052
4	1	3	-	3	2	2	37763.635	0.003
4	2	2	-	3	3	1	37645.409	-0.019
4	2	3	-	3	1	2	37978.762	0.019
4	2	3	-	3	3	0	36692.974	-0.017
4	2	2	-	3	1	3	39938.289	0.005
4	3	1	-	3	2	2	39389.783	0.042
4	3	2	-	3	2	1	38703.876	-0.001
4	3	2	-	3	0	3	40351.243	0.024
4	4	1	-	3	1	2	40602.361	0.015
4	4	1	-	3	3	0	39316.542	-0.052
4	4	0	-	3	3	1	39388.236	0.013
5	5	0	-	4	4	1	49248.813	-0.023
5	0	5	-	4	1	4	46696.606	0.009
5	1	4	-	4	2	3	47136.761	-0.023
5	2	4	-	4	1	3	47202.185	0.048
5	2	3	-	4	3	2	47313.356	-0.007
5	3	3	-	4	2	2	47900.153	0.011
5	4	1	-	4	3	2	49087.910	0.057
5	5	1	-	4	4	0	49222.031	-0.046

Table-4.3 Continued(1)

J'	K_a'	K_c'	-	J''	K_a''	K_c''	Frequency	Deviation
6	6	0	-	5	5	1	59123.405	-0.023
6	1	6	-	5	0	5	55989.883	-0.018
6	1	5	-	5	2	4	56452.219	-0.026
6	2	5	-	5	1	4	56467.451	-0.018
6	2	4	-	5	3	3	56817.984	-0.018
6	3	4	-	5	4	1	55283.376	-0.015
6	3	3	-	5	4	2	56697.845	0.050
6	3	4	-	5	2	3	57057.877	-0.003
6	3	4	-	5	0	5	60615.934	0.051
6	4	3	-	5	3	2	57887.951	-0.026
6	4	3	-	5	5	0	55510.128	0.026
6	4	3	-	5	1	4	60245.780	0.023
6	5	2	-	5	4	1	58649.872	-0.039
6	5	1	-	5	4	2	58854.721	0.029
6	5	2	-	5	2	3	60424.377	-0.023
6	6	1	-	5	5	0	59114.352	-0.032
7	7	1	-	6	6	0	69000.594	-0.007
7	0	7	-	6	1	6	65281.984	0.013
7	1	6	-	6	2	5	65749.468	-0.021
7	2	6	-	6	1	5	65752.477	-0.047
7	2	5	-	6	3	4	66191.671	-0.045
7	3	5	-	6	2	4	66264.136	-0.010
7	3	4	-	6	4	3	66387.420	-0.051
7	4	3	-	6	5	2	65918.728	0.061
7	4	3	-	6	3	4	69285.231	0.045
7	4	4	-	6	3	3	67002.657	-0.036
7	5	2	-	6	4	3	68659.083	-0.013
7	5	3	-	6	4	2	67915.235	-0.040
7	6	1	-	6	5	2	68678.972	0.010
7	6	2	-	6	5	1	68591.343	0.054
7	7	0	-	6	6	1	69003.508	0.036
8	7	1	-	7	6	2	78536.581	0.040
8	0	8	-	7	1	7	74574.091	0.001
8	1	8	-	7	0	7	74574.091	-0.005
8	2	6	-	7	3	5	75506.820	0.074
8	3	6	-	7	2	5	75524.336	-0.041
8	4	5	-	7	3	4	76123.716	0.007
8	5	4	-	7	4	3	77028.774	-0.049
8	6	3	-	7	5	2	77941.964	-0.042
8	7	2	-	7	6	1	78502.999	0.020
9	9	0	-	8	8	1	88767.512	0.003
9	2	7	-	8	3	6	84803.311	0.057
9	3	7	-	8	2	6	84806.965	-0.040
9	3	6	-	8	4	5	85251.205	0.017
9	4	6	-	8	3	5	85322.819	0.007
9	7	2	-	8	6	3	88124.235	0.010
9	8	1	-	8	7	2	88409.552	0.011

Table-4.3 Continued(2)

J'	K_a'	K_c'	-	J''	K_a''	K_c''	Frequency	Deviation
10	2	9	-	9	2	8	93625.680	-0.055
10	0	10	-	9	1	9	93157.746	-0.023
10	1	10	-	9	0	9	93157.746	-0.023
10	1	9	-	9	2	8	93625.680	-0.053
11	4	8	-	10	3	7	103861.598	0.048
11	0	11	-	10	1	10	102449.312	0.019
11	1	11	-	10	0	10	102449.312	0.019
11	1	10	-	10	2	9	102917.114	-0.005
11	2	10	-	10	1	9	102917.114	-0.007
11	3	8	-	10	4	7	103857.611	0.044
11	4	7	-	10	5	6	104312.719	-0.024
17	3	14	-	17	2	15	6723.636	0.093
18	4	15	-	18	3	16	7191.699	-0.028
18	3	16	-	18	2	17	7680.766	0.007
19	3	16	-	19	2	17	7659.640	-0.045
20	6	15	-	20	5	16	7136.561	0.014
20	5	16	-	20	4	17	7635.103	0.049
21	6	15	-	21	5	16	7101.813	0.052
21	4	17	-	21	3	18	8103.399	-0.045
21	4	18	-	21	3	19	8595.005	-0.027
21	5	16	-	21	4	17	7606.408	-0.005
22	7	16	-	22	6	17	7573.264	0.008
22	2	21	-	22	1	22	10034.209	-0.021
22	6	17	-	22	5	18	8075.790	0.031
23	21	2	-	23	20	3	7229.493	0.087
24	24	0	-	24	23	1	8433.758	-0.059
24	8	17	-	24	7	18	8007.522	-0.014
24	22	3	-	24	21	4	7592.568	-0.028
26	23	4	-	26	22	5	7884.000	0.070
26	1	25	-	26	0	26	11901.308	0.003
26	7	20	-	26	6	21	9452.514	0.001
26	9	18	-	26	8	19	8439.474	-0.064
27	17	10	-	27	14	13	10747.669	-0.039
27	7	20	-	27	6	21	9420.004	-0.020
28	25	4	-	28	24	5	8612.287	-0.099
29	19	10	-	29	16	13	11803.887	0.041
30	28	3	-	30	27	4	9768.256	0.045
30	8	23	-	30	7	24	10827.226	-0.021
30	9	22	-	30	8	23	10324.413	-0.068
30	15	16	-	30	14	17	7053.243	0.057
31	10	21	-	31	9	22	9771.523	-0.005
31	5	26	-	31	4	27	12285.370	-0.007
35	17	18	-	35	16	19	7735.081	-0.023
37	13	24	-	37	12	25	11046.135	-0.049
38	31	8	-	38	30	9	10471.273	0.001

Table-4.3 Continued(3)

J'	K_a'	K_c'	-	J''	K_a''	K_c''	Frequency	Deviation
39	29	10	-	39	28	11	9359.510	0.037
39	11	28	-	39	10	29	13027.964	0.088
39	14	25	-	39	13	26	11467.372	-0.026
39	27	12	-	39	26	13	8193.266	-0.016
40	28	13	-	40	27	14	8621.341	-0.017
40	11	30	-	40	10	31	14002.426	0.013
40	21	20	-	40	20	21	8415.825	0.066
42	24	19	-	42	23	20	7425.835	-0.020
44	27	18	-	44	26	19	7271.131	0.028
45	30	15	-	45	29	16	8743.339	-0.041
45	22	23	-	45	21	24	9750.560	0.033
47	26	21	-	47	25	22	7208.541	-0.044
48	25	24	-	48	24	25	10006.315	-0.021
50	31	20	-	50	30	21	8264.334	-0.035
50	30	21	-	50	29	22	8004.403	-0.007
54	32	23	-	54	31	24	8541.857	-0.055
56	31	26	-	56	30	27	10048.031	0.042
60	36	25	-	60	35	26	9305.988	0.037

Table-4.4
Observed Rotation Transition Frequencies(in MHz) of $F_2^{32}S^{16}O^{18}O$.

J'	K_a'	K_c'	-	J''	K_a''	K_c''	Frequency	Deviation
3	1	3	-	2	0	2	29297.472	0.050
3	0	3	-	2	1	2	29026.771	0.027
3	0	3	-	2	0	2	29186.309	0.049
3	1	3	-	2	1	2	29137.894	-0.013
3	1	2	-	2	1	1	29287.242	-0.064
4	4	1	-	3	3	0	40542.706	0.068
4	0	4	-	3	1	3	38774.140	0.026
4	0	4	-	3	0	3	38885.291	0.014
4	1	3	-	3	2	2	38503.314	0.057
4	1	4	-	3	1	3	38842.646	0.049
4	1	3	-	3	1	2	39037.838	-0.029
4	1	4	-	3	0	3	38953.783	0.024
4	2	3	-	3	2	2	38950.556	0.059
4	2	2	-	3	2	1	39022.123	-0.004
4	2	3	-	3	1	2	39485.062	-0.046
4	2	2	-	3	1	3	39896.206	0.002
4	3	2	-	3	2	1	40068.111	-0.062
4	3	1	-	3	2	2	40113.924	0.020
4	4	0	-	3	3	1	40543.529	-0.043
5	3	2	-	4	2	3	49896.867	0.035
5	0	5	-	4	1	4	48504.497	0.071
5	0	5	-	4	0	4	48572.925	0.016
5	1	5	-	4	1	4	48542.544	0.005
5	1	5	-	4	0	4	48611.003	-0.018

Table-4.4 Continued(1)

J'	K_a'	K_c'	-	J''	K_a''	K_c''	Frequency	Deviation
5	1	4	-	4	1	3	48775.857	-0.051
5	2	3	-	4	2	2	48800.224	-0.032
5	2	4	-	4	2	3	48677.708	-0.017
5	2	4	-	4	1	3	49125.002	0.036
5	3	3	-	4	3	2	48716.397	0.005
5	3	2	-	4	3	1	48733.366	-0.059
5	3	3	-	4	2	2	49762.389	-0.049
6	5	1	-	5	5	0	58455.495	-0.019
6	0	6	-	5	1	5	58218.697	-0.017
6	0	6	-	5	0	5	58256.813	-0.013
6	1	6	-	5	1	5	58238.405	-0.007
6	1	6	-	5	0	5	58276.510	-0.014
6	1	5	-	5	1	4	58496.778	-0.005
6	2	5	-	5	2	4	58398.490	-0.023
6	2	4	-	5	2	3	58574.045	0.004
6	2	5	-	5	1	4	58747.544	-0.027
6	3	3	-	5	2	4	59721.378	-0.053
6	5	2	-	5	5	1	58455.495	0.039
7	7	0	-	6	6	1	71118.169	-0.010
7	0	7	-	6	1	6	67921.567	0.004
7	0	7	-	6	0	6	67941.243	-0.017
7	1	6	-	6	1	5	68198.535	0.039
7	1	7	-	6	1	6	67931.230	-0.002
7	1	6	-	6	2	5	67947.690	-0.018
7	1	7	-	6	0	6	67950.926	-0.004
7	1	6	-	6	1	5	68198.507	0.011
7	2	6	-	6	2	5	68112.363	-0.004
7	2	5	-	6	2	4	68336.445	-0.039
7	3	5	-	6	3	4	68200.742	0.026
7	3	4	-	6	3	3	68283.657	-0.007
7	4	4	-	6	4	3	68211.384	0.002
7	4	3	-	6	4	2	68219.646	-0.054
7	6	2	-	6	6	1	68196.532	0.009
7	6	1	-	6	6	0	68196.532	0.004
7	7	1	-	6	6	0	71118.169	-0.009
8	7	1	-	7	7	0	77937.416	0.018
8	0	8	-	7	1	7	77617.376	-0.036
8	0	8	-	7	0	7	77627.104	0.023
8	1	8	-	7	0	7	77631.670	0.012
8	1	8	-	7	1	7	77621.993	0.005
8	1	7	-	7	2	6	77720.182	-0.012
8	2	7	-	7	2	6	77819.371	-0.044
8	3	6	-	7	3	5	77935.778	0.025
8	4	5	-	7	4	4	77961.445	0.041
8	7	2	-	7	7	1	77937.416	0.019
19	16	3	-	19	15	4	6960.283	0.027
21	16	5	-	21	15	6	6944.602	0.050
23	17	6	-	23	16	7	7386.594	-0.017

Table-4.4 Continued(2)

J'	K_a'	K_c'	-	J''	K_a''	K_c''	Frequency	Deviation
25	19	6	-	25	18	7	8289.453	0.019
26	20	6	-	26	19	7	8740.705	-0.070
27	24	3	-	27	23	4	10570.550	-0.017
30	19	11	-	30	18	12	8229.082	-0.069
34	33	1	-	34	32	2	14660.596	-0.022
34	32	2	-	34	31	3	14198.855	0.062
34	24	10	-	34	23	11	10504.090	0.086
35	20	15	-	35	19	16	8612.745	-0.054
36	36	1	-	36	35	2	16032.521	0.001
36	30	6	-	36	29	7	13257.603	0.042
37	36	2	-	37	35	3	16023.972	0.027
37	34	3	-	37	33	4	15097.514	0.007
37	31	6	-	37	30	7	13709.960	0.021
37	27	10	-	37	26	11	11858.933	-0.006
38	38	0	-	38	37	1	16943.467	0.050
38	37	1	-	38	36	2	16478.957	0.011
38	36	3	-	38	35	4	16015.013	0.047
38	33	5	-	38	32	6	14625.308	0.044
39	38	1	-	39	37	2	16934.274	0.033
39	37	2	-	39	36	3	16469.677	0.002
39	36	4	-	39	35	5	16005.634	0.066
40	39	2	-	40	38	3	17389.838	0.000
40	32	8	-	40	31	9	14141.226	-0.053
40	38	2	-	40	37	3	16924.641	-0.028
40	30	10	-	40	29	11	13214.036	0.012
40	20	20	-	40	19	21	8487.019	0.008
40	37	3	-	40	36	4	16459.961	-0.030
40	36	5	-	40	35	6	15995.700	-0.037
40	24	16	-	40	23	17	10412.591	0.029
41	41	0	-	41	40	1	18312.133	0.013
41	40	1	-	41	39	2	17845.744	-0.002
41	34	7	-	41	33	8	15057.410	-0.027
41	39	3	-	41	38	4	17379.915	-0.040
41	38	3	-	41	37	4	16914.721	0.034
41	31	10	-	41	30	11	13665.829	-0.027
41	37	4	-	41	36	5	16449.874	-0.005
41	36	6	-	41	35	7	15985.431	-0.026
42	42	0	-	42	41	1	18769.032	0.014
42	41	1	-	42	40	2	18301.921	-0.052
42	40	2	-	42	39	3	17835.561	0.019
42	39	4	-	42	38	5	17369.691	0.025
42	27	15	-	42	26	17	11788.545	-0.006
42	38	4	-	42	37	5	16904.284	0.000
42	37	5	-	42	36	6	16439.328	0.002
42	36	7	-	42	35	8	15974.764	0.049
43	43	0	-	43	42	1	19226.211	-0.050

Table-4.4 Continued(3)

J'	K_a'	K_c'	-	J''	K_a''	K_c''	Frequency	Deviation
43	42	1	-	43	41	2	18758.537	0.009
43	36	8	-	43	35	9	15963.513	0.020
43	41	2	-	43	40	3	18291.451	0.012
43	40	3	-	43	39	4	17824.963	0.027
43	39	5	-	43	38	6	17358.955	-0.006
43	38	5	-	43	37	6	16893.387	-0.059
43	37	6	-	43	36	7	16428.326	0.008
44	44	1	-	44	43	2	19683.891	0.032
44	43	1	-	44	42	2	19215.384	-0.036
44	37	7	-	44	36	8	16416.828	-0.010
44	42	2	-	44	41	3	18747.703	0.049
44	36	9	-	44	35	10	15951.750	-0.025
44	41	3	-	44	40	4	18280.508	0.002
44	40	4	-	44	39	5	17813.873	-0.045
44	39	6	-	44	38	7	17347.818	-0.008
44	33	11	-	44	32	12	14556.996	-0.043
44	38	6	-	44	37	7	16882.157	-0.002
45	44	2	-	45	43	3	19672.691	0.035
45	43	2	-	45	42	3	19204.202	0.006
45	37	8	-	45	36	9	16404.866	-0.008
45	42	3	-	45	41	4	18736.336	-0.048
45	41	4	-	45	40	5	18269.137	-0.027
45	27	18	-	45	26	19	11735.086	-0.002
45	40	5	-	45	39	6	17802.482	0.007
45	38	7	-	45	37	8	16870.437	0.027
46	43	3	-	46	42	4	19192.538	-0.040
46	42	4	-	46	41	5	18724.713	0.005
46	37	9	-	46	36	10	16392.377	-0.030
46	41	5	-	46	40	6	18257.367	-0.036
46	30	16	-	46	29	17	13128.234	0.035
46	40	6	-	46	39	7	17790.574	-0.022
46	38	8	-	46	37	9	16858.252	0.068
46	34	12	-	46	33	13	14995.494	-0.023
47	44	4	-	47	43	5	19649.123	0.024
47	43	4	-	47	42	5	19180.482	-0.077
47	42	5	-	47	41	6	18712.631	0.013
47	37	10	-	47	36	11	16379.419	-0.004
47	41	6	-	47	40	7	18245.203	-0.007
47	38	9	-	47	37	10	16845.463	-0.003
47	24	23	-	47	23	24	10247.539	0.038
48	43	5	-	48	42	6	19168.136	0.008
48	42	6	-	48	41	7	18700.072	-0.028
48	35	13	-	48	34	14	15433.218	0.015
48	41	7	-	48	40	8	18232.615	0.040
48	38	10	-	48	37	11	16832.232	-0.010
48	37	11	-	48	36	12	16365.897	-0.007

Table-4.4 Continued(4)

J'	K_a'	K_c'	-	J''	K_a''	K_c''	Frequency	Deviation
48	31	17	-	48	30	18	13563.049	0.029
48	32	16	-	48	31	17	14031.647	-0.048
49	44	6	-	49	43	7	19623.885	-0.058
49	38	11	-	49	37	12	16818.471	-0.024
49	27	22	-	49	26	23	11647.994	0.064
49	43	6	-	49	42	7	19155.282	0.007
49	42	7	-	49	41	8	18687.142	-0.003
49	37	12	-	49	36	13	16351.790	-0.044
49	41	8	-	49	40	9	18219.474	-0.011
50	47	3	-	50	46	4	21020.683	-0.015
50	46	4	-	50	45	5	20550.081	0.043
50	43	7	-	50	42	8	19141.992	0.003
50	38	12	-	50	37	13	16804.231	0.021
50	41	9	-	50	40	10	18205.960	0.031
50	42	8	-	50	41	9	18673.748	0.006
50	37	13	-	50	36	14	16337.202	0.007
51	49	2	-	51	48	3	21950.788	0.000
51	48	3	-	51	47	4	21478.618	0.012
51	45	6	-	51	44	7	20066.523	0.010
51	44	8	-	51	43	9	19597.071	-0.043
51	33	18	-	51	32	19	14448.839	0.043
51	43	8	-	51	42	9	19128.238	-0.022
51	41	10	-	51	40	11	18191.894	0.002
51	42	9	-	51	41	10	18659.868	-0.011
51	37	14	-	51	36	15	16321.956	-0.013
51	38	13	-	51	37	14	16789.347	-0.022
52	34	18	-	52	33	19	14900.428	0.030
52	43	9	-	52	42	10	19114.057	-0.020
52	37	15	-	52	36	16	16306.093	-0.043
52	30	22	-	52	29	23	13011.371	-0.069
52	38	14	-	52	37	15	16773.970	0.012
52	35	17	-	52	34	18	15369.544	-0.009
52	42	10	-	52	41	11	18645.549	0.005
52	41	11	-	52	40	12	18177.321	-0.043
53	51	2	-	53	50	3	22869.313	-0.007
53	38	15	-	53	37	16	16757.983	0.027
53	42	11	-	53	41	12	18630.699	-0.025
53	47	6	-	53	46	7	20978.975	-0.023
53	41	12	-	53	40	13	18162.346	0.016
53	44	10	-	53	43	11	19568.532	-0.001
53	37	16	-	53	36	17	16289.701	0.023
53	43	10	-	53	42	11	19099.435	0.006
54	41	13	-	54	40	14	18146.809	0.033
54	42	12	-	54	41	13	18615.440	0.032
54	46	8	-	54	45	9	20493.451	-0.020
54	43	11	-	54	42	12	19084.263	-0.042

Table-4.4 Continued(5)

J'	K_a'	K_c'	-	J''	K_a''	K_c''	Frequency	Deviation
54	37	17	-	54	36	18	16272.601	0.027
55	52	3	-	55	51	4	23313.981	-0.024
55	49	6	-	55	48	7	21892.804	0.007
55	41	14	-	55	40	15	18130.666	-0.024
55	37	18	-	55	36	19	16254.801	-0.004
55	48	7	-	55	47	8	21420.576	-0.042
55	42	13	-	55	41	14	18599.555	-0.028
55	44	12	-	55	43	13	19538.115	-0.001
55	43	12	-	55	42	13	19068.715	0.023
56	54	2	-	56	53	3	24250.195	0.030
56	50	6	-	56	49	7	22350.223	0.012
56	47	9	-	56	46	10	20933.544	0.003
56	37	19	-	56	36	20	16236.350	0.001
56	42	14	-	56	41	15	18583.252	0.016
56	45	11	-	56	44	12	19992.166	-0.003
56	32	24	-	56	31	25	13871.857	-0.073
56	43	13	-	56	42	14	19052.535	-0.045
56	41	15	-	56	40	16	18114.069	0.012
56	35	21	-	56	34	22	15294.452	-0.005
57	33	24	-	57	32	25	14324.962	0.023
57	53	4	-	57	52	5	23757.822	-0.003
57	52	5	-	57	51	6	23282.459	-0.015
57	51	6	-	57	50	7	22807.988	0.007
57	37	20	-	57	36	21	16217.167	-0.018
57	34	23	-	57	33	24	14800.163	0.003
57	46	11	-	57	45	12	20446.466	-0.006
57	45	12	-	57	44	13	19975.958	0.038
57	43	14	-	57	42	15	19035.967	0.012
57	41	16	-	57	40	17	18096.857	-0.004
57	42	15	-	57	41	16	18566.320	-0.033
57	44	14	-	57	43	15	19505.801	0.024
58	56	2	-	58	55	3	25172.887	0.028
58	55	3	-	58	54	4	24694.742	-0.005
58	41	17	-	58	40	18	18079.100	0.012
58	43	15	-	58	42	16	19018.785	-0.020
58	42	16	-	58	41	17	18548.933	0.012
58	45	13	-	58	44	14	19959.224	0.037
59	44	16	-	59	43	17	19471.433	0.009
59	45	14	-	59	44	15	19941.948	-0.011
59	41	18	-	59	40	19	18060.723	0.000
59	43	16	-	59	42	17	19001.146	0.029
59	42	17	-	59	41	18	18530.928	0.003
60	43	17	-	60	42	18	18982.894	0.016
60	54	6	-	60	53	7	24183.545	0.043
60	53	7	-	60	52	8	23707.392	-0.019
60	42	18	-	60	41	19	18512.407	0.056

Table-4.4 Continued(6)

J'	K_a'	K_c'	-	J''	K_a''	K_c''	Frequency	Deviation
60	35	25	-	60	34	26	15206.264	0.017
60	48	12	-	60	47	13	21338.545	-0.020
60	41	19	-	60	40	20	18041.778	0.028
61	57	4	-	61	56	5	25599.500	0.025
61	56	5	-	61	55	6	25120.634	-0.002
61	44	18	-	61	43	19	19434.954	-0.008
61	42	19	-	61	41	20	18493.196	0.012
61	55	6	-	61	54	7	24642.817	0.042
61	43	18	-	61	42	19	18964.102	0.028
61	52	9	-	61	51	10	23214.604	0.031
61	41	20	-	61	40	21	18022.193	0.042
61	46	15	-	61	45	16	20377.108	-0.018
61	47	14	-	61	46	15	20848.812	0.018
61	50	11	-	61	49	12	22266.385	-0.003
62	58	4	-	62	57	5	26060.973	0.021
62	43	19	-	62	42	20	18944.678	-0.014
62	42	20	-	62	41	21	18473.412	0.003
62	51	11	-	62	50	12	22722.127	0.037
63	57	6	-	63	56	7	25562.533	0.011
63	43	20	-	63	42	21	18924.673	-0.043
63	42	21	-	63	41	22	18453.044	0.034
63	34	29	-	63	33	30	14649.071	-0.013
63	49	14	-	63	48	15	21756.516	-0.031
64	61	3	-	64	60	4	27467.990	-0.011
64	60	4	-	64	59	5	26985.222	-0.022
64	59	5	-	64	58	6	26503.679	0.083
64	53	11	-	64	52	12	23634.369	-0.056
64	50	14	-	64	49	15	22210.812	0.018
64	58	6	-	64	57	7	26022.998	-0.015
64	54	10	-	64	53	11	24110.452	0.050
64	56	8	-	64	55	9	25064.869	0.008
64	46	18	-	64	45	19	20319.973	0.005
64	42	22	-	64	41	23	18431.962	-0.009
64	55	9	-	64	54	10	24587.167	-0.028
65	42	23	-	65	41	24	18410.219	-0.056
65	61	4	-	65	60	5	27448.116	0.041
65	60	5	-	65	59	6	26965.421	-0.032
65	59	6	-	65	58	7	26483.826	-0.100
65	46	19	-	65	45	20	20299.818	0.003
66	60	6	-	66	59	7	26945.193	-0.077
66	57	9	-	66	56	10	25504.055	-0.034
66	48	18	-	66	47	19	21224.646	0.005
66	59	7	-	66	58	8	26463.916	0.058
66	58	8	-	66	57	9	25983.489	0.008
66	52	14	-	66	51	15	23120.083	0.004
67	51	16	-	67	50	17	22625.121	-0.006

Table-4.4 Continued(7)

J'	K_a'	K_c'	-	J''	K_a''	K_c''	Frequency	Deviation
67	56	11	-	67	55	12	25005.349	-0.042
67	53	14	-	67	52	15	23575.169	0.033
67	55	12	-	67	54	13	24527.867	0.012
68	50	18	-	68	49	19	22130.083	0.052
69	49	20	-	69	48	21	21634.577	0.037
70	47	23	-	70	46	24	20664.349	-0.087
70	48	22	-	70	47	23	21138.373	0.012

Table-4.5

Observed Rotation Transition Frequencies(in MHz) of $F_2{}^{34}S^{16}O_2$.

J'	K_a'	K_c'	-	J''	K_a''	K_c''	Frequency	Deviation
2	1	1	-	1	1	0	20264.11*	-0.049
2	0	2	-	1	0	1	20245.51*	-0.069
2	1	2	-	1	1	1	20232.21*	0.002
3	0	3	-	2	0	2	30362.176	-0.035
3	1	3	-	2	1	2	30346.737	0.023
3	1	2	-	2	1	1	30394.332	-0.034
4	1	3	-	3	1	2	40521.917	-0.031
4	1	4	-	3	1	3	40459.648	-0.002
4	0	4	-	3	0	3	40473.455	0.053
5	1	4	-	4	1	3	50645.439	-0.036
5	1	5	-	4	1	4	50571.003	0.025
6	5	1	-	5	5	0	60750.421	0.017
6	0	6	-	5	0	5	60686.922	0.014
6	1	5	-	5	1	4	60763.539	0.090
6	1	6	-	5	1	5	60680.887	-0.001
6	2	5	-	5	2	4	60731.899	0.006
6	3	4	-	5	3	3	60751.623	0.060
6	3	3	-	5	3	2	60764.754	-0.034
6	5	2	-	5	5	1	60750.421	0.035
7	5	2	-	6	5	1	70876.549	-0.079
7	0	7	-	6	0	6	70792.947	-0.035
7	1	6	-	6	1	5	70875.162	-0.016
7	1	7	-	6	1	6	70789.673	-0.005
7	2	6	-	6	2	5	70847.320	-0.040
7	3	4	-	6	3	3	70901.665	0.045
7	5	3	-	6	5	2	70876.549	0.019

*-Reference [85][86]

Table-4.6
Observed Rotational Transition Frequencies(in MHz) of $F_2^{34}S^{18}O_2$.

J'	K_a'	K_c'	-	J''	K_a''	K_c''	Frequencies	Deviation
6	6	1	-	5	5	0	59093.082	-0.007
6	1	6	-	5	0	5	55971.150	-0.022
6	2	5	-	5	1	4	56450.133	0.050
7	7	1	-	6	6	0	68975.760	0.010
7	0	7	-	6	1	6	65259.968	0.016
7	1	7	-	6	0	6	65259.968	-0.021
7	1	6	-	6	2	5	65729.689	-0.011
7	2	5	-	6	3	4	66176.435	-0.044
7	2	6	-	6	1	5	65732.373	-0.040
7	3	5	-	6	2	4	66243.004	0.025
7	7	0	-	6	6	1	68978.950	0.033
8	7	2	-	7	6	1	78476.332	0.054
8	0	8	-	7	1	7	74548.816	0.061
8	1	8	-	7	0	7	74548.816	0.056
8	3	6	-	7	2	5	75502.029	-0.067
8	4	5	-	7	3	4	76094.918	-0.020
8	6	3	-	7	5	2	77908.184	-0.071

Table-4.7

Observed Rotational Transition Frequencies(in MHz) of $F_2^{32}S^{16}O_2$

(X-excited state, v_5=1, a_2 symmetry.)

J'	K_a'	K_c'	-	J''	K_a''	K_c''	Frequency	Deviation
2	1	1	-	1	1	0	20227.534	-0.083
2	1	2	-	1	1	1	20224.70*	-0.026
2	0	2	-	1	0	1	20226.11*	-0.008
3	1	3	-	2	1	2	30336.922	-0.075
3	0	3	-	2	0	2	30339.09*	0.023
3	1	2	-	2	1	1	30341.328	-0.028
4	1	4	-	3	1	3	40449.188	0.028
4	0	4	-	3	0	3	40451.939	0.057
4	1	3	-	3	1	2	40455.041	0.030
5	1	4	-	4	1	3	50568.529	-0.023
5	1	5	-	4	1	4	50561.193	0.017
6	5	2	-	5	5	1	60680.348	-0.024
6	1	5	-	5	1	4	60681.980	0.030
6	1	6	-	5	1	5	60672.980	-0.030
6	3	4	-	5	3	3	60678.658	0.055
6	3	3	-	5	3	2	60678.658	0.043
7	1	6	-	6	1	5	70795.144	-0.030
7	1	7	-	6	1	6	70784.624	-0.002
7	2	6	-	6	2	5	70790.288	-0.002
7	3	4	-	6	3	3	70791.300	-0.030
7	4	4	-	6	4	3	70792.193	0.007

Table-4.8

Observed Rotational Transition Frequencies(in MHz) of $F_2^{32}S^{16}O_2$

(Y-excited state, v_4=1, a_1 symmetry)

J'	K_a'	K_c'	-	J''	K_a''	K_c''	Frequency	Deviation
2	2	1	-	1	1	1	20251.58*	-0.044
2	1	1	-	1	0	1	20218.15*	0.014
2	2	0	-	1	1	0	20236.36*	-0.075
3	3	0	-	2	2	0	30358.29*	0.020
3	2	1	-	2	1	1	30328.187	0.050
3	3	1	-	2	2	1	30378.279	0.031
4	4	1	-	3	3	1	40505.790	0.063
4	2	2	-	3	1	2	40456.128	0.046
4	3	1	-	3	2	1	40439.368	0.000
4	3	2	-	3	2	2	40470.442	0.024
5	5	1	-	4	4	1	50634.188	0.024
5	4	1	-	4	3	1	50552.427	0.002

Table-4.8 Continued

J'	K_a'	K_c'	-	J''	K_a''	K_c''	Frequency	Deviation
6	6	1	-	5	5	1	60763.550	0.011
6	4	2	-	5	3	2	60667.358	-0.047
6	5	1	-	5	4	1	60668.006	-0.023
6	5	2	-	5	4	2	60709.831	-0.081
6	6	0	-	5	5	0	60746.583	-0.036
7	7	1	-	6	6	1	70893.802	0.075
7	5	2	-	6	4	2	70771.664	0.009
7	6	1	-	6	5	1	70787.070	0.095
7	4	4	-	6	3	4	70810.979	-0.083
7	2	5	-	6	1	5	70811.725	0.031
7	3	5	-	6	2	5	70811.725	0.022
7	7	0	-	6	6	0	70881.002	-0.071

*-Refrence [85][86]

Table-4.9
Observed Rotational Transition Frequencies(in MHz) of $F_2^{32}S^{16}O_2$
(U-excited state, v_3=1, a_1 symmetry)

J'	K_a'	K_c'	-	J''	K_a''	K_c''	Frequency	Deviation
3	1	3	-	2	1	2	30488.624	0.045
3	1	2	-	2	1	1	30506.555	-0.020
4	3	1	-	3	3	0	40664.674	-0.214
4	0	4	-	3	0	3	40658.986	0.020
4	1	3	-	3	1	2	40674.490	0.050
4	1	4	-	3	1	3	40650.730	0.020
4	3	2	-	3	3	1	40664.674	-0.069
5	3	3	-	4	3	2	50830.721	0.039
5	1	4	-	4	1	3	50841.419	0.015
5	1	5	-	4	1	4	50812.279	-0.020
6	1	5	-	5	1	4	61007.126	-0.065
6	1	6	-	5	1	5	60973.238	-0.062
7	2	6	-	6	2	5	71155.186	0.037
7	0	7	-	6	0	6	71139.301	0.009
7	1	6	-	6	1	5	71171.522	0.005
7	1	7	-	6	1	6	71133.716	0.012

Table-4.10
Observed Rotational Transition Frequencies(in MHz) of $F_2^{32}S^{16}O_2$
(Z-excited state, v_9=1, b_2 symmetry)

J'	K_a'	K_c'	-	J''	K_a''	K_c''	Frequency	Deviation
2	1	2	-	1	1	1	20248.800	0.095
2	0	2	-	1	0	1	20260.000	0.144
2	1	1	-	1	1	0	20275.000	0.179
3	0	3	-	2	0	2	30385.196	-0.004
4	2	2	-	3	2	1	40538.740	-0.051
6	2	5	-	5	2	4	60775.687	0.012
6	0	6	-	5	0	5	60740.159	-0.021
6	1	5	-	5	1	4	60803.340	0.012
6	1	6	-	5	1	5	60734.678	0.706
6	2	4	-	5	2	3	60819.403	0.010
7	5	2	-	6	5	1	70921.708	-0.025
7	0	7	-	6	0	6	70856.092	-0.030
7	1	7	-	6	1	6	70852.508	0.024
7	2	5	-	6	2	4	70956.942	0.001
7	2	6	-	6	2	5	70899.931	-0.017
7	3	4	-	6	3	3	70939.592	0.003
7	5	3	-	6	5	2	70921.708	0.028

Table-4.11
Observed Rotational Transition Frequencies(in MHz) of $F_2^{32}S^{16}O_2$
(W-excited state, v_7=1, b_1 symmetry)

J'	K_a'	K_c'	-	J''	K_a''	K_c''	Frequency	Deviation
2	0	2	-	1	0	1	20194.000	-0.081
3	2	1	-	2	2	0	30372.000	0.003
3	1	3	-	2	1	2	30240.300	-0.008
4	0	4	-	3	0	3	40317.730	0.032
4	1	3	-	3	1	2	40463.334	0.013
4	1	4	-	3	1	3	40308.172	-0.044
4	2	2	-	3	2	1	40511.001	0.006
4	2	3	-	3	2	2	40408.128	-0.019
6	0	6	-	5	0	5	60435.842	0.005
6	1	5	-	5	1	4	60586.228	0.049
6	1	6	-	5	1	5	60434.774	0.035
6	2	5	-	5	2	4	60563.563	0.031
7	5	3	-	6	5	2	70797.350	0.006
7	0	7	-	6	0	6	70497.045	-0.003
7	1	6	-	6	1	5	70640.295	-0.072
7	2	6	-	6	2	5	70630.704	0.002
7	3	4	-	6	3	3	70897.114	-0.004

Table-4.12
Observed Rotational Transition Frequencies(in MHz) of $F_2^{32}S^{18}O_2$
(K-excited state, $v_5=1$, a_2 symmetry)

J'	K_a'	K_c'	-	J''	K_a''	K_c''	Frequency	Deviation
3	3	0	-	2	2	1	29580.864	0.031
3	1	2	-	2	2	1	28475.352	-0.042
3	1	3	-	2	0	2	28126.442	0.080
4	4	1	-	3	3	0	39187.892	0.011
4	3	2	-	3	2	1	38595.324	-0.056
6	6	1	-	5	5	0	58948.089	-0.018
6	3	4	-	5	2	3	57006.913	0.001
6	4	3	-	5	3	2	57679.444	-0.007
6	6	0	-	5	5	1	58999.295	0.039
7	7	1	-	6	6	0	68812.305	-0.001
7	0	7	-	6	1	6	65281.165	0.008
7	1	6	-	6	2	5	65776.204	-0.006
7	2	5	-	6	3	4	66269.994	-0.005
7	3	5	-	6	2	4	66276.541	-0.014
7	6	1	-	6	5	2	68754.512	-0.014
7	7	0	-	6	6	1	68836.640	-0.013
8	8	1	-	7	7	0	78669.583	-0.063
8	0	8	-	7	1	7	74571.126	-0.007
8	1	8	-	7	0	7	74571.126	-0.007
8	2	7	-	7	1	6	75065.912	0.004
8	3	6	-	7	2	5	75562.037	0.052
8	4	5	-	7	3	4	76074.108	0.001
8	5	4	-	7	4	3	76715.294	-0.047
8	7	2	-	7	6	1	78292.776	0.054
8	8	0	-	7	7	1	78680.721	0.043

Table-4.13
Observed Rotational Transition Frequencies(in MHz) of $F_2^{32}S^{18}O_2$
(L-excited state, $v_4=1$, a_1 symmetry)

J'	K_a'	K_c'	-	J''	K_a''	K_c''	Frequency	Deviation
3	0	3	-	2	1	2	28000.956	-0.027
4	4	1	-	3	3	0	39261.647	0.023
6	6	1	-	5	5	0	59017.260	-0.009
6	0	6	-	5	1	5	55893.505	0.001
6	1	6	-	5	0	5	55895.621	0.017
6	2	5	-	5	1	4	56348.652	-0.008
6	4	3	-	5	3	2	57895.582	-0.019
6	3	4	-	5	2	3	57032.659	-0.016
6	5	2	-	5	4	1	58562.280	0.004
6	6	0	-	5	5	1	59018.830	0.000
7	6	1	-	6	5	2	68472.323	0.023
7	0	7	-	6	1	6	65175.274	0.022
7	1	6	-	6	2	5	65581.129	-0.031
7	2	6	-	6	1	5	65602.965	0.057
7	2	5	-	6	3	4	65867.287	0.003
7	6	2	-	6	5	1	68455.671	-0.024

Table-4.13 Continued

J'	K_a'	K_c'	-	J''	K_a''	K_c''	Frequency	Deviation
8	8	1	-	7	7	0	78760.135	0.038
8	0	8	-	7	1	7	74456.345	0.046
8	1	8	-	7	0	7	74456.345	-0.059
8	2	7	-	7	1	6	74874.827	-0.033
8	3	6	-	7	2	5	75356.495	0.018
8	5	4	-	7	4	3	77114.611	0.009
8	6	3	-	7	5	2	77857.793	-0.004
8	8	0	-	7	7	1	78760.135	-0.035

Table-4.14
Observed Rotational Transition Frequencies(in MHz) of $F_2^{32}S^{18}O_2$
(M-excited state, v_9=1, b_2 symmetry)

J'	K_a'	K_c'	-	J''	K_a''	K_c''	Frequency	Deviation
6	6	1	-	5	5	0	59151.806	-0.024
6	0	6	-	5	1	5	56010.691	0.075
6	6	0	-	5	5	1	59158.759	0.064
7	1	6	-	6	2	5	65767.765	-0.066
7	1	7	-	6	0	6	65307.135	-0.005
7	2	6	-	6	1	5	65772.221	-0.024
7	3	6	-	6	2	4	66290.079	-0.011
7	4	4	-	6	3	3	67059.356	-0.026
7	5	3	-	6	4	2	67976.738	0.035
7	6	2	-	6	5	1	68632.215	0.034
7	7	0	-	6	6	1	69046.529	-0.026
7	7	1	-	6	6	0	69044.410	-0.096
8	0	8	-	7	1	7	74603.292	0.015
8	1	8	-	7	0	7	74603.292	0.005
8	7	1	-	7	6	2	78570.133	0.055

Table-4.15
Observed Rotational Transition Frequencies(in MHz) of $F_2^{32}S^{18}O_2$
(N-excited state, v_7=1, b_1 symmetry)

J'	K_a'	K_c'	-	J''	K_a''	K_c''	Frequency	Deviation
6	0	6	-	5	1	5	55774.592	-0.041
7	0	7	-	6	1	6	65027.892	0.014
7	1	7	-	6	0	6	65027.892	-0.009
7	1	6	-	6	2	5	65542.889	0.047
7	2	6	-	6	1	5	65544.749	0.056
7	3	5	-	6	2	4	66091.688	-0.022
7	6	2	-	6	5	1	68575.751	-0.022
8	0	8	-	7	1	7	74281.271	0.026
8	1	8	-	7	0	7	74281.271	0.023
8	1	7	-	7	2	6	74796.420	-0.100
8	2	6	-	7	3	5	75310.450	0.004
8	8	0	-	7	7	1	78907.512	0.021

4.2 Infrared Results

A low resolution scan of our oxygen-18 enriched sample of F_2SO_2 in the region of the ν_1 fundamental is shown in Figure-4.6. We were able with the spectrometers available to scan the regions of all the stretching fundamentals only. Even at low resolution three of the fundamentals show Q-branch features easily attributed to $F_2^{32}S^{16}O_2$, $F_2^{32}S^{16}O^{18}O$ and $F_2^{32}S^{18}O_2$ respectively. At higher resolution the Q-branches were shown to consist of number of peaks forming a pattern which gradually degraded to low frequency. No isotopic structure was observed for the $887 cm^{-1}$ band, though, even at high resolution.

Our measured vibrational frequencies, reported in Tables 4.29-4.32, represent for each isotope the wavenumber of the strongest Q-branch feature discerned from high resolution scans.

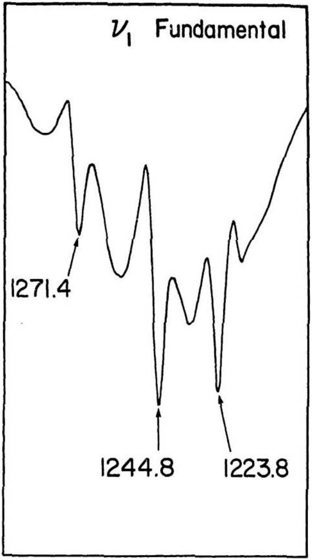

Figure-4.6 The Infrared Spectra of the ν_1 Fundamental for $F_2^{32}S^{16}O_2$, $F_2^{32}S^{16}O^{18}O$ and $F_2^{32}S^{18}O_2$ Species.

4.3 Calculation of the Rotational Constants and the Centrifugal Distortion Constants of Sulphuryl Fluoride

The observed line frequencies were used to calculate the rotational constants and quartic centrifugal distortion constants. Because one isotopomer of this molecule is a slightly asymmetric prolate rotor, the constants were derived using Watson's S-reduction[46][47] Hamiltonian in the I^r representation.

Lide's rotational constants[85][86] for $F_2^{32}S^{16}O_2$ and $F_2^{34}S^{16}O_2$ could only predict accurately very low J transition frequencies ($J<4$); quartic distortion constants, all of which were assumed to be zero in Lide's work, were needed to fit the higher J transitions. For $F_2^{34}S^{16}O_2$, only three quartic distortion constants were obtained; D_K and d_1 were constrained to values calculated from the force field discussed in Section 4.6. No sextic distortion constants were required to fit the data obtained for these two species. The ground state effective molecular geometry derived from the effective rotational constants of $F_2^{32}S^{16}O_2$ and $F_2^{34}S^{16}O_2$ was used to obtain rough estimates for the rotational constants of $F_2^{32}S^{18}O_2$, $F_2^{32}S^{16}O^{18}O$ and $F_2^{34}S^{18}O_2$, which gave reasonable predictions for the low J transitions of these three species. As higher J lines were found, distortion constants were required to fit the obtained frequencies; Q-branch transitions or higher K_a transitions were needed to obtain a good D_K value. Three different representations(I_r, II_r and III_r) were used to calculate these constants for $F_2^{32}S^{18}O_2$; the results are summarized in Table-4.23. Several very weak lines with $\Delta K_a = 3$ or $\Delta K_c = 3$, both in R and Q branches, were measured, which helped a lot in the distortion constant refinement; all of the quartic and sextic distortion constants , except for H_J, were derived for $F_2^{32}S^{18}O_2$. Even though more than three hundred lines of $F_2^{32}S^{16}O^{18}O$ were assigned, an accurate value for the distortion constants d_2 could still not be derived; because this isotopomer is almost a prolate symmetric rotor d_2 is expected to have a small value if Watson's S-reduction Hamiltonian in an I^r representation is employed. Several quartic distortion constants of $F_2^{32}S^{18}O_2$ were constrained to values calculated using the force field described in the last section of this chapter.

For the $F_2^{32}S^{16}O_2$ and $F_2^{32}S^{18}O_2$ excited states, there were insufficient data available to derive values for all of the quartic distortion constants. In these cases the distortion constants of the excited states were assumed to be the same as those of the corresponding ground state.

All of the derived spectroscopic constants are collected in Tables 4.16 to 4.22.

Table-4.16

Effective Rotational Constants of F_2SO_2

Species	A (MHz)	B (MHz)	C (MHz)	κ
$F_2{}^{32}S^{16}O_2$	5134.8874(32)	5073.0761(11)	5057.0581(14)	-0.5884
$F_2{}^{32}S^{18}O_2$	4941.7625(7)	4831.4802(7)	4646.3812(8)	+0.2533
$F_2{}^{32}S^{16}O^{18}O$	5096.0749(10)	4894.7017(12)	4844.6137(12)	-0.6016
$F_2{}^{34}S^{16}O_2$	5135.196(57)	5070.0471(41)	5054.0649(39)	-0.6060
$F_2{}^{34}S^{18}O_2$	4939.8697(62)	4831.6884(77)	4644.7311(67)	+0.2669

Table-4.17

Effective Moment of Inertia of F_2SO_2

Species	I^0_A ($amuA^2$)	I^0_B ($amuA^2$)	I^0_C ($aumA^2$)
$F_2{}^{32}S^{16}O_2$	98.42066(6)	99.61983(2)	99.93478(3)
$F_2{}^{32}S^{18}O_2$	102.26696(1)	104.60128(2)	108.76830(2)
$F_2{}^{32}S^{16}O^{18}O$	99.17025(2)	103.25021(3)	104.31771(3)
$F_2{}^{34}S^{16}O_2$	98.41692(108)	99.67940(81)	99.99449(8)
$F_2{}^{34}S^{18}O_2$	102.30603(105)	104.59681(186)	108.80678(121)

Table-4.18

Quartic Centrifugal Distortion Constants of F_2SO_2

Term	$F_2^{32}S^{16}O_2$	$F_2^{32}S^{18}O_2$	$F_2^{32}S^{16}O^{18}O$	$F_2^{34}S^{16}O_2$	$F_2^{34}S^{18}O_2$
D_J/MHz	1.4912(73)[b]	1.1795(44)	1.111(11)	1.519(39)	1.180(55)
D_{JK}/MHz	-1.576(27)	-0.04869(82)	1.0085(6)	-1.57(12)	-0.0615[c]
D_K/MHz	2.370(13)	0.11266(97)	-0.8541(2)	1.94[c]	0.119[c]
d_1/MHz	-0.0252(71)	-C.15624(36)	-0.0356(19)	-0.0309[c]	-0.157[c]
d_2/MHz	0.1402(36)	-0.02319(14)	0.0027(37)	0.1476[c]	-0.0223[c]
H_J/kHz		-0.00767(76)	0.00590(11)		
H_{JK}/kHz		0.00967(83)	-0.01039(17)		
H_K/kHz			0.00500(9)		
h_1/kHz		0.00058(21)			
h_2/kHz		-0.00027(14)			
h_3/kHz		-0.00049(3)			
κ^d	-0.5884	0.2533	-0.6016	-0.6060	0.2669
ε_{fit} (MHz)	0.026	0.036	0.033	0.048	0.043

a--Where no value is given for a constant it was constrained to zero.

b--Number in parentheses represent one standard deviation in the units of the last digits quoted.

c--Constrained to the value calculated from the Fit I force field.

d--Value of Ray's asymmetry parameter.

Table-4.19

Effective Rotational Constants of $F_2^{32}S^{16}O_2$ in Excited States.

States	$A_v(MHz)$	$B_v(MHz)$	$C_v(MHz)$	ε_{fit} (MHz)
X-state	5155.6161(127877)	5057.2629(71)	5055.8228(70)	0.0437
Y-state	5067.1085(89)	5050.4145(100)	4917.0898(3193)	0.0675
U-state	5140.4755(3780)	5086.0521(90)	5079.9963(74)	0.0480
W-state	5137.6351(241)	5075.0841(60)	5030.3765(47)	0.0397
Z-state	5132.2848(1602)	5071.9801(68)	5058.9216(85)	0.0622

Table-4.20

Effective Rotational Constants of $F_2^{32}S^{18}O_2$ in Excited States.

States	$A_v(MHz)$	$B_v(MHz)$	$C_v(MHz)$	ε_{fit} (MHz)
K-state	4925.5573(39)	4864.4615(83)	4645.3581(61)	0.0416
L-state	4835.9232(34)	4784.5340(146)	4640.7165(35)	0.0327
M-state	4945.3216(55)	4827.5754(114)	4648.3933(62)	0.0528
N-state	4943.1521(71)	4835.4527(190)	4626.3666(64)	0.0500

Table-4.21

The Excited State Quartic Centifugal Distortion Constants(kHz) of $F_2^{32}S^{16}O_2$

State	D_J	D_{JK}	D_K	d_1	d_2
$X-$	1.175(4)	-9.441(185)	a	0.180(44)	a
$Y-$	2.860(54)	9.805(741)	-1420.2(272)	0.2276(626)	0.7070(535)
$U-$	2.837(57)	-5.684(590)	a	-0.680(50)	a
$W-$	1.770(37)	-7.083(189)	a	-1.920(30)	a
$Z-$	1.483(73)	-1.772(179)	a	a	0.152(33)

a--Constrained to the value obtained for the ground state.

Table-4.22

The Excited State Quartic Centrifugal Distortion Constants(kHz) of $F_2^{32}S^{18}O_2$

State	D_J	D_{JK}	D_K	d_1	d_2
$K-$	7.380(74)	-20.02(26)	13.84(20)	-3.153(44)	0.0597(129)
$L-$	-4.428(99)	16.09(26)	-10.30(17)	2.890(63)	0.2354(159)
$M-$	1.109(56)	a	a	a	a
$N-$	-0.703(57)	a	a	a	a

a--Constrained to the value obtained for the ground state.

Table-23

Rotational Constants and Distortion Constants of $F_2^{32}S^{18}O_2$

in Different Representations

Terms	I^r	II^r	III^r
A (MHz)	4941.7625(7)	4941.7624(8)	4941.7629(8)
B (MHz)	4831.4802(7)	4831.4808(8)	4831.4806(8)
C (MHz)	4646.3812(8)	4646.3814(9)	4646.3815(9)
D_J (kHz)	1.1795(44)	0.9554(56)	1.3808(55)
D_{JK} (kHz)	-0.04869(82)	0.8560(77)	-0.7391(99)
D_K (kHz)	0.11266(97)	-0.2727(64)	0.2755(15)
d_1 (kHz)	-0.15624(36)	0.0824(5)	0.0737(4)
d_2 (kHz)	-0.02319(14)	-0.0618(6)	-0.0070(1)
H_J (Hz)	-0.00767(76)	-0.1056(63)	0.01136(51)
H_{JK} (Hz)	0.00967(83)	0.1016(69)	-0.0314(11)
H_K (Hz)			
h_1 (Hz)	0.00058(21)	-0.00143(30)	0.00065(24)
h_2 (Hz)	-0.00027(14)	-0.00764(39)	0.00100(16)
h_3 (Hz)	-0.000489(34)	0.000744(82)	0.000040(37)
ε_{fit} (MHz)	0.03774	0.03755	0.03769

4.4 The Molecular Geometry of Sulphuryl Fluoride

The ground state effective rotational constants of Table-4.16, have been converted to the principal moments of inertia, Table-4.17, which were used to calculate the ground state effective or r_0 molecular structure. This geometry was evaluated by a least squares procedure, which fitted the structural parameters to the experimental effective moments of inertia of $F_2^{32}S^{16}O_2$, $F_2^{32}S^{18}O_2$, $F_2^{32}S^{16}O^{18}O$ and $F_2^{34}S^{16}O_2$. The data for $F_2^{34}S^{18}O_2$ were not employed in the calculation. The resulting structural parameters are listed in the fourth row of Table-4.25. This geometry was employed subsequently in the force constant determination .

Although the effective structural parameters appear to be well defined it is well known that a neglect of vibrational effects can give rise to misleading results, particularly when an atom lies close to a principal inertial axis as does sulfur in this case. In order to obtain more reliable structural parameters for F_2SO_2 we have performed several average structure calculations. The calculation of the harmonic force field will be described in next section. The force constants presented in Table-4.33, Fit-I, have, however, been used here in the derivation of the average and equilibrium molecular structures.

Average structural parameters were first obtained from a least squares fit in which isotopic variations in bond distances were ignored and rotational constants were weighted inversely as the squares of assigned uncertainties (0.1% of the value of each constants). The structure parameters derived in this way, our uncorrected r_z structure, are also reported in Table-4.25.

We attempted further r_z structure calculations in which the isotopic variations in bond distances were considered. The harmonic vibration-rotation interaction constants derived from the harmonic force field, have been employed to calculate values for the ground state average rotational constants A_z,B_z and C_z using equation-1.3.15. The resulting ground state average rotational constants are collected in Table-4.24. Because there are four geometric parameters for this molecule, .t least two isotopic species are required to evaluate the whole molecular structure. Therefore the isotopic variations of the bond lengths were needed in this calculation; these were derived using equation-1.3.4 and the harmonic force constants obtained in the next section, Table-4.33. Values of the Morse anharmonicity parameters used in the calculation, were $a(SO) = 2.072\AA^{-1}$ and $a(SF) = 2.06\AA^{-1}$, both from Kuchitsu and Morino[92]. The value of $a(SF)$ was the average of $a(S_2)$ and $a(F_2)$. Isotopic variations in the mean square amplitude of vibration of the bond considered, $\delta\langle u^2\rangle$, and the corresponding changes in the mean square perpendicular amplitude correction, δK were evaluated from the harmonic force field[39]. All of the calculated δr_z's, typically about $10^{-5}\AA$, are given in Table-4.26 together with the values for $\delta\langle u^2\rangle$ and δK. A least squares procedure was again used to derive the ground state average molecular structure, r_z, of F_2SO_2 from a fit to the average rotational constants using the δr_z values of Table-4.25.

Finally, we refined values for the Morse parameters as well and obtained a somewhat better result; this is our preferred ground state average geometry of F_2SO_2. This r_z molecular structure is shown in Figure 4.8.

Using the above average molecular geometry as a starting point, we have evaluated a crude equilibrium molecular structure, with the help of equation-1.3.3 and the harmonic force field. In the calculation of both the average structure and the equilibrium structure, $F_2^{32}S^{16}O_2$ was used as the parent species.

The structure of F_2SO_2 has also been evaluated by both the usual[9] and a modified substitution method adopting $F_2^{32}S^{16}O_2$ as the parent and using as well the effective rotational constants for $F_2^{34}S^{16}O_2$ and $F_2^{32}S^{18}O_2$ taken from Table-4.1b. Because the sulfur atom lies close to the center of the principal inertial axes system, isotopic substitution of sulphur changes the principal moments of inertia only slightly. Relative to the parent the three principal moments of $F_2^{34}S^{16}O_2$ change by -0.00591(108)$u\mathring{A}^2$, 0.05952(8)$u\mathring{A}^2$ and 0.05919(8)$u\mathring{A}^2$ for ΔI_a, ΔI_b and ΔI_c, respectively. For a rigid molecule the ΔI_b and ΔI_c values should be equal and the ΔI_a value should be zero. In an initial calculation the a-coordinate of sulfur was taken to be 0.17418(25)$\mathring{A}$, the mean of the two values obtained using either ΔI_b or ΔI_c. The two oxygen coordinates were determined by the usual substitution methods[9] and the a-coordinate and c-coordinate of fluorine were found respectively using the center of mass condition and the effective A value for $F_2^{32}S^{16}O_2$. This uncorrected partial r_s structure, presented in Table-4.25, is in poor agreement with the r_0 and r_t geometries.

A modified substitution method, employed previously for F_2SeO_2[158], was also used to evaluate an r_s structure for F_2SO_2. This method assumes that the changes in moments of inertia which occur as a consequence of isotopic substitution can be expressed as the sum of two terms. One term equals the change that would be observed for a totally rigid molecule and the second gives the change resulting from zero-point vibrational effects. For the g^{th} inertial axis

$$(\Delta I_g)_{Observed} = (\Delta I_g)_{Rigid\ Top} + (\Delta I_g)_{Zero\ Point\ Vib.} \qquad (4.4.1)$$

It is desirable to subtract the zero-point term from the observed changes before performing a substitution calculation. For isotopic substitution at the central atom of a spherical top the zero-point term should be very nearly equal for all three principal moments since isotopic variations in the harmonic alpha constants are small and similar for all three rotational constants and, further, isotopic variations in bond distances should change all principal moments of inertia by a similar amount. For spherical tops one can therefore write

$$(\Delta I_a)_{Zero\ Point} \approx (\Delta I_b)_{Zero\ Point} \approx (\Delta I_c)_{Zero\ Point} \qquad (4.4.2)$$

In the second r_s calculation the change in I_a consequent to ^{34}S isotopic substitution has been subtracted from the observed changes in I_b and I_c and these corrected values were used to determine the a-coordinate of sulfur.

$$(\Delta I_g)_{Corrected} = (\Delta I_g)_{Rigid\ Top} = (\Delta I_g)_{Observed} - (\Delta I_a)_{Observed} \qquad g = b,c \tag{4.4.3}$$

The coordinates of the remaining atoms were determined as for the previous substitution structure. The resulting "corrected" substitution structure, also given in Table-4.25, is now quite consistent with the r_z structure.

If one applied the modified substitution method to the $F_2^{32}S^{18}O_2$ and $F_2^{34}S^{18}O_2$ isotopomers, and makes the very dubious assumption that the errors in the derived structural parameters are governed entirely by the experimental uncertainties in the rotational constants, then partial substitution parameters slightly different from above are obtained - for example, one obtains a value of 1.4008(4)Å for the r_{SO} bond length - again in good agreement with the r_z geometry.

Finally, we have evaluated a partial substitution structure in which the a-coordinate of sulfur in the normal isotopomer, $F_2^{32}S^{16}O_2$, was determined by the double substitution method of Pierce[159][160]. The calculation is complicated in this case by the fact that oxygen-18 substitution causes a reorientation of the principal inertial axes and also due to the fact that oxygen does not lie on an inertial axis. The required difference between the a-coordinate of sulfur in $F_2^{32}S^{16}O_2$ and the b-coordinate of sulfur in $F_2^{32}S^{18}O_2$ was therefore equated to the difference in the corresponding oxygen coordinate values (0.0313Å) as determined by the substitution method. Two second differences in moments of inertia can be used:

$$\Delta\Delta I_1 = I_b(F_2^{34}S^{16}O_2) - I_b(F_2^{32}S^{16}O_2) - [I_a(F_2^{34}S^{18}O_2) - I_a(F_2^{32}S^{18}O_2)] \tag{4.4.4}$$

$$\Delta\Delta I_2 = I_c(F_2^{34}S^{16}O_2) - I_c(F_2^{32}S^{16}O_2) - [I_c(F_2^{34}S^{18}O_2) - I_c(F_2^{32}S^{18}O_2)] \tag{4.4.5}$$

The experimental $\Delta\Delta I_1$ and $\Delta\Delta I_2$ values, 0.02033(15)uÅ^2 and 0.02054(18)uÅ^2, again are slightly different due to zero-point vibrational effects as well as experimental uncertainty. A partial substitution structure in which the average double substitution a-coordinate of sulfur was used is presented in Table-4.25. This structure is almost identical with that obtained by the modified substitution method.

The effective, substitution, average and crude equilibrium molecular structures of F_2SO_2, obtained in this work, are all collected in Table-4.25, and compared with the two previous microwave structures[84][85][86] and the more recent electron diffraction structure, r_a[88]. Table-4.25 also gives a theoretical structure for this molecule, which was derived from an ab-initio calculation using the Monstergauss program written by Poirier[65] and a 6-31G* basis set. Although the parameters listed in this table do not have the same physical meaning some differences between the r_z parameters of this work and the r_a electron diffraction values, for example, are evident. It transpires, as discussed by Hagen *et al*[88] in detail, that the evaluation of structural parameters for a near spherical molecule such as F_2SO_2 using electron diffraction is somewhat problematic, especially when, as in this case, the atoms bonded to the central atom have similar atomic numbers. Albeit not without considerable effort the present study has greatly increased the precision of the experimental structural determination for this molecule.

The F_2SO_2 molecule is very close to a spherical rotor and therefore it is possible to change the molecule's principal axes ori. ıtation by isotopic substitution. Figure-4.7 gives the principal axes coordinates of $F^{32}S^{16}O_2$, $F^{32}S^{18}O_2$ and $F^{32}S^{16}O^{18}O$, which shows the changes in the principal axes orientation caused by isotopic substitution. The species $F_2^{32}S^{16}O_2$, $F_2^{32}S^{16}O^{18}O$ and $F_2^{34}S^{16}O_2$ are slightly asymmetric prolate rotors with Ray's asymmetry parameter values [58], equation-1.1.8, κ of about -0.6. However, the species $F_2^{32}S^{18}O_2$ and $F_2^{34}S^{18}O_2$ are very asymmetric oblate tops, with κ about 0.25. The substitution of ^{18}O rotates the principal axes and exchanges the a-axis and the b-axis. Table-4.28 gives the principal axes coordinates of sulphuryl fluoride and shows that the S atom is very close to the mass center of the molecule. In $F_2^{32}S^{16}O^{18}O$, because of the asymmetric substitution of ^{18}O, the molecule loses C_{2v} symmetry. In this case the angle between the $S^{16}O$ bond and the b-axis is 20.89°, while the angle between the FSF plane and the b-axis is 41.60°.

The various molecular geometries obtained for sulphuryl fluoride are given in Table-4.25. It is seen from this table that both the bond lengths and bond angles show only slight variations from one structure to the next. This is because there is no light atom, such as hydrogen, in this molecule, and therefore the neglect of vibrational effects does not introduce large errors in the molecular coordinates. Both the SO and SF bond lengths follow the $r_z > r_0 > r_e > r_{ab-initio}$ trend, except that the r_0 and r_z values for the SF bond are almost equal. The normal substitution structure obtained for this molecule is in very poor agreement with all of the other spectroscopic structures. Table-4.27 gives a comparison of the structure of F_2SO_2 with the structures of molecules SO_2, F_2SO [95][133] and SF_2 [95][96][97]. The SO bond length of F_2SO_2 is about 0.012Å and 0.032Å shorter than that of F_2SO and that of SO_2, respectively. The FS bond is about 0.05Å shorter than that of F_2SO and F_2S. The SOS angle is about 5.5 ° bigger than that of SO_2. The angle FSF is about 2.9° smaller and 2.5° bigger than that of F_2S and F_2SO, respectively.

Table-4.24

Average Rotational Costants of F_2SO_2

Isotopomer	$A_z(MHz)$	$B_z(MHz)$	$C_z(MHz)$
$F_2^{32}S^{16}O_2$	5129.352	5067.096	5051.829
$F_2^{32}S^{18}O_2$	4935.952	4826.475	4641.848
$F_2^{32}S^{16}O^{18}O$	5090.231	4889.381	4839.746
$F_2^{34}S^{16}O_2$	5129.669	5064.081	5048.850
$F_2^{34}S^{18}O_2$	4934.074	4826.685	4640.206

Table-4.25 Molecular Geometry of F_2SO_2

Parameter	$Bond_{SO}/\AA$	$Bond_{SF}/\AA$	$Angle_{OSO}/^{\circ}$	$Angle_{FSF}/^{\circ}$
r_0 [a]	1.370(10)	1.570(10)	129.63(50)	92.78(50)
r_0 [b]	1.405(3)	1.530(3)	123.97(20)	96.12(17)
r_a [c]	1.397(2)	1.530(2)	122.6(12)	96.7(11)
r_0	1.4003(13)[d]	1.5361(15)	125.03(20)	95.41(12)
r_z (Uncorrected)[e]	1.4004(15)	1.5376(19)	125.11(24)	95.36(15)
r_z (Corrected)[f]	1.40121(60)	1.53670(73)	124.988(94)	95.435(59)
r_z (Corrected)[g]	1.40174(24)	1.53610(29)	124.910(37)	95.485(23)
r_e	1.3985	1.5311		
r_s (Usual)	1.4036[h]	1.5260	124.43	96.30
r_s (Modified)	1.3996(13)[i]	1.5365(38)	125.04(21)	95.43(31)
r_s (Double)	1.3997(12)[j]	1.5364(34)	125.03(19)	95.44(28)
$r_{ab\text{-}initio}$ [k]	1.3959	1.5306	124.733	95.201

a--Reference[84]. b--Reference[86]. c--Reference[88].

d--Errors quoted are twice the estimated standard deviations obtained from a weighted least squares fit to the rotational constants.

e--Obtained from a fit to the average rotational constants of Table-4.33(Fit-I). Isotopic variations in bond distances were ignored.

f--Isotopic variations in bond distances were calculated using fixed Morse anharmonicity parameter values of $a(SO)$=2.07$\AA^{-1}$ and $a(SF)$=2.06$\AA^{-1}$ from reference[92].

g--Isotopic variations in bond distances were calculated using Morse anharmonicity parameter values of $a(SO)$=2.80(20)$\AA^{-1}$ and $a(SF)$=2.54(44)$\AA^{-1}$ refined in this work.

h--No uncertainties are quoted since with this method the experimental errors in the moments of inertia are much smaller than uncertainties introduced by the neglect of zero-point vibrational effects.

i--The uncertainties are assumed to arise entirely from the error in the a-coordinate of sulfur and correspond to two standard errors in the rotational constants values of Table-4.16.

j--Mean value. See the text. k--6.31G* basis set.

Table-4.26.

Parameters Describing the Isotopic Variation in the Average Bond Lengths of Sulphuryl Fluoride

Parameter		$F_2^{32}S^{16}O_2$	$F_2^{32}S^{18}O_2$	$F_2^{32}S^{16}O^{18}O$	$F_2^{34}S^{16}O_2$
u	$S^{16}O$	0.03386		0.03385	0.03371
(Å)	$S^{18}O$		0.03318	0.03318	
	SF	0.04005	0.04005	0.04005	0.03985
$\delta\langle u^2\rangle$	$S^{16}O$			0.00	-0.00001
(Å^2)	$S^{18}O$		-0.000045	-0.000045	
	SF		0.0	0.0	-0.000016
K	$S^{16}O$	0.001568		0.001585	0.001555
(Å)	$S^{18}O$		0.001470	0.001453	
	SF	0.001144	0.001180	0.001162	0.001131
δK	$S^{16}O$			0.000017	-0.000013
(Å)	$S^{18}O$		-0.000098	-0.000115	
	SF		0.000036	0.000018	-0.000013
δr	$S^{16}O$			-0.000017	-0.000018
(Å)	$S^{18}O$		-0.000042	-0.000025	
	SF		-0.000036	-0.000018	-0.000037

Table-4.27.

Comparison Between the Geometries

of SO_2, SF_2, F_2SO and F_2SO_2

Parameter		$Bond_{SO}/\AA$	$Bond_{SF}/\AA$	$Angle_{OSO}/^\circ$	$Angle_{FSF}/^\circ$
r_0	F_2SO_2 [c]	1.4003	1.5361	125.03	95.41
	F_2SO [d]	1.412	1.585		92.82
	SO_2 [a]	1.4322		119.535	
	FO_2 [b]		1.589		98.27
r_e	F_2SO_2 [c]	1.3985	1.5361		
	SO_2 [a]	1.4308		119.33	
	SF_2 [b]		1.5875		98.048
r_z	F_2SO_2 [c]	1.40174	1.53610	124.910	95.485
	SF_2 [b]		1.5921		98.197

a--Reference [95][96].

b--Reference[97].

c--This work.

d--Reference [133].

Table-4.28 Principal Axes Coordinates of F_2SO_2

Species	Atoms	a	b	c
$F_2^{32}S^{16}O_2$	O	0.8290	1.2423	0.0000
	O	0.8290	-1.2423	0.0000
	S	0.1819	0.0000	0.0000
	F	-0.8511	0.0000	1.1362
	F	-0.8511	0.0000	-1.1362
$F_2^{32}S^{16}O^{18}O$	^{16}O	0.4071	1.4487	0.0000
	^{18}O	-1.4509	-0.2008	0.0000
	S	-0.0923	0.1400	0.0000
	F	0.5935	-0.6325	1.1362
	F	0.5935	-0.6325	-1.1362
$F_2^{32}S^{18}O_2$	O	1.2423	0.7977	0.0000
	O	-1.2423	0.7977	0.0000
	S	0.0000	0.1506	0.0000
	F	0.0000	-0.8824	1.1362
	F	0.0000	-0.8824	-1.1362
$F_2^{34}S^{16}O_2$	O	0.8256	1.2423	0.0000
	O	0.8256	-1.2423	0.0000
	S	0.1784	0.0000	0.0000
	F	-0.8545	0.0000	1.1362
	F	-0.8545	0.0000	-1.1362

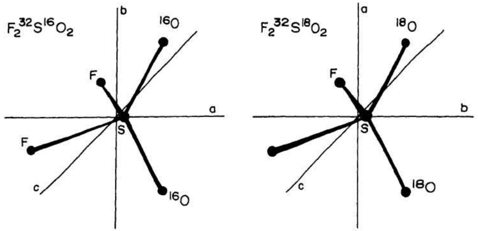

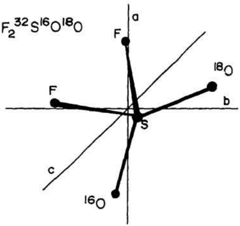

Figure-4.7

The Principal Inertial Axes Coordinates, r_o, of $F_2^{32}S^{16}O_2$, $F_2^{32}S^{18}O_2$ and $F_2^{32}S^{16}O^{18}O$, Which Show the a and b Principal Axes Reorientations Caused by ^{18}O Substitution.

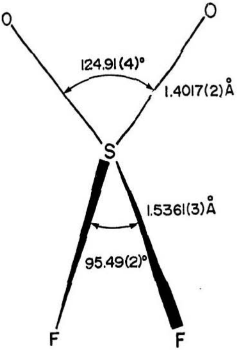

Table-8 The Preferred Ground State Average Molecular Structure of Sulfuryl Fluoride.

4.5 Coriolis Interaction Constants

After comparing Table-4.16 with Table-4.19 and Table-4.20, we note some unusual changes in rotational constant values that occur with vibrational excitation. For $F_2^{32}S^{16}O_2$, the rotational constant C of the Y excited state is $217.80MHz$ smaller than the rotational constant A of the ground state; the other two constants, however, change by only about $6MHz$. Because we have employed single vibrational state rotational Hamitonians throughuot, the Y state effectively has c-type transitions; we compared its C rotational constant with the A value of the ground state and its A and B with B and C of ground state, respectively. For $F_2^{32}S^{18}O_2$, the changes in the B rotational constants are much bigger than those of A and C; this is seen when comparing the excited states K and L with the ground state. Because the A rotational constant of the excited state X of $F_2^{32}S^{16}O_2$ was not well determined and not all of its distortion constants were obtained , Table-4.19 and Table-4.21, this state was not considered in the calculation of the Coriolis constant $\zeta^{\xi_{4,5}}$. Similarly, the changes in the values of the distortion constants τ_{aaaa} of $F_a^{32}S^{16}O_2$ and τ_{bbbb} of $F_2^{32}S^{18}O_2$ are much bigger than those of other distortion constants. The unusual variations in values of rotational constants and centrifugal distortion constants show that there is a Coriolis interaction between these two excited states.

According to the symmetry analysis, the three rotations R_x, R_y and R_z of F_2SO_2 under the C_{2v} point group belong to the species b_2, b_1 and a_2, respectively. The v_4 and v_5 modes, which belong to the a_1 and a_2 species respectively, have almost the same vibrational frequency. According to group theory, using the direct product of the representations of the two vibrational modes.

$$a_1 \times a_2 = a_2 \supseteq R_z \tag{4.5.1}$$

it follows that the nonzero Coriolis coupling constant is $\zeta_{4,5}^{\xi}$ [94]. Similarly, for the v_3

and ν_7 modes, which belong to the b_1 and b_2 species respectively, we have:

$$a_1 \times b_2 = b_2 \supseteq R_v \tag{4.5.2}$$

the nonzero Coriolis coupling constant is $\zeta^y_{3,7}$. Here the z axis is the a principal inertial axis for $F_2^{32}S^{16}O_2$ but is the b principal inertial axis for $F_2^{32}S^{18}O_2$. The y axis is the c principal inertial axis for both isotopomers.

Hirota and Sahara[98] suggested an approximate method to calculate the Coriolis coupling constant using rotational constant and distortion constant values for Coriolis perturbed states. They assumed that any changes in rotational constants and distortion constants caused by the excitation of the vibration are due only to the Coriolis interaction and are specified by the following equation

$$\zeta^a_{i,j} = \frac{(\Delta A)^{3/2}}{A_{g.s}(\Delta\tau_{aaaa})^{1/2}} \tag{4.5.3}$$

with similar equations for $\zeta^b_{i,j}$ and $\zeta^c_{i,j}$. The difference between the vibrational energies of the two states, $\Delta E_{i,j}$, can also be obtained as

$$\Delta E_{i,j} = \frac{4(\Delta A)^2}{\Delta\tau_{aaaa}} \tag{4.5.4}$$

Where $A_{g.s}$ is the ground state rotational constant, and

$$\Delta A = A_{g.s} - A_i = -(A_{g.s} - A_j) \tag{4.5.5}$$

$$\Delta\tau_{aaaa} = \tau^{g.s}_{aaaa} - \tau^{i}_{aaaa} = -(\tau^{g.s}_{aaaa} - \tau^{j}_{aaaa}) \tag{4.5.6}$$

This approximate method was used in our work to derive the Coriolis coupling constants. The constant $\zeta^z_{3,5}$ of $F_2^{32}S^{16}O_2$ was calculated using the Y- state constants. In the Y- state the z axis is the c principal inertial axis; therefore equations 4.4.5 and 4.4.6 become

$$\Delta A = A_{g.s} - C_Y \tag{4.5.7}$$

and

$$\Delta\tau_{aaaa} = \tau^{q.s}_{aaaa} - \tau^{Y}_{cccc} \tag{4.5.8}$$

respectively. The resulting constant $\zeta^{z}_{4,5}$ is found to have the value 0.264. The energy difference between ν_4 and ν_5 of $F_2^{32}S^{16}O_2$, derived by equation-4.4.4, is $1.12 cm^{-1}$. Both the K and L excited state data of $F_2^{32}S^{18}O_2$ were employed to calculate the Coriolis constant $\zeta^{z}_{4,5}$ for this species and an average value of 0.24 is obtained, which is smaller than that of $F_2^{32}S^{16}O_2$. The average energy difference between ν_4 and ν_5 of $F_2^{32}S^{18}O_2$ is $4.51 cm^{-1}$, calculated using equation-4.4.4. The Coriolis coupling constant $\zeta^{y}_{3,7}$ is calculated as 0.24 for $F_2^{32}S^{16}O_2$. In this calculation we used the vibrational frequencies listed in Table-4.29.

Having analyzed the Coriolis interactions, we can assign the excited state X to ν_5, Y to ν_4, U to ν_3, W to ν_7 and Z to ν_9 for the $F_2^{32}S^{16}O_2$ species, and K to ν_5, L to ν_4, M to ν_9 and N to ν_7 for the $F_2^{32}S^{16}O_2$ species, respectively.

4.6 The Harmonic Molecular Force Field of Sulphuryl Fluoride

Several force fields have been published for F_2SO_2 [79][80][81], all of which used Lide's rigid rotor approximate geometry[86] and had only one available set of vibrational frequencies for the normal species($F_2^{32}S^{16}O_2$) which were not reliably assigned. They were therefore forced to constrain almost all of the non-diagonal force constants to be zero. It therefore is possible to derive a better force field using our microwave geometry revised vibrational assignments, centrifugal distortion constants, remeasured vibrational frequencies of several isotopic species and the additional data provided by the Coriolis coupling constant$\zeta_{4,5}^{z}$.

F_2SO_2 belongs to the point group C_{2v} and the nine normal modes are distributed among the four possible irreducible symmetry species[73][79][80][81][86][90]:

$$C_{2v} = 4a_1(\nu_1,\nu_2,\nu_3,\nu_4) + a_2(\nu_5) + 2b_1(\nu_6,\nu_7) + 2b_2(\nu_8,\nu_9) \qquad (4.6.1)$$

In $F_2^{32}S^{16}O^{18}O$, the unsymmetric substitution of ^{18}O reduces the C_{2v} symmetry to C_s symmetry. For this case the nine normal modes are redistributed into two irreducible representations of the C_s group, that are:

$$C_s = 6a' + 3a'' \qquad (4.6.2)$$

The a_1 and b_1 species of C_{2v} become the a' species of C_s, the a_2 and b_2 species of C_{2v} construct the a'' species of C_s. In our refinement of the force field, the experimental data of $F_2^{32}S^{16}O^{18}O$ were used, therefore C_s symmetry was applied in the procedure. The nonredundant symmetry coordinates of F_2SO_2 used in the calculation are given in Table-1.3, in which the coefficients a, b, c, and so on, were derived using the effective geometry(r_0) listed in Table-4.25 and equations-1.8.3 to 1.8.6.

The quartic distortion constants listed in Table-4.18, with the exception of those of $F_2^{34}S^{18}O_2$, were employed to fit the force field. An uncertainty of 3% was also used for the distortion constants of $F_2^{32}S^{16}O_2$, $F_2^{32}S^{16}O^{18}O$ and $F_2^{32}S^{18}O_2$, except for D_K of $F_2^{32}S^{16}O_2$, to which a higher value of 5% was assigned; 5% uncertainties were assigned to all $F_2^{34}S^{16}O_2$ distortion constants. Two procedures were used to derive the force field for this molecule. In procedure(I) the Coriolis constant $\zeta_{4,5}^{a}$ of $F_2^{32}S^{16}O_2$ was employed in the calculation to fit the force field. An uncertainty of 5% was assigned to this constant. In procedure(II) the Coriolis constant was not considered in the calculation. The Coriolis constant $\zeta_{4,5}^{a}$ of $F_2^{32}S^{18}O_2$ was not used in either of the calculations but was used to check the result. The effective structure, Table-4.25, was used in this calculation to fit the force field. The calculated results showed little variation between procedure(I) and procedure(II). The infrared frequencies of $F_2^{32}S^{16}O_2$, $F_2^{32}S^{16}O^{18}O$, $F_2^{32}S^{18}O_2$ and $F_2^{34}S^{16}O_2$, Tables 4.29 to 4.32, were used in these calculations and all were accorded 1% uncertainties in the weighted least squares fits.

The wavenumbers of all four stretching fundamentals are well established from earlier work[73][86][89][90][91][93]. Two almost degenerate modes near $380cm^{-1}$ are assigned to ν_4 and ν_5. ν_5, the torsion mode, is infrared inactive. There have been several papers reporting the observation of this mode in the Raman spectrum[73][90] and the frequency has been assigned to about $388cm^{-1}$. However, the frequencies of ν_4 and ν_5, are both Raman active and are so close to each other that only one Raman line in this range has been reported . Sportouch and Clark[91] considered that the torsional mode, although Raman active, is too weak to be observed in the Raman spectrum. Their experiments suggested the assignment of the line observed in this range, at $385cm^{-1}$, to the ν_4 mode. Our data confirm that ν_4 and ν_5 are affected by a strong a-type Coriolis interaction and suggest that ν_5 is best estimated at $384cm^{-1}$, a little lower than ν_4. The centrifugal distortion constant data are quite sensitive to the value of force constant F_{55}. When no value for ν_5 of $F_2^{32}S^{16}O_2$ was included in the fit this fundamental was predicted to occur at 383 cm^{-1} in very good agreement with the result obtained from our excited state microwave data. The near coincidence of ν_4 and ν_5 is therefore reliably demonstrated.

Three near degenerate bending funda· ·ntals are known to occur at 552, 544 and 539 cm^{-1} respectively and have been variously attributed to ν_3, ν_7 and ν_9. Previous microwave studies of F_2SO_2 in various excited states ruled out the possibility of ν_3 being the lowest frequency of these three fundamentals,[85] while later Raman work suggested that ν_3 be assigned at $552cm^{-1}$ [91]. We have extended the earlier microwave studies of vibrationally excited F_2SO_2[85]. Our result show that ν_3 and ν_7 are affected by a weak c-type Coriolis interaction and that $\nu_3 > \nu_7$. Further, the combination of the vibrational and microwave data together with force field calculations shows that it is most reasonable to assign ν_3, ν_7 and ν_9 at 552, 544 and 539 cm^{-1} respectively.

The force field obtained is given in Table-4.33. All seventeen force constants have been refined and appear to have reasonable magnitudes and signs. In Table-4.33, the least squares errors given for the force constants are rather small and perhaps underestimate the actual uncertainties in these parameters. Since no allowance for the effects of anharmonicity has been made it is difficult to reliably assess uncertainties for these parameters.

Tables 4.29 to 4.32 give a comparison between the observed and calculated vibrational frequencies, which shows how well the force field reproduces the input data. The calculated vibrational frequency, using procedure(I), of ν_5 is $1.5cm^{-1}$ lower than that of ν_4 for the $-^{16}O_2$ species and $3.4cm^{-1}$ lower for the $-^{18}O_2$ species, which is consistent with the values, $1.1cm^{-1}$ and $4.5cm^{-1}$, derived from Coriolis interactions in Section 4.4. The quartic distortion constants are listed in Tables 4.34 to 4.37. All of the calculated distortion constants are consistent with the observed values, the worst agreement occurs for D_K of $F_2^{32}S^{16}O_2$. The reason is that the observed value of D_K for $F_2^{32}S^{16}O_2$ was not well determined; because this species is a nearly symmetric prolate rotor with a-type transitions, to obtain a good estimate of D_K for such a rotor, Q-branch or higher K_a, especially $\Delta K_a = 2$, transitions are necessary. The distortion constants of $F_2^{34}S^{18}O_2$ derived from the force field, using procedure(I), together with the rotational constants derived from the calculated effective molecular geometry, were used to obtain a very good prediction of the rotational frequencies for this species, which helped greatly in assigning these lines. The Coriolis constants $\zeta_{4,5}^{c}$ of $F_2^{32}S^{16}O_2$ and $F_2^{32}S^{18}O_2$ refined , using procedure(I), from the harmonic force field are 0.233 and 0.215, respectively, which are in good agreement with the observed values 0.264 and 0.24 obtained in section 4.4.

This study has removed ambiguities in the vibrational assignment of F_2SO_2 and provided a good harmonic force field for this molecule. Since all literature force fields are based on fragmentary data and often incorrect vibrational assignments comparisons with the present force field are unwarranted. Our force field study of F_2SO_2 has suggested that a detailed study of excited vibrational states would be both profitable and interesting and some results have already been reported here. Here again the force field predicts and experiment confirms that isotopic substitution at oxygen should have unusual effects. For example, whereas the $v_4 = 1$ and $v_5 = 1$ states of $F_2^{32}S^{16}O_2$ should be perturbed by a strong a-type Coriolis resonance the corresponding excited states of $F_2^{32}S^{18}O_2$ should be affected by a rather weaker b-type Coriolis interaction.

Table-4.29 Vibrational Frequencies of $F_2^{32}S^{16}O_2$ (cm^{-1})

Modes	Obs.	Cal.(I)	Dif.(I)	Cal.(II)	Dif.(II)
ν_1	1271.4	1270.6	0.8	1270.7	0.7
ν_2	848.6	848.4	0.2	848.2	0.4
ν_3	552.2	552.3	-0.1	552.2	0.0
ν_4	385.0	385.1	-0.1	384.8	0.2
ν_5	384.0	383.6	0.4	383.8	0.2
ν_6	1504.8	1504.3	0.5	1504.0	0.8
ν_7	544.3	544.3	0.0	544.3	0.0
ν_8	887.0	886.9	0.1	887.0	0.0
ν_9	539.3	539.2	0.1	539.3	0.0

Table-4.30 Vibrational Frequencies of $F_2^{32}S^{16}O^{18}O$ (cm^{-1})

Modes	Obs.	Cal.(I)	Dif.(I)	Cal.(II)	Dif.(II)
ν_1	1244.8	1244.1	0.7	1244.3	0.5
ν_2	843.9	843.5	0.4	843.3	0.6
ν_3		546.2		546.3	
ν_4		380.7		380.1	
ν_5		377.9		378.2	
ν_6	1485.1	1484.5	0.6	1484.3	0.8
ν_7		536.6		536,7	
ν_8	887.0	886.7	0.3	886.8	0.2
ν_9		532.5		532.5	

Table-4.31 Vibrational Frequencies of $F_2^{32}S^{18}O^2$ (cm^{-1})

Modes	Obs.	Cal.(I)	Dif.(I)	Cal.(II)	Dif.(II)
ν_1	1223.8	1222.3	1.5	1222.7	1.1
ν_2	838.6	838.4	0.2	838.1	0.5
ν_3		538.9		539.7	
ν_4		376.2		375.2	
ν_5		372.8		373.0	
ν_6	1460.9	1460.2	0.7	1460.0	0.9
ν_7		530.0		530.0	
ν_8	887.0	886.4	0.6	886.7	0.3
ν_9		525.3		525.3	

Table-4.32 Vibrational Frequencies of $F_2^{34}S^{16}O_2$ (cm^{-1})

Modes	Obs.	Cal.(I)	Dif.(I)	Cal.(II)	Dif.(II)
ν_1	1261.5	1259.6	1.9	1259.6	1.9
ν_2		842.8		842.8	
ν_3		549.4		549.2	
ν_4		385.1		384.8	
ν_5		383.6		383.8	
ν_6	1484.3	1483.0	1.3	1482.7	1.6
ν_7		541.6		541.1	
ν_8	874.6	874.1	0.5	874.7	-0.1
ν_9		536.1		535.9	

Table-4.33 The Force Constants of F_2SO_2

a_1	1(I)	11.823(74)			
	1(II)	11.782(72)			
	2(I)	0.40(11)	5.794(64)		
	2(II)	0.35(11)	5.833(66)		
	3(I)	0.202(80)	-0.409(45)	1.182(31)	
	3(II)	0.319(92)	-0.468(54)	1.100(35)	
	4(I)	0.31(19)	0.214(88)	-0.099(12)	1.856(85)
	4(II)	0.39(21)	0.236(85)	-0.095(11)	2.024(100)
a_2	5(I)	1.119(6)			
	5(II)	1.112(7)			
b_1	6(I)	11.69(10)			
	6(II)	11.69(11)			
	7(I)	-0.289(78)	1.620(14)		
	7(II)	-0.292(78)	1.619(15)		
b_2	8(I)	5.33(13)			
	8(II)	5.45(13)			
	9(I)	-0.643(79)	2.143(36)		
	9(II)	-0.723(81)	2.117(37)		

The units are $aJ\dot{A}^{-2}$ for stretch-stretch, $aJ\dot{A}^{-1}$ for stretch-bend and aJ for bend-bend constants.

(I) The Coriolis constant ζ^z_{45} was considered in this force field refinement.

(II) The Coriolis constant ζ^z_{45} was not considered.

Table-4.34

Quartic Distortion Constants of $F_2^{32}S^{16}O_2$ (kHz)

Modes	Observed	Calculated	Difference
$D_J(I)$	1.491	1.502	-0.011
$D_J(II)$		1.499	-0.008
$D_{JK}(I)$	-1.576	-1.576	0.000
$D_{JK}(II)$		-1.643	0.067
$D_K(I)$	2.375	1.946	0.429
$D_K(II)$		1.948	0.427
$d_1(I)$	-0.0252	-0.0325	0.0073
$d_1(II)$		-0.0325	0.0073
$d_2(I)$	0.1402	0.1472	-0.0070
$d_2(II)$		0.1480	-0.0078

(I) Coriolis constant was considered in this force field refinement.

(II) Coriolis constant was not considered.

Table-4.35

Quartic Distortion Constants of $F_2^{32}S^{16}O^{18}O$ (kHz)

Modes	Observed	Calculated	Difference
$D_J(I)$	1.111	1.101	0.010
$D_J(II)$		1.098	0.0013
$D_{JK}(I)$	1.0085	0.9916	0.0169
$D_{JK}(II)$		0.9928	0.0157
$D_K(I)$	-0.8541	-0.8393	-0.0148
$D_K(II)$		-0.8414	-0.0127
$d_1(I)$	-0.0356	-0.0363	0.0007
$d_1(II)$		-0.0360	-0.0010
$d_2(I)$	0.0027	0.0038	-0.0011
$d_2(II)$		0.0041	-0.0014

(I) Coriolis constant was considered in this force field refinement.

(II) Coriolis constant was not considered.

Table-4.36

Quartic Distortion Constants of $F_2^{32}S^{18}O_2$ (kHz)

Modes	Observed	Calculated	Difference
$D_J(I)$	1.1795	1.1801	-0.0006
$D_J(II)$		1.1772	0.0023
$D_{JK}(I)$	-0.0487	-0.0487	0.0000
$D_{JK}(II)$		-0.0487	0.0000
$D_K(I)$	0.1127	0.1128	-0.0001
$D_K(II)$		0.1128	-0.0001
$d_1(I)$	-0.1562	-0.1572	0.0010
$d_1(II)$		-0.1569	0.0007
$d_2(I)$	-0.0232	-0.0232	-0.0000
$d_2(II)$		-0.0231	-0.0001

(I) Coriolis constant was considered in this force field refinement.

(II) Coriolis constant was not considered.

Table-4.37

Quartic Distortion Constants of $F_2^{34}S^{16}O_2$ (kHz)

Modes	Observed	Calculated	Difference
$D_J(I)$	1.518	1.49[illegible]	0.019
$D_J(II)$		1.4954	0.023
$D_{JK}(I)$	-1.568	-1.632	0.065
$D_{JK}(II)$		-1.635	0.063
$D_K(I)$		1.9423	
$D_K(II)$		1.9427	
$d_1(I)$		-0.0309	
$d_1(II)$		-0.0309	
$d_2(I)$		0.1468	
$d_2(II)$		0.1476	-0.0468

(I) Coriolis constant was considered in this force field refinement.

(II) Coriolis constant was not considered.

CHAPTER 5

THE MICROWAVE SPECTRUM AND MOLECULAR STRUCTURE OF DIMETHYL SULPHONE

The molecular structure of dimethyl sulphone was first determined by Sands, in 1963, using X-ray crystallography[100]; he reported that $r_{SC} = 1.78Å$, $r_{SO} = 1.44Å$, $angle_{CSC} = 103.2°$ and $angle_{OSO} = 117.9°$. The geometry of the two methyl groups was not obtained. A gas electron diffraction measurement was done by Heinz and Werner[101], who derived the complete structure of the molecule including the structure of the methyl groups. They assumed that the six r_{CH} bonds and six $angle_{HCH}$ had the same values with $r_{CH} = 1.077(9)Å$ and $angle_{HCH} = 109.8(13)°$. The microwave spectra of two isotopic species of dimethyl sulphone, $(^{12}CH_3)_2^{32}S^{16}O_2$ and $(^{12}CH_3)(^{13}CH_3)^{32}S^{16}O_2$, have been investigated by Saito and Marino[99], in 1972. In their observed frequency range, from $16000MHz$ to $46000MHz$, only the R-branch transitions with J lower than 6 could be found. They observed about 30 transitions for the normal species and 10 for the ^{13}C species. The molecule showed b-type transitions. The centrifugal distortion effect was disregarded in their work because only low J, for J up to 5, transitions were measured. The rotational constants of these two species were calculated using the rigid rotor approximation, which showed that this molecule is a nearly prolate asymmetric rotor, with Ray's asymmetry parameter[58], equation-1.18, having the value -0.49. They evaluated an effective molecular structure from these rotational constants by assuming that the structure of the methyl group of dimethyl sulphone is the same as that of dimethyl sulfide. The geometry of the methyl group of dimethyl sulfide was obtained by Pierce and Hayashi[102]; in their study the six CH bonds and six HCH angles were assumed to be the same. The second order Stark effect was measured and the dipole moment μ_b was derived from the Stark coefficients, as $4.432(41)D$.

The purpose of this study was to investigate the rotational spectra of several isotopomers, to derive accurate values of rotational constants and distortion constants and then to calculate the effective and substitution molecular structures for dimethyl sulphone.

5.1 Observed Microwave Spectrum and Assignments of Dimethyl Sulphone

The microwave spectra of eight isotopic species,

$(^{12}CH_3)_2^{32}S^{16}O_2$, $(^{12}CD_3)_2^{32}S^{16}O_2$, $(^{12}CH_3)_2^{32}S^{16}O^{18}O$,

$(^{13}CH_3)_2^{32}S^{16}O_2$, $(^{12}CH_3)_2^{34}S^{16}O_2$, $(^{12}CH_3)(^{13}CH_3)^{32}S^{16}O_2$,

$(^{12}CH_3)(^{12}CH_2D)^{32}S^{16}O_2(I)$, $(^{12}CH_3)(^{12}CH_2D)^{32}S^{16}O_2(II)$,

were observed in the gas phase over the frequency range from $40000MHz$ to $85000MHz$. At room temperature, each solid sample was kept in a small flask and its vapour was pumped continuously through a $7.2 \times 3.4cm$ Stark cell, in which the gas pressure was maintained below 5 microns. For all eight of these species only R-branch transitions were measured. The predictions indicated that all the strong Q-branch lines would fall below the frequency range of this work. High Stark fields of about $700Vcm^{-1}$ were used. The number of observed lines, and the highest J value observed for each isotopic species and conformer are listed in Table-5.1.

The rotational frequencies and rotational constants obtained by Saito and Marino[99] were used to calculate the initial prediction for the species $(^{12}CH_3)_2^{32}S^{16}O_2$, which gave good agreement with the measurement for the low J lines. Quartic centrifugal distortion constants were needed to fit the higher J lines. This species, which is a Fermi particle, showed b-type transitions, therefore the $eo-oe$ transitions should be stronger than $oo-ee$ transitions. Because there are three pairs of identical nuclei with non-zero spin, all hydrogen atoms, the effect of the spin statistics was very small(Table-1.1). No hyperfine structure due to the internal rotation of the two methyl groups was found, however, the lines were slightly broadened with a half width of about $1MHz$(Figures 5.1, 5.2 and 5.3). The frequencies of $(^{12}CH_3)_2^{34}S^{16}O_2$ were for the most part about $10MHz$ to $20MHz$ lower than the corresponding transitions of $(^{12}CH_3)_2^{32}S^{16}O_2$, Figure-5.1. Since a 92% enriched sample of ^{34}S was used, there was no difficulty in assigning the lines for this species after the assignment of $(^{12}CH_3)_2^{32}S^{16}O_2$ was completed. We also used Saito and Marino's frequencies and rotational constants for $(^{12}CH_3)(^{13}CH_3)^{32}S^{16}O_2$ [99] to make the first prediction of the rotational lines of this isotopomer. Only b-type transitions were found for this species, the a-type transitions due to the asymmetric substitution of ^{13}C were too weak to be observed in this work. An approximate relation,

$$2G_{(^{12}CH_3)(^{13}CH_3)^{32}S^{16}O_2} = G_{(^{12}CH_3)_2^{32}S^{16}O_2} + G_{(^{13}CH_3)_2^{32}S^{16}O_2} \tag{5.1.1}$$

where G is either a rotational constant or a distortion constant, was used to facilitate the initial spectral prediction for $(^{13}CH_3)_2^{32}S^{16}O_2$ using the constants obtained for $(^{12}CH_3)^{32}S^{16}O_2$ and $(^{12}CH_3)(^{13}CH_3)^{32}S^{16}O_2$. Like the normal species, $(^{13}CH_3)_2^{32}S^{16}O_2$ showed b-type transitions. Because of the substitution of ^{18}O in $(^{12}CH_3)_2^{32}S^{16}O^{18}O$, both b-type and c-type transitions were observed. Figure-5.2 shows that the lines of the b-type transitions were stronger those that of the c-type transitions. The substitution of D for the six lightest atoms in $(^{12}CD_3)_2^{32}S^{16}O_2$ shifted the frequencies lower by about 6000 to $7000MHz$. This species, which also showed b-type transitions, is a Bose particle and therefore oo-ee transitions should be stronger than eo-oe transitions. Because of the higher nuclear spin of D, $I = 1$, the effect of the nuclear spin statistics on the rotational spectrum was not obvious for this species (Table-1.1). Two series of rotational transitions were observed for the mono-deutero substituted species, which were assigned to two different possible conformers, $(^{12}CH_3)(^{12}CH_2D)^{32}S^{16}O_2(I)$ and

$(^{12}CH_3)(^{12}CH_2D)^{32}S^{16}O_2(II)$(Figure-5.4). The transitions of conformer II were stronger than the corresponding transitions of conformer I. Both of the conformers have strong b-type lines. Although mono-deutero substitution could produce a dipole moment along the a-axis or the c-axis, it would be quite small; no a-type or c-type transition was found in this work. Figure-5.3 shows two lines of these two conformers. Since they are not transitions with the same quantum numbers their intensities are not directly comparable. The line strength of the higher frequency transition shown in Figure-5.3 is roughly twice that of the lower lower frequency transition. Therefore the population of conformer(II) is double that of conformer(I)(Figure-5.4).

Table-5.1 The Number of Observed Lines(N) and Highest J Value Observed for Dimethyl Sulphone

Species	N	J
$(^{12}CH_3)_2^{32}S^{16}O_2$	75	10
$(^{12}CD_3)_2^{32}S^{16}O_2$	55	11
$(^{13}CH_3)_2^{32}S^{16}O_2$	43	10
$(^{12}CH_3)_2^{32}S^{16}O^{18}O$	51	9
$(^{12}CH_3)_2^{34}S^{16}O_2$	34	9
$(^{12}CH_3)(^{12}CH_2D)^{32}S^{16}O_2(I)$	29	9
$(^{12}CH_3)(^{12}CH_2D)^{32}S^{16}O_2(II)$	29	8
$(^{12}CH_3)(^{13}CH_3)^{32}S^{16}O_2$	36	9

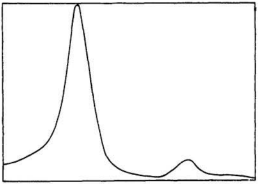

Figure 5.1 The $8_{1,8} \leftarrow 7_{0,7}$ Transitions of $(^{12}CH_3)_2^{32}S^{16}O_2$ (67061.633MHz) and $(^{12}CH_3)_2^{34}S^{16}O_2$ (67059.496MHz). Obtained Using a 92% ^{34}S Enriched Sample.

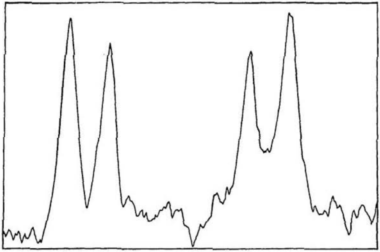

Figure-5.2 The b-Type and c-Type Transitions of $(^{12}CH_3)_2^{32}S^{16}O^{18}O$, $7_{6,2}\leftarrow6_{5,1}$ (61541.414MHz), $7_{6,1}\leftarrow6_{5,1}$ (61542.517MHz), $7_{6,2}\leftarrow6_{5,2}$ (61546.647MHz) and $7_{6,1}\leftarrow6_{5,2}$ (61547.645MHz).

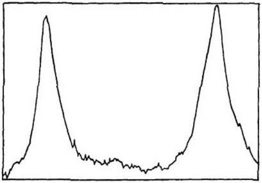

Figure-5.3 The Transitions $8_{2,7}\leftarrow7_{1,6}$ (65286.701MHz) of $(^{12}CH_3)(^{12}CH_2D)^{32}S^{16}O_2(I)$ and $8_{2,6}\leftarrow7_{3,5}$ (65278.730MHz) of $(^{12}CH_3)(^{12}CH_2D)^{32}S^{16}O_2(II)$.

Table-5.2

Observed Rotational Transition Frequencies (in MHz) of $({}^{12}CH_3)_2^{32}S^{16}O_2$.

J'	K_a'	K_c'	-	J''	K_a''	K_c''	Frequency	Deviation
2	2	0	-	1	1	1	18235.73*	-0.052
2	0	2	-	1	1	1	16576.64*	0.032
3	0	3	-	2	1	2	25071.70*	0.013
3	2	1	-	2	1	2	26922.32*	0.040
4	3	1	-	3	2	2	35981.21*	0.051
4	1	3	-	3	2	2	33194.18*	0.013
4	0	4	-	3	1	3	33529.75*	-0.011
4	2	2	-	3	1	3	35772.55*	0.014
5	4	1	-	4	3	2	45199.552	-0.013
5	0	5	-	4	1	4	41946.147	-0.011
5	1	5	-	4	0	4	42065.775	0.001
5	2	4	-	4	1	3	42980.962	-0.005
5	3	2	-	4	2	3	44598.786	0.010
5	3	3	-	4	2	2	44179.245	-0.007
5	4	2	-	4	3	1	45171.421	-0.057
6	5	2	-	5	4	1	54461.096	-0.092
6	0	6	-	5	1	5	50332.384	-0.026
6	1	5	-	5	2	4	50428.864	-0.039
6	2	5	-	5	1	4	51195.147	-0.004
6	2	5	-	5	3	2	48428.914	-0.089
6	3	3	-	5	2	4	53349.451	0.044
6	3	4	-	5	2	3	52441.415	-0.063
6	3	4	-	5	4	1	48119.320	-0.019
6	4	3	-	5	3	2	53601.612	-0.062
6	4	2	-	5	3	3	53711.476	-0.009
6	6	0	-	5	5	1	55259.876	-0.029
6	6	1	-	5	5	0	55259.876	0.019
7	7	1	-	6	6	0	64535.674	-0.005
7	0	7	-	6	1	6	58701.426	0.052
7	1	7	-	6	0	6	58725.278	-0.012
7	1	6	-	6	2	5	58958.580	0.051
7	2	6	-	6	1	5	59414.447	0.046
7	3	5	-	6	2	4	60634.407	0.047
7	4	4	-	6	3	3	61964.029	0.026
7	5	3	-	6	4	2	62928.492	0.000
7	5	2	-	6	4	3	62948.951	0.030
7	7	0	-	6	6	1	64535.674	-0.010
8	8	1	-	7	7	0	73811.193	-0.041
8	0	8	-	7	1	7	67061.633	0.002
8	1	8	-	7	0	7	67071.589	0.057
8	2	6	-	7	3	5	67136.534	-0.008
8	2	7	-	7	3	4	64350.474	-0.006
8	1	7	-	7	2	6	67421.495	0.070
8	2	7	-	7	1	6	67665.663	0.013
8	3	5	-	7	4	4	65912.177	-0.051

*-Reference [99]

Table-5.2 Continued(1)

J'	K_a'	K_c'	-	J''	K_a''	K_c''	Frequency	Deviation
8	3	6	-	7	2	5	68780.821	0.041
8	3	6	-	7	4	3	64902.271	-0.052
8	4	5	-	7	3	4	70233.753	-0.023
8	4	5	-	7	5	2	64385.969	0.087
8	4	4	-	7	3	5	70932.623	-0.038
8	5	4	-	7	4	3	71370.183	0.010
8	5	3	-	7	4	4	71442.998	0.056
8	6	3	-	7	5	2	72215.684	-0.051
8	7	1	-	7	6	2	73015.726	-0.016
8	7	2	-	7	6	1	73015.726	0.044
8	8	0	-	7	7	1	73811.193	-0.041
9	9	1	-	8	8	0	83086.522	0.010
9	0	9	-	8	1	8	75417.775	-0.036
9	1	9	-	8	0	8	75421.697	-0.084
9	2	7	-	8	3	6	75812.901	0.063
9	1	8	-	8	2	7	75834.786	-0.021
9	2	8	-	8	1	7	75955.146	-0.057
9	3	7	-	8	2	6	76912.815	0.026
9	3	7	-	8	4	4	73116.662	-0.008
9	4	5	-	8	5	4	73271.425	0.026
9	4	6	-	8	3	5	78409.763	0.041
9	4	6	-	8	5	3	72879.063	0.055
9	4	5	-	8	3	6	79739.266	0.017
9	5	5	-	8	4	4	79759.777	-0.022
9	5	4	-	8	4	5	79965.817	-0.037
9	8	1	-	8	7	2	82291.268	0.020
9	8	2	-	8	7	1	82291.268	0.026
9	9	0	-	8	8	1	83086.522	0.010
10	6	5	-	9	7	2	79775.374	-0.040
10	1	10	-	9	0	9	83773.707	0.027
10	2	9	-	9	1	8	84273.723	-0.050

Table-5.3

Observed Rotational Transition Frequencies (in MHz) of $(^{12}CD_3)_2^{32}S^{16}O_2$.

J'	K_a'	K_c'	-	J''	K_a''	K_c''	Frequency	Deviation
5	5	0	-	4	4	1	40779.259	0.036
5	5	1	-	4	4	0	40776.875	-0.064
6	5	1	-	5	4	2	47843.886	-0.032
6	0	6	-	5	1	5	41166.590	0.020
6	1	6	-	5	0	5	41205.858	0.004
6	1	5	-	5	2	4	41670.490	-0.045
6	2	5	-	5	1	4	42413.154	-0.009
6	5	2	-	5	4	1	47823.464	-0.019
7	7	1	-	6	6	0	57332.608	0.038
7	1	7	-	6	0	6	47985.558	-0.004
7	4	4	-	6	3	3	53105.041	-0.008

Table-5.3 Continued(1)

J'	K_a'	K_c'	-	J''	K_a''	K_c''	Frequency	Deviation
7	4	3	-	6	3	4	54154.168	0.015
7	5	3	-	6	4	2	54828.688	-0.012
7	5	2	-	6	4	3	54927.857	-0.019
7	7	0	-	6	6	1	57332.608	-0.003
8	8	1	-	7	7	0	65609.509	0.028
8	0	8	-	7	1	7	54768.603	-0.008
8	1	8	-	7	0	7	54773.422	-0.023
8	5	3	-	7	4	4	62073.056	-0.054
8	5	4	-	7	4	3	61733.420	0.072
8	6	2	-	7	5	3	63173.855	-0.025
8	6	3	-	7	5	2	63153.639	0.076
8	8	0	-	7	7	1	65609.509	0.023
9	9	1	-	8	8	0	73886.141	0.000
9	0	9	-	8	1	8	61562.803	0.012
9	1	9	-	8	0	8	61564.410	0.010
9	1	8	-	8	2	7	62389.696	-0.019
9	2	8	-	8	1	7	62453.461	-0.015
9	2	7	-	8	3	6	62886.606	0.080
9	3	7	-	8	2	6	63730.595	0.012
9	4	5	-	8	3	6	69895.853	0.035
9	4	6	-	8	3	5	65986.407	0.002
9	5	5	-	8	4	4	68460.026	0.000
9	5	4	-	8	4	5	69362.126	-0.037
9	6	3	-	8	5	4	70244.043	-0.038
9	6	4	-	8	5	3	70159.608	0.039
9	7	2	-	8	6	3	71446.474	-0.002
9	7	3	-	8	6	2	71442.858	0.034
9	8	1	-	8	7	2	72667.942	-0.085
9	8	2	-	8	7	1	72667.942	-0.009
9	9	0	-	8	8	1	73886.141	-0.001
10	7	3	-	9	6	4	78499.493	0.018
10	1	9	-	9	2	8	69199.334	0.034
10	2	8	-	9	3	7	69890.690	-0.026
10	2	9	-	9	1	8	69223.655	0.052
10	3	8	-	9	2	7	70300.379	-0.039
10	4	7	-	9	3	6	72276.802	-0.006
10	5	6	-	9	4	5	74963.899	0.005
10	6	5	-	9	5	4	77080.981	-0.019
10	7	4	-	9	6	3	78481.732	-0.008
11	1	10	-	10	2	9	75997.715	-0.014
11	2	10	-	10	1	9	76006.630	0.011
11	2	9	-	10	3	8	76786.298	-0.065
11	3	9	-	10	2	8	76968.016	-0.026
11	4	8	-	10	3	7	78587.476	0.053

Table-5.4
Observed Rotational Transition Frequencies (in MHz) of $(^{13}CH_3)_2^{32}S^{16}O_2$.

J'	K_a'	K_c'	-	J''	K_a''	K_c''	Frequency	Deviation
5	4	1	-	4	3	2	44182.394	-0.060
5	0	5	-	4	1	4	40133.579	-0.029
5	1	5	-	4	0	4	40236.683	-0.011
5	3	2	-	4	2	3	43562.832	0.032
5	4	2	-	4	3	1	44124.267	-0.022
6	4	3	-	5	3	2	52185.873	0.069
6	0	6	-	5	1	5	48137.152	-0.005
6	1	6	-	5	0	5	48179.565	-0.148
6	2	5	-	5	1	4	49138.087	0.021
6	3	4	-	5	2	3	50674.458	-0.011
6	3	3	-	5	2	4	52186.896	-0.047
7	7	1	-	6	6	0	63357.754	0.050
7	0	7	-	6	1	6	56123.212	0.007
7	1	7	-	6	0	6	56139.677	-0.001
7	3	5	-	6	4	2	53638.745	0.055
7	4	4	-	6	3	3	60129.554	0.034
7	5	3	-	6	4	2	61400.783	-0.016
7	5	2	-	6	4	3	61450.899	0.038
7	6	2	-	6	5	1	62395.532	-0.038
7	7	0	-	6	6	1	63357.754	0.033
8	8	1	-	7	7	0	72476.755	-0.012
8	0	8	-	7	1	7	64101.474	0.005
8	1	8	-	7	0	7	64107.571	-0.002
8	1	7	-	7	2	6	64651.943	-0.030
8	2	7	-	7	1	6	64830.998	0.015
8	2	6	-	7	3	5	64595.408	0.082
8	3	6	-	7	2	5	66105.194	-0.020
8	3	6	-	7	4	3	61517.966	-0.077
8	4	5	-	7	3	4	67933.782	0.048
8	4	5	-	7	5	2	61115.868	0.036
8	5	4	-	7	4	3	69475.486	-0.062
8	6	3	-	7	5	2	70545.641	-0.026
8	8	0	-	7	7	1	72476.755	-0.013
9	6	4	-	8	5	3	78677.049	-0.017
9	0	9	-	8	1	8	72076.495	0.008
9	1	9	-	8	0	8	72078.706	0.027
9	1	8	-	8	2	7	72672.238	-0.012
9	2	8	-	8	1	7	72750.490	-0.023
9	2	7	-	8	3	6	72911.532	0.044
9	3	7	-	8	2	6	73809.706	-0.068
9	3	7	-	8	4	4	69145.707	-0.016
9	3	6	-	8	4	5	71954.499	-0.074
9	5	5	-	8	6	2	68387.438	-0.035
9	5	5	-	8	4	4	77445.062	0.059
10	5	6	-	9	6	3	76627.471	0.042
10	4	7	-	9	5	4	77256.111	0.015

Table-5.5
Observed Rotational Transition Frequencies (in MHz) of $(^{12}CH_3)_2^{32}S^{16}O^{18}O$.

J'	K_a'	K_c'	-	J''	K_a''	K_c''	Frequency	Deviation
5	4	1	-	4	3	2	43763.521	0.049
5	3	2	-	4	2	2	43040.567	-0.023
5	3	3	-	4	2	3	43335.742	-0.008
5	4	2	-	4	3	1	43654.496	0.011
5	4	1	-	4	3	1	43677.508	0.013
5	4	2	-	4	3	2	43740.374	-0.089
6	5	2	-	5	4	2	52636.209	0.044
6	2	5	-	5	1	4	49836.384	-0.054
6	3	4	-	5	2	3	50776.844	0.005
6	3	3	-	5	2	3	51438.183	-0.049
6	2	4	-	5	1	4	51493.037	0.024
6	4	3	-	5	3	2	51844.330	0.006
6	3	4	-	5	2	4	51848.680	-0.007
6	4	3	-	5	3	3	52132.256	0.025
6	4	2	-	5	3	3	52235.103	-0.072
6	5	2	-	5	4	1	52613.150	-0.005
6	5	1	-	5	4	1	52618.294	-0.040
7	7	1	-	6	6	1	62123.167	-0.038
7	2	6	-	6	1	5	57943.212	0.027
7	3	4	-	6	2	4	59951.003	0.062
7	4	3	-	6	3	3	60221.560	-0.016
7	5	3	-	6	4	2	60888.196	-0.004
7	5	3	-	6	4	3	60991.172	0.028
7	5	2	-	6	4	2	60916.967	-0.039
7	5	2	-	6	4	3	61019.921	-0.029
7	6	2	-	6	5	1	61541.414	-0.016
7	6	2	-	6	5	2	61546.647	0.038
7	6	1	-	6	5	2	61547.645	-0.013
7	6	1	-	6	5	1	61542.517	0.037
7	7	0	-	6	6	1	62123.167	-0.052
7	7	1	-	6	6	0	62123.167	0.045
7	7	0	-	6	6	0	62123.167	0.032
8	8	1	-	7	7	1	71038.593	0.006
8	3	5	-	7	4	3	65699.641	0.012
8	3	6	-	7	4	3	63867.595	-0.011
8	3	6	-	7	2	6	69019.448	-0.036
8	4	5	-	7	3	5	69067.027	-0.009
8	4	5	-	7	5	2	64168.543	0.021
8	5	3	-	7	4	3	69171.249	-0.016
8	5	3	-	7	4	4	69482.667	-0.013
8	5	4	-	7	4	3	69060.972	0.014
8	6	2	-	7	5	3	69893.722	0.026
8	6	3	-	7	5	2	69857.958	-0.004
8	6	3	-	7	5	3	69886.814	0.046
8	8	1	-	7	7	0	71038.593	0.020
8	8	0	-	7	7	1	71038.593	0.004

Table-5.5 Continued(1)

J'	K_a'	K_c'	-	J''	K_a''	K_c''	Frequency	Deviation
8	8	0	-	7	7	0	71038.593	0.018
9	9	1	-	8	8	1	79953.717	-0.026
9	4	5	-	8	3	5	77051.811	-0.009
9	8	1	-	8	7	2	79376.427	-0.081
9	9	0	-	8	8	1	79953.717	-0.026
9	9	1	-	8	8	0	79953.717	-0.024
9	9	0	-	8	8	0	79953.717	-0.024

Table-5.6
Observed Rotational Transition Frequencies (in MHz) of $(^{12}CH_3)_2^{34}S^{16}O_2$.

J'	K_a'	K_c'	-	J''	K_a''	K_c''	Frequency	Deviation
6	6	1	-	5	5	0	55248.559	0.054
6	4	3	-	5	3	2	53591.678	-0.014
6	5	1	-	5	4	2	54455.647	0.069
6	5	2	-	5	4	1	54451.207	-0.082
6	6	0	-	5	5	1	55248.559	0.005
7	7	1	-	6	6	0	64522.271	-0.048
7	0	7	-	6	1	6	58691.561	0.040
7	1	7	-	6	0	6	58714.657	-0.032
7	1	6	-	6	2	5	58955.264	0.031
7	4	3	-	6	3	4	62269.384	-0.025
7	5	2	-	6	4	3	62938.998	0.047
7	5	3	-	6	4	2	62917.693	-0.030
7	7	0	-	6	6	1	64522.271	-0.053
8	8	1	-	7	7	0	73795.882	0.013
8	0	8	-	7	1	7	67049.991	-0.017
8	1	8	-	7	0	7	67059.496	-0.047
8	1	7	-	7	2	6	67414.716	-0.041
8	2	7	-	7	1	6	67652.257	0.016
8	3	6	-	7	2	5	68762.239	0.025
8	4	4	-	7	3	5	70932.534	0.078
8	4	5	-	7	3	4	70216.388	0.004
8	5	3	-	7	4	4	71433.270	0.004
8	5	4	-	7	4	3	71357.706	-0.015
8	6	3	-	7	5	2	72203.286	-0.059
8	7	1	-	7	6	2	73001.942	0.006
8	7	2	-	7	6	1	73001.942	0.070
8	8	0	-	7	7	1	73795.882	0.012
9	5	5	-	8	4	4	79744.091	-0.048
9	0	9	-	8	1	8	75404.523	0.011
9	1	9	-	8	0	8	75408.338	0.025
9	1	8	-	8	2	7	75825.135	-0.004
9	2	7	-	8	3	6	75816.088	-0.013
9	2	8	-	8	1	7	75941.423	-0.027
9	3	7	-	8	2	6	76892.572	0.063
9	5	4	-	8	4	5	79957.694	-0.019

Table-5.7
Observed Rotatinal Transition Frequencies (in MHz)
of $(^{13}CH_3)(^{12}CH_2D)^{32}S^{16}O_2$(I).

J'	K_a'	K_c'	-	J''	K_a''	K_c''	Frequency	Deviation
6	6	1	-	5	5	0	55043.560	0.004
6	6	0	-	5	5	1	55043.560	-0.004
7	7	1	-	6	6	0	64312.530	0.021
7	0	7	-	6	1	6	56267.102	-0.026
7	3	5	-	6	2	4	59178.596	0.003
7	4	4	-	6	3	3	60788.144	0.024
7	4	3	-	6	3	4	60916.437	-0.005
7	5	3	-	6	4	2	62014.001	-0.050
7	6	1	-	6	5	2	63166.044	-0.058
7	6	2	-	6	5	1	63166.044	0.027
7	7	0	-	6	6	1	64312.530	0.021
8	8	1	-	7	7	0	73581.153	-0.056
8	0	8	-	7	1	7	64298.611	-0.006
8	1	8	-	7	0	7	64352.574	0.014
8	1	7	-	7	2	6	64421.374	0.018
8	2	7	-	7	1	6	65286.701	0.018
8	3	6	-	7	2	5	66993.505	0.014
8	3	5	-	7	2	6	68821.526	-0.004
8	4	4	-	7	3	5	69104.950	-0.008
8	4	5	-	7	3	4	68796.387	-0.001
8	5	4	-	7	4	3	70122.793	-0.017
8	7	1	-	7	6	2	72435.089	0.082
8	7	2	-	7	6	1	72435.089	0.089
8	8	0	-	7	7	1	73581.153	-0.056
9	2	8	-	8	1	7	73145.473	-0.061
9	0	9	-	8	1	8	72318.500	0.026
9	1	9	-	8	0	8	72345.614	-0.003
9	1	8	-	8	2	7	72597.239	0.020
9	2	7	-	8	3	6	71803.619	-0.006

Table-5.8
Observed Rotational Transition Frequencies (in MHz) of $(^{12}CH_3)(^{12}CH_2D)^{32}S^{16}O_2$(II).

J'	K_a'	K_c'	-	J''	K_a''	K_c''	Frequency	Deviation
6	6	1	-	5	5	0	53945.819	-0.017
6	3	4	-	5	2	3	50710.413	-0.033
6	4	3	-	5	3	2	52107.470	-0.054
6	4	2	-	5	3	3	52395.172	0.005
7	7	1	-	6	6	0	63006.261	0.023
7	4	3	-	6	3	4	60845.395	-0.055
7	5	2	-	6	4	3	61356.331	0.000
7	6	1	-	6	5	2	62169.389	0.084
7	7	0	-	6	6	1	63006.261	-0.009
8	8	0	-	7	7	1	72066.264	-0.015
8	1	7	-	7	2	6	65135.776	0.048
8	2	6	-	7	3	5	65278.730	-0.025
8	3	6	-	7	3	5	65642.883	0.025
8	2	6	-	7	2	5	65928.668	-0.015
8	3	5	-	7	3	4	66346.172	-0.028
8	4	4	-	7	3	5	69518.233	0.029
8	4	4	-	7	4	3	66179.481	-0.030
8	4	5	-	7	3	4	67917.050	0.047
8	4	5	-	7	4	4	65877.072	0.044
8	5	3	-	7	4	4	69644.986	0.037
8	8	1	-	7	7	0	72066.264	-0.011
9	9	1	-	8	8	0	81126.006	-0.003
9	1	8	-	8	1	7	73227.719	-0.038
9	2	7	-	8	3	6	73565.334	-0.027
9	3	6	-	8	4	5	72989.332	0.025
9	3	7	-	8	2	6	74108.522	0.032
9	5	5	-	8	4	4	77370.958	-0.025
9	6	4	-	8	5	3	78560.703	-0.037
9	9	0	-	8	8	1	81126.006	-0.003

Table-5.9
Observed Rotational Transition Frequencies (in MHz) of $(^{12}CH_3)(^{13}CH_3)^{32}S^{16}O_2$.

J'	K_a'	K_c'	-	J''	K_a''	K_c''	Frequency	Deviation
6	6	1	-	5	5	0	54821.329	0.032
6	3	4	-	5	2	3	51595.305	0.025
6	4	2	-	5	3	3	53072.270	0.023
6	4	3	-	5	3	2	52932.521	0.012
6	6	0	-	5	5	1	54821.329	-0.033
7	7	1	-	6	6	0	64033.023	0.061
7	0	7	-	6	1	6	57382.113	0.017
7	1	7	-	6	0	6	57406.166	-0.038
7	1	6	-	6	2	5	57704.776	-0.028
7	2	6	-	6	1	5	58183.406	0.061
7	3	5	-	6	2	4	59564.350	-0.010
7	4	3	-	6	3	4	61487.624	-0.018
7	4	4	-	6	3	3	61095.208	-0.026
7	5	3	-	6	4	2	62207.886	-0.073
7	7	0	-	6	6	1	64033.023	0.055
8	8	1	-	7	7	0	73244.339	-0.034
8	0	8	-	7	1	7	65548.665	-0.009
8	1	8	-	7	0	7	65558.349	-0.074
8	1	7	-	7	2	6	65981.581	0.042
8	2	6	-	7	3	5	65716.564	0.003
8	2	7	-	7	1	6	66231.470	0.081
8	3	6	-	7	2	5	67482.181	-0.072
8	4	4	-	7	3	5	70024.023	-0.013
8	4	5	-	7	3	4	69147.008	-0.020
8	5	4	-	7	4	3	70467.758	0.037
8	5	3	-	7	4	4	70563.832	0.024
8	6	2	-	7	5	3	71438.728	0.010
8	8	0	-	7	7	1	73244.339	-0.035
9	3	7	-	8	2	6	75388.728	0.006
9	0	9	-	8	1	8	73711.013	0.000
9	1	9	-	8	0	8	73714.856	0.024
9	1	8	-	8	2	7	74203.429	-0.051
9	2	8	-	8	1	7	74323.566	0.035
9	2	7	-	8	3	6	74235.298	0.029
9	3	6	-	8	4	5	73109.050	-0.015

5.2 The Rotational Constants and Distortion Constants of Dimethyl Sulphone

The observed rotational frequencies, listed from Table-5.2 to Table-5.9, were used to calculate the effective rotational constants and centrifugal distortion constants of dimethyl sulphone. Watson's S-reduction[46][47], in the I^r representation, was also used in this calculation. Saito and Marino's rotational constants for $(^{12}CH_3)_2^{32}S^{16}O_2$ and $(^{12}CH_3)(^{13}CH_3)^{32}S^{16}O_2$ [99] were used to fit the low J transitions and to give the initial predictions for these two species. Quartic distortion constants were required to fit the higher J lines. Greatly improved rotational constants were obtained for these two species. All five quartic distortion constants of $(^{12}CH_3)_2^{32}S^{16}O_2$ were derived. However, the distortion constants D_{JK} and d_2 of $(^{12}CH_3)(^{13}CH_3)^{32}S^{16}O_2$ were not obtained and the constants of the normal species were used in the calculations for this mono-^{13}C substituted species. The rotational constants and quartic distortion constants of six other species have been well determined and fitted with the measured frequencies. The standard deviations of fit for all of the species studied were smaller than $0.045MHz$, with the exception of that of $(^{12}CH_3)(^{13}CH_3)^{32}S^{16}O_2$, which was bigger than $0.075MHz$, for this species the distortion constants D_{JK} and d_2 were not well determined. No sextic distortion constants were needed in the fits.

The derived rotational constants show that $(^{12}CH_3)_2^{32}S^{16}O^{18}O$ is more asymmetric and $(^{12}CH_3)(^{12}CH_2D)^{32}S^{16}O_2$(I) is more symmetric than any of the other species. Ray's values of asymmetry parameter κ for the two species are -0.192 and -0.649, respectively, while the parameters for the other species are from -0.3 to -0.5. The rotational constant and the distortion constant D_J of $(^{12}CH_3)(^{13}CH_3)^{32}S^{16}O_2$ are almost the average of those of $(^{12}CH_3)_2^{32}S^{16}O_2$ and $(^{13}CH_3)_2^{32}S^{16}O_2$. The inertial defects Δ_c, $\Delta_c = I_c^0 - I_a^0 - I_b^0$, of $(^{12}CH_3)_2^{32}S^{16}O_2$, $(^{13}CH_3)_2^{32}S^{16}O_2$ and $(^{12}CH_3)(^{12}CH_2D)^{32}S^{16}O_2(I)$ are $-105.62 \, lu\AA^2$, $-105.621 u\AA^2$ and $-105.645 u\AA^2$, respectively. The difference between the inertial defects, Δ_c, of $({}^{12}CH_3)_2^{32}S^{16}O_2$ and $({}^{12}CH_3)({}^{12}CH_2D)^{32}S^{16}O_2$ is almost three times bigger than that of $({}^{12}CH_3)_2^{32}S^{16}O_2$ and $({}^{13}CH_3)_2^{32}S^{16}O_2$. We attribute the larger difference to the effect of the vibration of the light atom hydrogen, these variations are. however, all small, which suggests that the atoms $H(I)$ are located on the CSC plane. The inertial defect Δ_c of $({}^{12}CH_3)_2^{32}S^{16}O_2(II)$ is -106.423$u\AA^2$, which means that $H(II)$ atoms are out of the CSC plane. The rotational constants and distortion constant D_J of $({}^{12}CH_3)({}^{12}CH_2D)^{32}S^{16}O_2(I)$ and $({}^{12}CH_3)({}^{12}CH_2D)^{32}S^{16}O_2(II)$ are between those of the normal species and the D_6 substituted species and there is the following approximate relation between these constants:

$$\frac{G_{({}^{12}CH_3)({}^{12}CH_2D)^{32}S^{16}O_2(I)} + 2G_{({}^{12}CH_3)({}^{12}CH_2D)^{32}S^{16}O_2(II)}}{3} \tag{5.2.1}$$

$$\propto \frac{5G_{({}^{12}CH_3)_2^{32}S^{16}O_2} + G_{({}^{12}CD_3)_2^{32}S^{16}O_2}}{6}$$

where G may be either one of the rotational constants A, B and C or a distortion constant D_J. This approximate relation helped to assign these two mono-deutero species.

Table-5.10 Effective Rotational Constants and Distortion Constants of $(CH_3)_2SO_2$

Isotopomer	$(^{12}CH_3)_2^{32}S^{16}O_2$	$(^{12}CD_3)_2^{32}S^{16}O_2$	$(^{13}CH_3)_2^{32}S^{16}O_2$
A (MHz)	4638.2247(18)	4138.7767(23)	4559.9750(30)
B (MHz)	4295.4408(17)	3639.5545(49)	4157.8888(29)
C (MHz)	4177.1287(15)	3396.6720(18)	3987.0419(22)
D_J (kHz)	1.2218(102)	0.8927(183)	1.1928(146)
D_{JK} (kHz)	-0.5409(405)	-0.7422(539)	-0.6733(543)
D_K (kHz)	0.7329(302)	0.9897(359)	0.9313(406)
d_1 (kHz)	-0.1598(57)	-0.1521(117)	-0.1477(94)
d_2 (kHz)	0.0078(25)	0.0159(38)	0.0165(36)
κ	-0.487	-0.345	-0.404
ε_{fit} (MHz)	0.0349	0.0359	0.0394

Table-5.10 Continued(1)

Isotopomer	$(^{12}CH_3)_2^{32}S^{16}O^{18}O$	$(^{12}CH_3)_2^{34}S^{16}O_2$	$(^{12}CH_3)(^{13}CH_3)^{32}S^{16}O_2$
A (MHz)	4458.0844(22)	4637.2112(46)	4606.1041(56)
B (MHz)	4235.5809(22)	4295.6112(78)	4219.7493(69)
C (MHz)	4084.7486(41)	4176.3349(51)	4080.2318(62)
D_J (kHz)	1.1668(344)	1.2117(360)	1.2616(397)
D_{JK} (kHz)	-0.2807(871)	-0.6069(1116)	a
D_K (kHz)	0.3274(503)	0.7766(673)	0.5990(713)
d_1 (kHz)	-0.1361(196)	-0.1532(241)	-0.1659(186)
d_2 (kHz)	0.1127(66)	0.0194(79)	a
κ	-0.192	-0.482	-0.469
ε_{fit} (MHz)	0.0246	0.0437	0.0767

a--Constrained to the value obtained for $(^{12}CH_3)_2^{32}S^{16}O_2$.

Table-5.10 Continued(2)

Isotopomer	$(^{12}CH_3)(^{12}CH_2D)^{32}S^{16}O_2(I)$	$(^{12}CH_3)(^{12}CH_2D)^{32}S^{16}O_2(II)$
A (MHz)	4634.8199(50)	4530.4685(37)
B (MHz)	4114.4465(60)	4188.9947(51)
C (MHz)	4003.8231(41)	4018.1981(53)
D_J (kHz)	0.9647(307)	1.0959(303)
D_{JK} (kHz)	0.30548(931)	0.1042(836)
D_K (kHz)	0.1818(496)	0.2505(469)
d_1 (kHz)	-0.0775(145)	-0.1279(133)
d_2 (kHz)	0.0187(64)	-0.0534(109)
κ	-0.649	-0.333
ε_{fit} (MHz)	0.0295	0.0323

Table-5.11 Principal Moments of Inertia of Dimethyl Sulfone

Species	I_a^0 $(u\dot{A}^2)$	I_b^0 $(u\dot{A}^2)$	I_c^0 $(u\dot{A}^2)$
$(^{12}CH_3)_2^{32}S^{16}O_2$	108.95958(4)	117.65475(5)	120.98718(4)
$(^{12}CD_3)_2^{32}S^{16}O_2$	122.10830(7)	138.85738(19)	148.78652(8)
$(^{13}CH_3)_2^{32}S^{16}O_2$	110.82934(7)	121.54702(9)	126.75538(7)
$(^{12}CH_3)_2^{32}S^{16}O\,^{18}O$	113.36237(6)	119.31752(6)	123.72340(12)
$(^{12}CH_3)_2^{34}S^{16}O_2$	108.98339(11)	117.65008(21)	121.01017(15)
$(^{12}CH_3)(^{13}CH_3)^{32}S^{16}O_2$	109.71934(12)	119.76518(12)	123.86039(10)
$(^{12}CH_3)(^{12}CH_2D)^{32}S^{16}O_2$(I)	109.03962(11)	122.83037(19)	126.22411(12)
$(^{12}CH_3)(^{12}CH_2D)^{32}S^{16}O_2$(II)	111.55116(7)	120.64446(17)	125.77254(16)

5.3 The Calculation of the Molecular Structure of Dimethyl Sulphone

The effective rotational constants obtained, as listed in Table-5.10, were used to derive the effective molecular geometry of dimethyl sulphone. In the calculation of the effective structure, the effect of zero point vibrations is usually ignored and the structure is assumed to be unaffected by isotopic substitution. If there is a light atom, such as hydrogen, in a molecule, the effect of isotopic substitution on the molecular structure should be large. Because there are six hydrogen atoms in dimethyl sulphone the effect on the zero point vibrations of deuterium substitution is very large, and the effective geometry is not easy to determine. Three different effective geometries were derived.

Method(1): The $r_{CH(I)}$ and $r_{CH(II)}$ bonds, Figure-5.4, were assumed to be the same and all the rotational constants of the eight observed species were used in the calculation.

Method(2): The $r_{CH(I)}$ and $r_{CH(II)}$ bonds, Figure-5.4, were assumed to be the same and all the rotational constants of the eight observed species, except that of $({}^{12}CD_3)_2^{32}S^{16}O_2$, were used in the calculation.

Method(3): The $r_{CH(I)}$ and $r_{CH(II)}$ bonds, Figure-5.4, were assumed to be different and all the rotational constants of the eight observed species were used in the calculation.

The procedure used for sulphuryl chloride and sulphuryl fluoride was also used here.

A substitution structure was evaluated from the following isotopic species:

$({}^{12}CH_3)_{2_{32}}S^{16}O_2$, $({}^{13}CH_3)_2^{12}S^{16}O_2$, $({}^{12}CH_3)_2^{32}S^{16}O^{18}O$,

$({}^{12}CH_3)_2^{34}S^{16}O_2$, $({}^{12}CH_3)({}^{12}CH_2D)^{32}S^{16}O_2(I)$ and $({}^{12}CH_3)({}^{12}CH_2D)^{32}S^{16}O_2$,

In this calculation $({}^{12}CH_3)_2^{32}S^{16}O_2$ was used as the parent species. The S atom is so close to the center of mass that the isotopic substitution produces only very small changes in the moments of inertia, ΔI_a and ΔI_c.

$$\Delta I_a = I_a^{({}^{12}CH_3)_2^{34}S^{16}O_2} - I_a^{({}^{12}CH_3)_2^{32}S^{16}O_2} \tag{5.3.1}$$

$$= 0.02382u\dot{A}^2$$

$$\Delta I_c = I_c^{({}^{12}CH_3)_2^{34}S^{16}O_2} - I_c^{({}^{12}CH_3)_2^{32}S^{16}O_2} \tag{5.3.2}$$

$$= 0.02300u\dot{A}^2$$

The small changes may be significantly affected by the zero-point vibrational effects. Therefore the effects of vibration cannot be ignored and the location of the S atom cannot be well determined by the Kraitchman equation[28]. Because the S atom is located on the principal b-axis, if this molecule is a rigid rotor, ΔI_b should be zero. However, actually we have

$$\Delta I_b = I_b^{({}^{12}CH_3)_2^{34}S^{16}O_2} - I_b^{({}^{12}CH_3)_2^{32}S^{16}O_2} \tag{5.3.3}$$

$$= -0.004669u\dot{A}^2$$

Here, we assume that ΔI_b reflects only vibrational effects and that ΔI_a and ΔI_c reflect both inertial changes and vibrational effects. Because this molecule is a nearly spherical rotor, with $I_a \approx I_b \approx I_c$, we assume that the three vibration-rotation interaction constants are almost the same, $\alpha^a \approx \alpha^b \approx \alpha^c$ and that the ΔI change due to vibrations are the same for all the three principal moments of inertia. We correct ΔI_a and ΔI_c by subtraction of ΔI_b from them, that is:

$$\Delta I_{a_{corrected}} = \Delta I_a - \Delta I_b = 0.02848(4)u\dot{A}^2 \tag{5.3.4}$$

$$\Delta I_{c_{corrected}} = \Delta I_c - \Delta I_b = 0.02767(5)u\dot{A}^2 \tag{5.3.5}$$

Then the corrected $\Delta I_{a_{corrected}}$ and $\Delta I_{c_{corrected}}$ are used to derive the coordinates of the S atom using the Kraitchman equation. The coordinates of all other atoms in this molecule were evaluated by the Kraitchman equation[28]. The principal axes coordinates of $(^{12}CH_3)_2^{32}S^{16}O_2$ are given in Table-5.12.

All the resulting r_0 structures are collected in Table-5.13 together with Saito and Marino's effective structure[99]. A theoretical structure derived from an ab-initio calculation, using the Gaussian-86 program[83] with the 6-31G* basis set, is also listed in this table. Figure-5.4 is the view of the $(^{12}CH_3)_2^{32}S^{16}O_2$ isotopomer in its principal inertial axes system.

Table-5.13 shows that the bond length of $r_{CH(I)}$ is determined much less accurately than those of r_{SO}, r_{SC} and $r_{CH(II)}$. The reason could be that hydrogen(I)s are located very close to the principal axis.

The molecular structure obtained for this molecule has C_{2v} symmetry. The two $H(I)$ atoms are located on the CSC plane and the distance between $H(I)$ atoms is longer than that between $H(II)$ atoms, as shown in Figure-5.4. The methyl groups are deformed a little from C_{3v} symmetry, however, and the symmetry axes of the methyl groups are not coincident with the SC bond axes. $\angle SCH(II)$ is about 3.7° bigger than $\angle SCH(I)$ and $\angle H(II)CH(II)$ is about 2° bigger than $\angle H(I)CH(II)$. The center of mass of the three hydrogen atoms in one methyl group is not located on the extension of the SC bond. The angle between the extension of SC bond and the line joining the mass center of the three hydrogen atoms and the C atom is 3.265°. Pierce and Hayashi calculated the same angle for dimethyl sulfide and gave 2.75° [102]. The structures of the two methyl groups in dimethyl sulphone are similar to the structure of the methyl groups in dimethyl sulfide obtained by Pierce and Hayashi[102]. There are also two kinds of hydrogen atoms in dimethyl sulfide, with $H(I)$ on the CSC plane. However, the structures of the methyl groups in dimethyl sulphoxide obtained by Typke[137][138] are much different. In dimethyl sulphoxide, which does not have C_{2v} symmetry, there were three different kinds of hydrogen atoms and the $H(I)$s were not located on the CSC plane. Typke found the angle between CSC plane and the $CH(I)$ bond to be only 1°, and he gave a very short $r_{CH(I)}$ bond length, only 1.054Å (r_s) and 1.052Å (r_z)[137][138]. Table-5.14 gives a comparison between the effective structures of dimethyl sulphone, dimethyl sulfide[102], dimethyl sulphoxide[138] and sulfur dioxide [95][96], in which the structure of dimethyl sulphone derived from method(1) is listed. The SO bond of dimethyl sulphone is only about 0.006Å longer than that of sulphur dioxide but more than 0.04° shorter than that of dimethyl sulphoxide. The $\angle OSO$ angle of dimethyl sulphone and sulfur dioxide are almost the same, the dimethyl sulphone angle is only 0.31° larger. In comparison with dimethyl sulfide, the methyl groups of dimethyl sulphone are not much different, but the CS bond is about 0.03Å smaller. The CSC angle of dimethyl sulphone increases by more than 7° and 5° in comparison with those of dimethyl sulphoxide and dimethyl sulfide, respectively.

Figure-5.4 The Substitution Coordinate of $(^{12}CH_3)_2^{32}S^{16}O_2$.

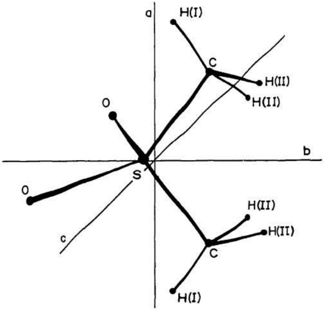

Table-5.12

Substitution Coordinates of Dimethyl Sulphone $\dot{A}$ *

Atoms	a	b	c
S	0.0	0.11985(18)	0.0
O	0.0	0.83555(1)	±1.24299(3)
C	±1.39326(1)	-0.97633(2)	0.0
$H(I)$**	±2.26777(2)	-0.33593(26)	0.0
$H(II)$**	±1.37187(3)	-1.58696(4)	±0.89758(12)

*--$(^{12}CH_3)_2^{32}S^{16}O_2$ was the parent species.

**--See Figure-5.4

Table-5.13 Geometry of Dimethyl Sulphone.

Parameters	r_0^a	r_0^b	r_0^c
$r_{SO}/\dot{A}$	1.431(4)	1.4380(16)	1.4369(15)
$r_{SC}/\dot{A}$	1.777(6)	1.7743(19)	1.7752(17)
$r_{CH(I)}/\dot{A}$	1.091^e	1.0899(12)	1.0827(40)
$r_{CH(II)}/\dot{A}$	1.091^e	1.0899(12)	1.0827(40)
$<OSO/^\circ$	121.02(25)	119.845(227)	120.143(252)
$<CSC/^\circ$	103.28(17)	103.917(157)	103.742(144)
$<SCH(I)/^\circ$		105.326(119)	105.844(227)
$<SCH(II)/^\circ$		109.026(67)	109.554(214)
$<H(I)CH(II)/^\circ$	109.57^e	110.792(184)	110.386(678)
$<H(II)CH(II)/^\circ$	109.57^e	111.649(146)	110.958(605)
$\varepsilon_{fit}(MHz)$		0.275	0.226

Table-5.13 Continued

Parameters	r_0^d	r_s	$r_{ab-initio}^f$
$r_{SO}/\dot{A}$	1.4373(15)	1.4343(23)	1.4368(4)
$r_{SC}/\dot{A}$	1.7749(17)	1.7728(28)	1.7742(2)
$r_{CH(I)}/\dot{A}$	1.0704(75)	1.0839(9)	1.0819(1)
$r_{CH(II)}/\dot{A}$	1.0890(11)	1.0858(2)	1.0811(0)
$<OSO/^\circ$	119.935(207)	120.135(191)	120.073(4)
$<CSC/^\circ$	103.874(141)	103.611(163)	104.272(1)
$<SCH(I)/^\circ$	106.459(459)	105.590(251)	106.469(0)
$<SCH(II)/^\circ$	109.070(62)	109.506(194)	109.775(0)
$<H(I)CH(II)/^\circ$	110.119(187)	110.375(113)	109.752(3)
$<H(II)CH(II)/^\circ$	111.846(155)	111.607(46)	111.208(2)
$\varepsilon_{fit}(MHz)$	0.241		

a--Reference[99].

b--This work method(1)

c--This work method(2)

d--This work method(3)

e--Reference[102]

f--6-31G* basis set, using Gaussian-86 program[83].

Table-5.14

The Comparison Between the Structures, r_0, of $(CH_3)_2SO_2$, $(CH_3)_2SO$, $(CH_3)_2S$ and SO_2.

Parameters	$(CH_3)_2SO_2$	$(CH_3)_2SO$ [c]	$(CH_3)_2S$ [a]	SO_2 [b]
$r_{SO}/\dot{A}$	1.4380(16)	1.482(50)		1.4322
$r_{SC}/\dot{A}$	1.7743(19)	1.807(31)	1.802(2)	
$r_{CH(I)}/\dot{A}$	1.0899(12)	1.094(9)	1.091(5)	
$r_{CH(II)}/\dot{A}$	1.0899(12)		1.091(5)	
$\langle OSO/^\circ$	119.845(227)			119.535
$\langle CSC/^\circ$	103.917(157)	96.52(10)	98.87(17)	
$\langle SCH(I)/^\circ$	105.326(119)		106.63	
$\langle SCH(II)/^\circ$	109.026(67)		110.75	
$\langle H(I)CH(II)/^\circ$	110.792(184)		109.53(33)	
$\langle H(II)CH(II)/^\circ$	111.649(146)		109.53(33)	

a--Reference[102].

b--Reference[95][96].

c--Reference[138].

5.4 The Raman Spectra of Dimethyl Sulphone

According to the X-ray analyses by Sands[149] and Langs[150], the space group of the $(CH_3)_2SO_2$ crystal is D_{2h}^{17}-$Amma$. The infrared and polarized Raman spectra of single crystals of dimethyl sulphone and dimethyl sulphone-D_6 were recorded by Geiseler[148] and Kuroda[147]. The normal coordinate analysis was carried out by them also.

In this present work the solid phase Raman spectra of $(^{12}CH_3)_2^{32}S^{16}O_2$ and $(^{12}CD_3)_2^{32}S^{16}O_2$ were remeasured and those of $(^{13}CH_3)_2^{32}S^{16}O_2$ were measured for the first time. Limited by the sensitivity and resolution of the Raman spectrometer used in this work and the low vapor pressure of this molecule, the gas phase spectra could not be observed. Therefore a meaningful harmonic force field for this molecule could not be obtained. The observed spectra are shown in Figure-5.5 and the measured frequencies are given in Table-5.15 together with Kuroda's data[148]. We did not try to reassign these peaks and Kuroda's assignments were used here.

Figure-5.5 The Raman Spectra of Crystalline $(^{12}CH_3)_2^{32}S^{16}O_2$, $(^{13}CH_3)_2^{32}S^{16}O_2$ and $(^{12}CD_3)_2^{32}S^{16}O_2$

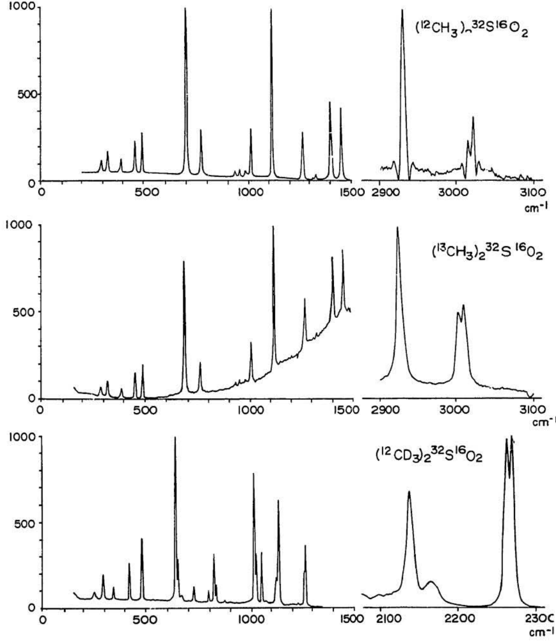

Table-5.15 The Vibrational Frequencies (cm^{-1})

of $(^{12}CH_3)_2^{32}S^{16}O_2$, $(^{13}CH_3)_2^{32}S^{16}O_2$, and $(^{12}CD_3)_2^{32}S^{16}O_2$.

Modes		$(^{12}CH_3)_2^{32}S^{16}O_2$		$(^{12}CD_3)_2^{32}S^{16}O_2$		$(^{13}CH_3)_2^{32}S^{16}O_2$
Species	Modes	a	b	a	b	b
a_1	ν_{a,CH_3}	3018.	3015.2	2270.	2263.2	3002.8
	ν_{s,CH_3}	2936.	2932.1	2147.	2137.9	2926.9
	δ_{a,CH_3}	1451.	1450.5	1143.	1239.2	1446.2
	δ_{s,CH_3}	1337.	1334.2	1051.	1052.1	1326.1
	$\nu_{s,SO}$	1121.	1119.3	1019.	1014.2	1117.3
	ρ_{CH_3}	1013.	1010.8	827.	824.3	1000.7
	ν_{CS}	703.	702.1	648.	642.1	685.2
	β_{SO_2}	496.	496.2	486.	483.5	491.5
	δ_{CSC}	294.	293.9	253.	252.0	286.5
a_2	ν_{a,CH_3}	3024.	3021.5		2269.3	3010.1
	δ_{a,CH_3}	1405.	1403.6	1027.	1023.1	1399.8
	ρ_{CH_3}	937.	936.5	730.	723.3	928.5
	t_{SO_2}	326.	325.0	296.	294.1	319.1
	τ					
b_1	ν_{a,CH_3}	3025.	3021.4	2275.	2269.3	3010.1
	δ_{a,CH_3}	1428.		1273.	1267.5	
	$\nu_{a,SO}$	1269.	1267.6	1020.		1266.9
	ρ_{CH_3}	986.	985.5	803.	795.1	974.0
	ρ_{SO_2}	396.	391.7	350.	344.1	386.1
	τ	262.		195.		

Table-5.15 continued

Modes		$(^{12}CH_3)_2^{32}S^{16}O_2$		$(^{12}CD_3)_2^{32}S^{16}O_2$		$(^{13}CH_3)_2^{32}S^{16}O_2$
Species	Modes	a	b	a	b	b
b_2	$\nu_{a.CH_3}$	3017.	3015.2	2270.	2263.2	3002.8
	$\nu_{s.CH_3}$	2936.	2932.1	2146.	2137.9	2926.1
	$\delta_{a.CH_3}$	1438.	1436.4	1056.		
	$\delta_{s.CH_3}$	1322.	1318.3	1023.		1307.5
	ρ_{CH_3}	958.	956.8	834.	833.5	949.2
	$\nu_{a.CSC}$	771.	770.1	658.	653.0	757.1
	ω_{SO_2}	465.	463.5	430.	426.0	458.3

a--Refrence[147].

b--This work.

ν--Stretching.

δ--Deformation.

β--Bending.

ω--Wagging.

ρ--Rocking.

t--Twisting.

τ--Torsion.

CHAPTER 6

DISCUSSION OF THE STRUCTURES AND FORCE FIELDS OF SULPHURYL FLUORIDE, SULPHURYL CHLORIDE AND DIMETHYL SULPHONE

In Table-6.1, we compare the properties of the SO bonds of sulphuryl fluoride, sulphuryl chloride and dimethyl sulphone. From the symmetry analysis we know the relations between the symmetry coordinate force constants and the internal coordinate force constants:

$$F_{11} = F_{SO} + F_{rr} \tag{6.1}$$

and

$$F_{66} = F_{SO} - F_{rr} \tag{6.2}$$

so that we have F_{SO} as the average of F_{11} and F_{66}. Here F_{11} and F_{66} are the symmetric and asymmetric SO stretching force constants, respectively. F_{SO} is the SO stretching force constant and F_{rr} is the interaction force constant between the two SO bonds in internal coordinates. We assume that the vibrational frequencies ν_{SO} are the average of the SO symmetric stretch vibrational frequency, $\nu_{SO\ sy.str.}$, and the SO asymmetric stretch vibrational frequency, $\nu_{SO\ asy.str.}$. The vibrational frequency of dimethyl sulphone was obtained from the solid state data and those of the other two molecules were obtained from gas phase data.

Table-6.1 shows some regularities. The properties of the SO bonds are sensitive to the electronegativities of the attached groups X. As noted by Gillespie and Robinson the frequencies of these SO stretching vibrations increase with increasing electronegativity of the attached groups X in sulphones and sulphoxides[124]. The highest observed SO bond stretching frequency was found for F_2SO_2 ($1388.1cm^{-1}$) followed by that of Cl_2SO_2 ($1320.3cm^{-1}$), while the lowest was that of $(CH_3)_2SO_2$ ($1193.3cm^{-1}$). The nature of the sulphuryl molecules, X_2SO_2, has long been a subject of controversy. Wells[122] and Gillespie[123] investigated the bond lengths and the bond angles of SO_2 groups in sulphuryl molecules and wrote the SO bonds as classical double bonds. An ab-initio calculation, using the 6-31G* basis set, showed the bond orders of the SO bonds in the three molecules are between 1.6 and 1.8. The SO bonds of sulphuryl fluoride have the largest bond order (1.79) and those of dimethyl sulphone have the smallest bond order (1.62) of the three molecules. The calculated force constant F_{SO} of sulphuryl fluoride, $11.76aJ\AA^{-2}$, is bigger than that of sulphuryl chloride, $10.68aJ\AA^{-2}$. Because vibrational frequencies could not be obtained for a sufficient number of isotopomers, the force constants of dimethyl sulphone could not be derived in this work. However, we can infer from the force constants of sulphuryl fluoride and sulphuryl chloride that the force constant F_{SO} of dimethyl sulphone is smaller than that of sulphuryl chloride. All of the properties discussed above, force constant F_{SO}, vibrational frequency ν_{SO} and bond order of SO bond, change in the same direction with a change of electronegativity, $\chi_{F_2SO_2}(3.98) > \chi_{Cl_2SO_2}(3.16) > \chi_{(CH_3)_2SO_2}(2.30)$. The SO bond length, however, decreases with an increase in the electronegativity of the X group. Here sulphuryl fluoride has the shortest SO bond length (1.4002 Å), dimethyl sulphone has the longest (1.4380Å). Many publications have given a detailed discussion of the sulphur-oxygen bond, which has been described in terms of π-bonds formed between oxygen $2p$ orbitals and $3d_{x^2-y^2}$ and $3d_{z^2}$ orbitals of sulphur[125][126][127][128][129]. In sulphuryl molecules the multiple bond character of the SO bond may arise from a back donation of $2p$ electrons on the oxygen atoms to vacant $3d_{z^2}$ or $3d_{x^2-y^2}$ orbitals of the sulphur atom. This process and thus the bond order depends on the electron density around the sulphur atom. The larger the electron density around the sulphur atom, the larger the multiple bond character of the SO bond. Hence the bond strength increases, and then the bond length decreases, with increasing electronegativity of the attached group X, from dimethyl sulphone, sulphuryl chloride to sulphuryl fluoride. The diagonal SO stretching force constant (F_{SO}) and vibrational frequency (ν_{SO}) increases in magnitude with decreasing SO bond length. The sulphoxides X_2SO have been found to be similar, the highest SO stretching frequency and shortest SO bond length were also observed for F_2SO and the lowest frequency and longest bond length were for $(CH_3)_2SO$. The SO stretching vibrational frequencies of F_2SO, Cl_2SO and $(CH_3)_2SO$ are $1385cm^{-1}$ [131], $1229cm^{-1}$ [131] and $1109cm^{-1}$ [135], respectively. The SO bond lengths of the three molecules are 1.412 Å [133], 1.428 Å [95][134][136] and 1.47Å [135], respectively. Goggin *et al* [132] showed that in SOF_4 the SO stretching frequency is higher than that of F_2SO, which is consistent with the presence of two additional highly electronegative F ligands. Table-3.21 and Table-4.27 show that the SO bond lengths of sulphuryl chloride, sulphuryl fluoride, thionyl chloride and thionyl fluoride are all shorter than that of sulfur dioxide. The SO bond stretching vibrational frequencies of the four molecules are higher than that of sulfur dioxide[104][131]. Brooker[104] gave the SO stretching vibrational frequencies of SO_2 as $1151.3cm^{-1}$ and $1361.5cm^{-1}$, the average is $1256.4cm^{-1}$. It is an obvious fact that the presence of the more electronegative groups Cl and F strengthen the SO bonds. Dimethyl sulphone and dimethyl sulphoxide, however, have longer SO bond lengths and lower SO stretching vibrational frequencies than sulfur dioxide[104][139][140]. The methyl group weakens the SO bond. Table-3.21, Table-4.27 and Table-5.14 show that the SO bond lengths of the sulphones are all shorter than those of the corresponding sulphoxides and the SO bond stretching vibrational frequencies of the sulphones are all higher than those of the corresponding sulphoxides. Fluorine, chlorine and oxygen atoms have bigger electronegativities (3.98, 3.16 and 3.5[118][119] respectively), than the sulfur atom (2.5[118][119]). The methyl group has an electronegativity of 2.3[120][121], which is smaller than that of the sulfur atom. The nature of the SO bond seems to depend on the relative values of the electronegativities of the S atom and the attached group. The attached group shortens the SO bond length and increases the SO stretching vibrational frequency if the group is more electronegative than sulfur atom, otherwise the attached group increases the SO bond length and lowers the SO stretching vibrational frequency.

Cruickshank[129] assumed that there is a linear relationship between bond length and bond order for sulphuryl molecules. A general relation between force constant and bond length was suggested by Linnett[130], as

$$kr^n = C \tag{6.3}$$

Here k is the SO stretching force constant, in $aJ\mathring{A}^{-2}$, r is the SO bond length, in $\mathring{A}$, and n and C both are constants. After studying more than twenty SO bond containing molecules, Gillespie and Robinson showed that the constants were about $n = 7.4$ and $C = 1.41 \times 10^2 aJ\mathring{A}^{n+2}$ for SO bonds[124]. They also obtained an expression for the vibrational frequency and the bond length.

$$\nu r^m = D \tag{6.4}$$

where ν is the SO stretch vibrational frequency, in cm^{-1}, r is the SO bond length, in $\mathring{A}$, and m and D are constants, with m=3.7 and $D = 4.79 \times 10^3 cm^{-1}\mathring{A}^m$. Both equations 6.1 and 6.2 are empirical equations and have no defined physical meaning. The C constant of sulphuryl fluoride obtained in our work is 1.42×10^2, which is very close to the value found by Gillespie. The constant for sulphuryl chloride, however, is a little smaller at 1.37×10^2. This may be because in the calculation of the force constants of sulphuryl chloride, the following force constants, $F_{1,2}$, $F_{1,3}$, $F_{1,4}$ and $F_{6,7}$, were assumed to be zero, which may decrease the value determined for the SO stretching force constants. The D constants are 4.82×10^3, 4.74×10^3 and 4.58×10^3 for F_2SO_2, Cl_2SO_2 and $(CH_3)_2SO_2$, respectively. The constants of sulphuryl fluoride and sulphuryl chloride fit with Gillespie's value well. The constant of dimethyl sulphone is much lower; the reason may be partly that the vibrational frequency of this molecule was measured in the crystal state.

The angles OSO of the three molecules change in the opposite direction to the SO bond lengths, as shown in Table-6.1. The shorter the SO bond length, the bigger the OSO angle. Thus the OSO angles of sulphuryl fluoride(125.051°) and sulphuryl chloride(123.230°) are bigger than that of sulfur dioxide(119.535°), while the angle of dimethyl sulphone is smaller than that of sulfur dioxide(119.845°). There are two possible reasons for the variations in the OSO angles. One is that the electron density in the SO bonds increases with increasing bond order, hence the repulsion between the two SO bonds in the SO_2 group will increase and therefore the bond angle should increase. The second reason is that, with shortening of the SO bond length, the repulsion between the two oxygen atoms in the SO_2 group will increase and the bond angle OSO should also increase accordingly.

Table-6.1

Comparison of the SO Bonds of X_2SO_2 Molecules

(X can be Cl, F or (CH_3))

Parameter	F_2SO_2	Cl_2SO_2	$(CH_3)_2SO_2$
r_{SO} /Å	1.4002	1.4122	1.4380
$Angle_{OSO}/°$	125.051	123.230	119.845
$Angle_{XSX}/°$	95.40	100.12	103.87
$F_{SO}\,(aJÅ^{-2})$	11.76	10.68	
ν_{SO} $(cm^{-1})^{e}$	1388.1	1320.3	1193.3[f]
Bond order$_{SO}$ [d]	1.786	1.658	1.621
χ [c]	3.98[a]	3.16[a]	2.30[b]

a--References [118] and [119].

b--References [120] and [121].

c--Electronegativity of the X atom or group on the Pauling scale.

d--Ab-initio result, obtained using the 6-31G* basis set and program Guassian-86.

e--$\nu_{SO} = (\nu_{sy.} + \nu_{asy.})/2$.

f--Vibrational frequency of crystal line $(CH_3)_2SO_2$.

g--Force constant of the SO bond stretch.

REFERENCES

[1] E. Fermi, *Z. Physik*, **71**, 251(1931).

[2] S. Califano, *Vibrational States*, John Wiley and Sons(1976).

[3] J. Michael Hollas, *High Resolution Spectroscopy*, Butterworths(1982).

[4] H. C. Allen, Jr. and P. C. Cross, *Molecular Vib-Rotors*, John Wiley and Sons, Inc., New York and London, (1963).

[5] D. C. McKean, *Spectrochimica Acta*, **29A**, 1559(1973).

[6] J. L. Duncan, D. Ellis and I. J. Wright, *Molecular Physics*, **20**, 673 (1971).

[7] A. D. Dickson, I. M. Mills and B. L. Crawford, *J. Chem. Phys.*, **27**, 445 (1957).

[8] C. H. Townes and A. L. Schawlow, *Microwave Spectroscopy*, McGraw-Hill Book Company, New York, Toronto, London, (1955).

[9] W. Gordy and R. L. Cook, *Microwave Molecular Spectra*, John Wiley and Sons, Inc. (1984).

[10] J. H. Schachtschneider and R. G. Snyder, *Spectrochim. Acta*, **19**, 117 (1963).

[11] R. G. Snyder and J. H. Schachtschneider, *Spectrochim. Acta*, **21**, 169 (1965).

[12] T. Shimanouchi, *Pure and Appl. Chem.*, **7**, 131(1963).

[13] R. W. Davis and M. C. L. Gerry, *J. Mol. Spect.*, **65**, 455(1977).

[14] Y. Morino and S. Saito, *J. Mol. Spect.*, **19**, 435(1966).

[15] H. Takeo, E. Hirota and Y. Morino, *J. Mol. Spect.*, **34**, 370(1970).

[16] Y. Morino, Y. Kikuchi, S. Saito, and E.Hirota, *J. Mol. Spect.*, **13**, 95(1964).

[17] F. Tanaka and Y. Morino, *J. Mol. Spect.*, **33**, 538(1970).

[18] W. Gordy and R. L. Cook, *Technique of Organic Chemistry*, Vol.9, 2nd edn., Wiley-Interscience, New York, (1970).

[19] J. Sheridan, *Advances in Infrared and Raman Spec.*, **5**, 276(1978).

[20] J. G. Smith and J. K. G.Watson, *J Mol. Spect.*, **69**, 47(1978).

[21] M. D. Harmony, R. J. Berry, and W.H.Taylor, *J. Mol. Spect.*, **127**, 324(1988).

[22] M. D. Harmony and W. H. Taylor, *J. Mol. Spect.*, **118**, 163(1986).

[23] E. B. Wilson Jr., J. C. Decius and P. C. Cross, *Molecular Vibrations*, McGraw-Hill, (1955).

[24] F. A. Cotton, *Chemical Applications of Group Theory*, John Wiley and Sons, Inc. New York. London. Sydney. (1963).

[25] E. R. Cohen and B. N. Taylor, *Physics Today*, BG11, (1987).

[26] O. M. Matsumura C. and Y. Morino, *J. Mol. Spec.*, **28**, 316(1968).

[27] T. Shimanouchi, *J. Phys. Chem. Ref. Data*, **6**, 1036(1977).

[28] J. Kraitchman, *Am. J. Phys.*, **21**, 17(1953).

[29] B. Bak, D. Christensen, W. B. Dixon, L. Hansen-Nygaard, and J. Rastrup-Andersen, *J. Chem. Phys.*, **37**, 2027(1962).

[30] R. W. Davis and M. C. L. Gerry, *J. Mol. Spec.*, **57**, 118(1975).

[31] C. C. Costain, *J. Chem. Phys.*, **29**, 864(1958).

[32] Y. Morino, K. Kuchitsu, and T. Oka, *J. Chem. Phys.*, **36**, 1108(1962).

[33] D. R. Herschbach and V. W. Laurie, *J. Chem. Phys.*, **37**, 1668(1962).

[34] D. R. Herschbach and V. W. Laurie, *J. Chem. Phys.*, **37**, 1687(1962).

[35] K. Kuchitsu and L. S. Bartell, *J. Chem. Phys.*, **36**, 2460(1962).

[36] K. Kuchitsu and L. S. Bartell, *J. Chem. Phys.*, **36**, 2470(1962).

[37] K. Kuchitsu, *J. Chem. Phys.*, **49**, 4456(1968).

[38] K. Kuchitsu, T. Fukuyama and Y. Morino, *J. Mol. Struc.*, **4**, 41(1969).

[39] R. Stolevik, H. M. Seip and S. J. Cyvin, *Chem. Phys. Lett.*, **15**, 263 (1972).

[40] I. M. Mills, *Molecular Spectroscopy: Modern Research*, (K. N. Rao and C. W. Mathews Editors), Academic Press, New York, (1972).

[41] J. K. G. Watson, *J. Mol. Spect.*, **48**, 479(1973).

[42] D. Kivelson and E. B. Wilson, Jr., *J. Chem. Phys.*, **21**, 1229(1953).

[43] J. H. Meal and S. R. Polo, *J. Chem. Phys*, **24**, 1119(1956).

[44] E. B. Wilson, Jr., and J. B. Howard, *J. Chem. Phys.*, **4**, 260(1936).

[45] J. K. G. Watson, *J. Chem. Phys.*, **46**, 1935(1967).

[46] J. K. G. Watson, *J. Chem. Phys.*, **45**, 1360(1966)

[47] J. K. G. Watson, *Vibrational Spectra* and *Structure*, *a Series of Advances*, (J. R. Durig, Ed.), Elsevier, New York, **6**, 1(1977).

[48] J. L. Duncan, *Croatica Chemica Acta*, **61(2)**, 463(1988).

[49] G. Herzberg, *Molecular Spectra* and *Molecular Structure. II. Infrared* and *Raman Spectra of Polyatomic Molecules*. D. Van Nostrand Company Inc. New York. (1966).

[50] J. H. Meal and S. R. Polo, *J. Chem. Phys.*, **24**, 1119(1956).

[51] J. H. Meal and S. R. Polo, *J. Chem. Phys.*, **24**, 1126(1956).

[52] E. Teller, *Hand-und Jahrbuch der Chem. Physik*, **IX,2**, 125(1934).

[53] I. M. Mills, *Spectrochim Acta*, **16**, 35(1960).

[54] I. M. Mills, *J. Mol. Spec.*, **5**, 334(1960).

[55] I. M. Mills, *J. Mol. Spec.*, **17**, 164(1965).

[56] G. W. King, R. M. Hainer and P. C. Cross, *J. Chem. Phys.*, **11**, 27 (1943).

[57] R. S. Mulliken, *Phys. Rev.*, **59**, 873(1941).

[58] B. S. Ray, *Z. Physik*, **78**, 74(1932).

[59] S. C. Wang, *Phys. Rev.*, **34**, 243(1929).

[60] H. H. Nielsen, *Rev. Mod Phys.*, **23**, 90(1951).

[61] D. Kivelson and E. B. Wilson, Jr., *J. Chem. Phys.*, **20**, 1575(1952).

[62] D. Kivelson and E. B. Wilson, Jr., *Phys. Rev.*, **87**, 214A(1952).

[63] W. H. Kirchhoff, *J. Mol. Spec.*, **41**, 333(1972).

[64] C. E. Cleeton and N. H. Williams, *Phys. Rev.*, **45**, 234(1934).

[65] R. A. Poirier, M. R. Peterson and A. Yadav, MUNGAUSS, Chemistry Department, Memorial University of Newfoundland, St. John's, Newfoundland, Canada, (1989).

[66] J. Burie and D. Boucher, *Mol. Phys.*, **32**, 289(1976).

[67] T. J. Balle, E. J. Campbell, M. R. Keenan and W. H. Flygare, *J. Chem. Phys.*, **71**, 2723(1979).

[68] D. J. Millen, *J. Mol. Struc.*, **45**, 1(1978).

[69] MM. A. Dubrulle and D. Boucher, *C. R. Acad. Sc. Paris*, **278**, B211(1974).

[70] MM. A. Dubrulle and J. L. Destombes, *C. R. Acad. Sc. Paris*, **274**, B181(1972).

[71] I. Hargittai, *Acta. Chim. Hung.*, **57**, 403(1968).

[72] I. Hargittai, *Acta. Chim. Hung.*, **60**, 231(1969).

[73] M. Hargittai and I. Hargittai, *J. Mol. Struc.*, **73**, 253(1981).

[74] T. Shimanouchi, *J. Phys. Chem. Ref. Data*, **6**, 1037(1977).

[75] D. E. Martz and R. T. Lagemann, *J. Chem. Phys.*, **22**, 1193(1954).

[76] R. Vogel-Hogler, *Klasse*, **81**, 34(1944).

[77] R. Vogel-Hogler, *Acta. Phys. Austriaca*, **1**, 323(1948).

[78] R. J. Gillespie and E. A. Robinson, *Can. J. Chem. Phys.*, **39**, 2171(1961).

[79] G. R. Hunt and M. K. Wilson, *Spec. Acta*, **18**, 959(1962).

[80] H. Toyuki and K. Shimizu, *Bull. Chem. Soc. Japan*, **39**, 2364(1966).

[81] R. A. Suthers and T. Henshall, *Z. Anorg. Allg. Chem.*, **388**, 257(1972).

[82] H. Siebert, *Z. Anorg. U. Allegem. Chem.*, **275**, 210(1954).

[83] M. J. Frish, J. S. Binkly, H. B. Schlegel, K. Raghavachari, *Carnegie-Mellon Quantum Chemistry Publishing Unit. Pittsburgh PA*, (1984).

[84] R. M. Fristrom, *J. Chem. Phys.*, **20**, 1(1952).

[85] D. R. Lide, Jr., D. E. Mann and J. J. Comeford, *Spec. Acta*, **21**, 497(1964).

[86] D. R. Lide, Jr. and D. E. Mann, *J. Chem. Phys.*, **26**, 734(1957).

[87] D. P. Stevenson and H. Russel, *J. Am. Chem. Soc.*, **61**, 3264(1939).

[88] K. Hagen, V. R. Cross and K. Hedberg, *J. Mol. Struc.* **44**, 187(1978).

[89] G. R. Hunt and M. K. Wilson, *Spec. Acta*, **16**, 570(1960).

[90] P. Bender and J. M. Wood, *J. Chem. Phys.*, **23**, 1316(1955).

[91] S. Sportouch, R. J. H. Clark and R. Gaufres, *J. Raman Spec.*, **2**, 153(1974).

[92] K. Kutchisu and Y. Morino, *Bull. Chem. Soc. Japan*, **38**, 805(1965).

[93] C. Nolin, J. Tremblay and R. Savoie, *J. Raman Spec.*, **2**, 71(1974).

[94] H. A. Jahn, *Phys. Rev.*, **56**, 680(1939).

[95] O. Madelung, *Structure Data of Polyatomic Molecules*, Springer-Verlag Berlin Heidelberg, New York, London Paris, Tokyo, 131(1987).

[96] A. Barbe, C. Secroun, P. Jouve, and B. Duterage, *J. Mol. Spect.*, **55**, 319(1975).

[97] Y. Endo, S. Saito and E.Hirota, *J. Mol. Spec.*, **77**, 222(1979).

[98] E. Hirota and M. Sahara, *J. Mol. Spec.*, **56**, 21(1975).

[99] S. Saito and F. Marino, *Bull. of Chem. Soc. of Japan*, 45, 92(1972).

[100] D. E. Sands, *Z Kristall.*, **119**, 245(1963).

[101] O. Heinz and Z. Werner, *J. Mol. Struc.*, **6**, 399(1970).

[102] L. Pierce and M. Hayashi, *J. Chem. Phys.*, **35**, 479(1961).

[103] H. Stammreich, K. Kawai and Y. Tavares, *Spec. Acta.*, **15**, 438(1959).

[104] M. H. Brooker and H. H. Eysel, *J. Raman Spec.*, **11**, 322(1981).

[105] H. J. Emeleus and J. F. Wood, *J. Chem. Soc.*, 60, 2183(1948).

[106] R. M. Fristrom, *J. Chemical Physics.*, 20, 1(1952).

[107] H. B. Henbest and S. A. Khan, *Chemical Communications*, 17, 1036 (1968).

[108] A. Schriver, L. Schriver and J. P. Perchard, *J. Molecular Spectroscopy*, 127, 125(1988).

[109] A. Okruszek, *J. of Labelled Compound* and *Radiopharmaceuticals*, Vol. XX, No 6, 741(1983).

[110] G. Courtois, *Compt. Rend. Sciences Acad. Sei.*, 207, 1220(1938).

[111] W. Klemm, H. Sodomann and P. Langmesser, *Z Anorg. Allg. Chem.*,

241, 281(1939)

[112] Yuji Shiro, Masaru Ohsaku, Michiro Hayashi and Hiromu Murata, *Bulletin of Chemical Society of Japan*, **43**, 609(1970).

[113] S. Firth and R. W. Davis, *J. Mol. Spec.*, **127**, 209(1988).

[114] R. H. Hughes and E. B. Wilson, Jr., *Phys. Rev.*, **71**, 562(1947).

[115] M. W. P. Strandberg and T. Wentink, Jr., *Phys. Rev.*, **75**, 270(1950).

[116] K. B. McAfee, Jr., R. H. Hughes and E. B. Wilson, Jr., *Rev. Sci. Instr.*, **20**, 821(1949).

[117] G. Biermann and H. Ziegler, *Anal. Chem.*, **58**, 536(1986).

[118] A. L. Allred, *J. Inorg. Nucl. Chem.*, **17**, 215(1961).

[119] J. E. Huheey, *Inorganic Chemistry*, Harper & Row, Publishers, New York, Evanston, San Francisco, London, (1972).

[120] J. Hinze, M. A. Whitehead and H. H. Jaffe, *J. Am. Chem. Soc.*, **85**, 148(1963).

[121] P. R. Wells, *Progr. Phys. Org. Chem.*, **6**, 111(1968).

[122] A. F. Wells, *Structural Inorganic Chemistry*, 3rd. ed. Oxford University Press, (1962).

[123] R. J. Gillespie, *J Chem. Educ.*, **40**, 295(1963).

[124] R. J. Gillespie and E.A.Robinson, *Canadian J. Chem.*, **41**, 2074(1963).

[125] L. Pauling, *J. Phys. Chem.*, **56**, 361(1952).

[126] W. Moffitt, *Proc. Roy. Soc. (London), Ser.*, A, **200**, 409(1950).

[127] H. H. Jaffe, *J. Phys. Chem.*, **58**, 185(1954).

[128] C. C. Price and S. Oae, *Sulphur Bonding*, The Ronald Press Co., New York, (1962).

[129] D. W. J. Cruickshank, *J. Chem. Soc.*, 5486(1961).

[130] J. W. Linnett, *Quart. Rev. Chem. Soc.*, **1**, 73(1947).

[131] R. J. Gillespie and E. A. Robinson, *Can. J. Chem.*, **39**, 2171(1961).

[132] P. L. Goggin. H. L. Roberts and L.A.Woodward, *Trans. Faraday Soc.*, **57**, 1877(1961).

[133] R. C. Ferguson, *J. Am. Chem. Soc.*, **76**, 850(1954).

[134] K. J. Palmer, *J. Am. Chem. Soc.*, **60**, 2360(1938).

[135] O. Bastiansen and H. Viervoll, *Acta Chem. Scand*, **2**, 702(1948).

[136] S. Suzuki, M. Yamaguchi, M. Onda, T.Sakaizumi, O.Ohashi, and I. Yamaguchi, *J. Mol. Struct.*, **73**, 41(1981).

[137] W. Feder, H. Dreizler, H. D. Rudolph and V. Typke, *Z. Naturforschung*, **24A**, 266(1969).

[138] V. Typke, *Z. Naturforschung*, **33A**, 842(1978).

[139] W. D. Horrocks and F. A. Cotton, *Spect. Acta*, **16**, 358(1960).

[140] W. D. Horrocks and F. A. Cotton, *Spect. Acta*, **17**, 134(1961).

[141] S. Suzuki, M. Yamaguchi, M. Onda, T. Sakaizumi, O. Ohashi and I. Yamaguchi, *et. al. J. Mol. Struc.*, **73**, 41(1981).

[142] J. M. B. Kellogg, I. I. Rabi and N. F. Ramsey, Jr., *Phys. Rev.*, **57**, 677(1940).

[143] J. K. Bragg and C. H. Townes, *Phys. Rev.*, **75**, 735(1949).

[144] G. W. Robinson and C. D. Cornwell, *J. Chem. Phys.*, **21**, 1436(1953).

[145] W. H. Flygare and W. D. Gwinn, *J. Chem. Phys.*, **36**, 787(1962).

[146] R. W. Davis and M. C. L. Gerry, *J. Mol. Spec.*, **60**, 117(1976).

[147] K. Machida and Y. Kuroda, *Spec. Acta.*, **35A(7)**, 835(1979).

[148] G. Geiseler and G. Hanschmann, *J. Mol. Struc.*, **11**, 283(1972).

[149] D. E. Sands, *Z. Kristallogr*, **119**, 245(1963).

[150] D. A. Langs, J. V. Silverton and W. M. Bright, *Chem. Soc. Chem. Commun*, 1653(1970).

[151] A. L. McClellan, *Table of Experimental Dipole Moments*, W. H. Freeman and Company, San Francisco and London, (1963).

[152] I. E. Coop and L. E. Sutton, *Transaction Faraday Soc. London*, **35**, 505(1939).

[153] K. Jug and R. Iffert, *J. Computational Chem.*, **8**, 1004(1987).

[154] D. Patel, D. Margolese and T. R. Dyke, *J. Chem. Phys.*, **70**, 2740(1979).

[155] J. H. Van Vleck and V. F. Weisskopf, *Revs. Modern Phys.*, **17**, 227(1945).

[156] S. Golden and E. B. Wilson, Jr., *J. Chem. Phys.*, **16**, 669(1948).

[157] G. W .Robinson and C. D. Cornwell, *J. Chem. Phys.*, **21**, 1436(1953).

[158] S. Firth, H. J. Clase and R. W. Davis, *J. Mol. Spec.*, in press (1990).

[159] L. Pierce, *J. Mol. Spec.*, **3**, 575(1959).

[160] L. C. Krisher and L. Pierce, *J. Chem. Phys.*, **32**, 1619(1960).

[161] T. Oka, *J. Chem. Phys.*, **45**, 752(1966).

[162] E. Hirota, *Molecular Spectroscopy: Modern Research*, Ed. K. N. Rao, **III**, 297(1985).

[163] E. Hirota, *High-Resolution Spectroscopy of Transient Molecules*, Springer-Verlag, Berlin, Heidelberg ,New York, Tokyo, (1985).

[164] F. C. De Lucia, *Molecular Spectroscopy: Modern Research*, Ed. K. N. Rao, **II**, 69(1976).

[165] A. F. Krupnov and A. V. Burenin, *Molecular Spectroscopy: Modern Research*, Ed. K. N. Rao, **III**, 297(1985).

[166] A. C. Legon and C. A. Rego, *Chem. Phys. Lett.*, **154**, 468(1989).

[167] Y. Ohshima, M. Iida, and Y. Endo, *J. Chem. Phys.*, **92**, 3990(1990).